

## **INFORMATION TO USERS**

**The most advanced technology has been used to photograph and reproduce this manuscript from the microfilm master. UMI films the text directly from the original or copy submitted. Thus, some thesis and dissertation copies are in typewriter face, while others may be from any type of computer printer.**

**The quality of this reproduction is dependent upon the quality of the copy submitted. Broken or indistinct print, colored or poor quality illustrations and photographs, print bleedthrough, substandard margins, and improper alignment can adversely affect reproduction.**

**In the unlikely event that the author did not send UMI a complete manuscript and there are missing pages, these will be noted. Also, if unauthorized copyright material had to be removed, a note will indicate the deletion.**

**Oversize materials (e.g., maps, drawings, charts) are reproduced by sectioning the original, beginning at the upper left-hand corner and continuing from left to right in equal sections with small overlaps. Each original is also photographed in one exposure and is included in reduced form at the back of the book.**

**Photographs included in the original manuscript have been reproduced xerographically in this copy. Higher quality 6" x 9" black and white photographic prints are available for any photographs or illustrations appearing in this copy for an additional charge. Contact UMI directly to order.**

# **U·M·I**

University Microfilms International  
A Bell & Howell Information Company  
300 North Zeeb Road, Ann Arbor, MI 48106-1346 USA  
313/761-4700 800/521-0600



**Order Number 9108197**

**Electron transport in semiconductor**

**Zheng, Ting-Fang, Ph.D.**

**City University of New York, 1990**

**U·M·I**  
300 N. Zeeb Rd.  
Ann Arbor, MI 48106



A

# **Electron Transport in Semiconductor**

by

**Ting-Fang Zheng**

**A dissertation submitted to the Graduate Faculty in Physics in partial  
fulfillment of the requirements for the degree of Doctor of Philosophy,  
The City University of New York**

**1990**

This manuscript has been read and accepted for the Graduate Faculty in Physics in satisfaction of the dissertation requirement for the degree of Doctor of Philosophy.

5/17/90  
Date

Malvin Fax  
Chairman of Examining Committee

5/17/90  
Date

[Signature]  
Executive Officer

Eugene M. Chudnovsky  
A. Levi

Nadine Tsou  
Supervisory Committee

### **Acknowledgements**

I am greatly indebted to Professor Melvin Lax for his support and guidance during the years I spent in the City College. I am also grateful to all people with whom I have had the pleasure to work during the course of my education.

My deep gratitude goes to Professor Fu-Jia Yang for his constant help and advice since I entered the field of physics.

For my old parents, whose complete devotion which I can hardly make up.

For my lovely son, who is always my inspiration.

For my dearest wife, Su-Hua Men, whose patience, encouragement, and help have been beyond measure and generously given.

## Table of Contents

	Page
<b>Acknowledgements</b>	iii
<b>Part I. Electron Tunneling at Presence of Inelastic Scattering</b>	
<b>Section 1 Long Wave Length Approximation with Solvable Model</b>	
1.1). Introduction	1
1.2). Solution of Wave Function	3
1.3). Boundary Condition	6
1.4). Result and Discussion	8
<b>Section 2 General Case via Green's Function</b>	
2.1). General Description of the Method	11
2.2). Green's Function Formula	13
2.3). Inelastic Steady State via Green's Function	21
2.4). Scattering $S$ Matrix of Elastic Potential	25
2.5). Complete Set via $S$ Matrix	29
2.6). Unperturbed Retarded Green's Function	30
2.7). Result and Discussion	36

<b>Part II.</b>	<b>Nonequilibrium Transport of an electron-phonon-hole System in a Semiconductor Well</b>	
1).	Introduction	38
2).	Scattering Mechanism	40
3).	Two-Dimensional Balance Equation	46
4).	Results and Discussions	56
<b>Part III.</b>	<b>Quasianalytical Simulation of Ultrafast Relaxation of Photoexcited Electrons in Semiconductor</b>	
1).	Introduction	60
2).	Approach	63
3).	Results and Discussions	71
<b>Part IV.</b>	<b>Resonant Level Lifetime in GaAs/AlGaAs Double-Barrier Structure with Consideration of <math>\Gamma</math>-X Mixing</b>	
	1). Introduction	74
	2). Model	76
	3). Results and Discussions	79
	Figures to part I	82
	Figures to part II	86
	Figures to part III	91
	Figures to part IV	94
	Bibliography	100

## **Part I: Electron Tunneling at Presence of Inelastic Scattering**

### **Section 1: Long Wave Length at Presence of Inelastic Scattering**

#### **1.1 Introduction**

Since the pioneering work of Esaki and Tsu (1970),<sup>1</sup> there has been great interest in double-barrier resonant tunneling. It not only provides an exciting prospect in electronic device application, but also gives rise to some substantial problems in theoretical research. One of the most important problems in the study of these devices is the effect of inelastic scattering on the tunneling current. These inelastic scatterings are mainly due to electron-phonon scattering and electron-photon scattering. As pointed by Gelfand, Schmitt-Rink, and Levi (1989),<sup>7</sup> the unitarity condition (ie. the current conservation) leads to a feedback mechanism by which inelastic scattering processes change the probability of elastic scattering. Since these devices, general speaking, are the compositions of barriers and wells or even more complicated, the conventional theoretical approach based on homogeneous systems can not be applied to these cases, or they can merely give some rough estimate in some aspect. Some tentative research has been done in this field that is far from complete.

In this part, we present a theoretical frame to solve the tunneling problem in the presence of electron-phonon inelastic scattering. In principle, our method can be generalized to the electron-photon inelastic scattering case.

The problem can be well defined in Fig. 1: an electron, injected from region I,

passes through region II, a so-called interaction region, which contains a lattice potential such as a single barrier or a double barrier and electron-phonon interaction. The purpose is to determine the tunneling current in region III and the reflected current.

We divide our theoretical frame into two sections. In section I, we deal with long wave length electron-phonon interactions. In this case, the electron-phonon interaction potential is approximately  $x$  independent in the interaction region. We present the first calculation of an optical phonon associated with electron tunneling through an actual double barrier. Using a solvable model for the electron-phonon interaction we propose an approach to calculate the 1D electron tunneling with dissipation in an arbitrary barrier, and indicate how the boundary conditions uniquely determine the transmitted current and the reflected current of an electron. We find a general electron wave function solution in the interaction region. By matching this solution with incident wave and out-going wave functions in the other region in each energy sideband at boundary, we can uniquely determine the tunneling current. Our approach also clearly shows why phonon-assisted resonant tunneling appears when the electron injects at sideband  $E \pm n\omega$  ( $E$  is the energy level of elastic resonant tunneling;  $\omega$  is the energy of optical phonon) in a double barrier structure. (Units in which  $\hbar=1$  are chosen.)

In section II, we remove the above long-wavelength approximation and deal with an electron-phonon interaction that is  $x$  dependent via a Green Function method. We derive the steady state in the presence of inelastic interaction with a steady incident current. Since the situation is non uniform in space, we carefully construct the unperturbed Green Function, by which we can calculate the tunneling current.

## 1.2 Solution of Wave Function

An incident electron from the left lead ( in region I,  $x < 0$ ), enters the barrier region II and is scattered by phonons (between  $x=0$  and  $x=d$ ), and arrives at the right lead (in region III,  $x > d$ ). The general Hamiltonian for electron-optical phonon interactions has the form :

$$H_{\text{int}} = [\sum_{\mathbf{q}} M(\mathbf{q}) e^{i\mathbf{q}\cdot\mathbf{R}} e^{-i\omega t} a_{\mathbf{q}} + \text{H. C.}] \Theta(x) \Theta(d-x), \quad (1.2.1)$$

with  $a_{\mathbf{q}}$  and  $a_{\mathbf{q}}^{\dagger}$ , respectively, the phonon annihilation and creation operators, and  $M(\mathbf{q})$  the electron-phonon scattering matrix, and  $\mathbf{R}$  is the electron position,  $\Theta(x)$  is the Heaviside step function. The Heaviside factors confine the interaction region to region II. In the following we use a model of long wave length approximation that replaces  $e^{i\mathbf{q}\cdot\mathbf{R}}$  by 1 in  $H_{\text{int}}$ . This model is similar to the independent boson model<sup>4</sup>, used to describe electron-phonon scattering. Using this model, the Schrödinger equation for a one-dimensional electron in a barrier with arbitrary shape,  $V_0(x)$ , in the region II is given by ( $\hbar=1$ )

$$i \frac{\partial \psi^{\text{II}}}{\partial t} = -\frac{1}{2} \frac{\partial}{\partial x} \left[ \frac{1}{m(x)} \frac{\partial \psi^{\text{II}}}{\partial x} \right] + [V_0(x) + V e^{-i\omega t} + V^{\dagger} e^{i\omega t}] \psi^{\text{II}}, \quad (1.2.2)$$

where

$$V = \sum_{\mathbf{q}} M(\mathbf{q}) a_{\mathbf{q}} \quad V^{\dagger} = \sum_{\mathbf{q}} M^*(\mathbf{q}) a_{\mathbf{q}}^{\dagger} .$$

Here  $m(x)$  is the effective mass of the electron. In the regions I and III the electron is in free motion. By neglecting the effect of the electron-phonon interaction on the phonon system, we assume phonon variables are in free motion and in equilibrium with a heat bath. Equation (1.2.2) is separable in space and time. The general solution of Eq.

(1.2.2) can be written as

$$\psi^{\text{II}}(x, t) = \exp \left[ \frac{V}{\omega} e^{-i\omega x} - \frac{V^\dagger}{\omega} e^{i\omega x} \right] \int dE' [A_{E'} \phi_{E'}^a(x) + B_{E'} \phi_{E'}^b(x)] e^{-iE't}, \quad (1.2.3)$$

where  $\phi_{E'}^a(x)$  and  $\phi_{E'}^b(x)$  are the two independent eigenfunctions at eigenvalue  $E'$  for the equation without phonons. The coefficients  $A_{E'}$  and  $B_{E'}$  are constants, to be determined by the boundary conditions. We assume the electron injects at energy  $E$ , with time independent amplitude,  $A^{\text{in}}$ , (the steady state case). In this case only components of  $\psi(x, t)$  with energy  $E + n\omega$  ( $n=0, \pm 1, \dots$ ) exist. In region II,

$$\psi^{\text{II}}(x, t) = \sum_n \psi_{E+n\omega}^{\text{II}}(x) \exp[-i(E+n\omega)t],$$

with

$$\psi_{E+n\omega}^{\text{II}}(x) = \sum_j \sum_k \frac{(V/\omega)^k}{k!} \frac{(-V^\dagger/\omega)^{j-n+k}}{(j-n+k)!} [A_j^{\text{II}} \phi_j^a(x) + B_j^{\text{II}} \phi_j^b(x)], \quad (1.2.4)$$

where sub-index  $j$  corresponds the energy  $E + j\omega$  ( $j=0, \pm 1, \dots$ ),  $k \geq 0$ ,  $j-n+k \geq 0$ .

To obtain Eq. (1.2.4) we have used

$$e^{A+B} = e^A e^B e^{-1/2[A, B]}$$

for phonon operators. It is easy to see that the magnitudes of  $A_n^{\text{II}}$  and  $B_n^{\text{II}}$  have the order of  $|V| |n|$ . Assuming the electron-phonon interaction is weak, a cutoff of  $|n|$  and  $|m|$  up to  $N$  will ensure the results for the transmitted and the reflected current with accuracy up to  $|V|^{2N}$ . In Eq. (1.2.4) terms for  $n$ -th branch should be maintained to order  $|V|^{2N-|n|}$ . For example, for computing the current with accuracy up to  $|V|^2$ , we should keep the following terms:

$$\psi_{E+\omega}^{\text{II}}(x) = \frac{V}{\omega} [A_0^{\text{II}} \phi_0^a(x) + B_0^{\text{II}} \phi_0^b(x)] + [A_{+1}^{\text{II}} \phi_{+1}^a(x) + B_{+1}^{\text{II}} \phi_{+1}^b(x)] , \quad (1.2.5a)$$

$$\psi_E^{\text{II}}(x) = \left[ 1 - \frac{VV^\dagger}{\omega^2} \right] [A_0^{\text{II}} \phi_0^a(x) + B_0^{\text{II}} \phi_0^b(x)] + \frac{V}{\omega} [A_{-1}^{\text{II}} \phi_{-1}^a(x) + B_{-1}^{\text{II}} \phi_{-1}^b(x)] - \frac{V^\dagger}{\omega} [A_{+1}^{\text{II}} \phi_{+1}^a(x) + B_{+1}^{\text{II}} \phi_{+1}^b(x)] , \quad (1.2.5b)$$

$$\psi_{E-\omega}^{\text{II}}(x) = \frac{-V^\dagger}{\omega} [A_0^{\text{II}} \phi_0^a(x) + B_0^{\text{II}} \phi_0^b(x)] + [A_{-1}^{\text{II}} \phi_{-1}^a(x) + B_{-1}^{\text{II}} \phi_{-1}^b(x)] . \quad (1.2.5c)$$

In the incident channel it is necessary to keep the terms  $\psi_E^{(2)} - |V|^2$ , which is related to the coherent double phonons process, since the cross term of  $|\psi_E^{(0)} + \psi_E^{(2)}|^2$  contributes the lowest order of phonon effect to the current in the incident channel.

In region I and region III, the electron wave function satisfies a free particle Schdinger equation:

$$i \frac{\partial \psi^{\text{I,III}}}{\partial t} = -\frac{1}{2m_{\text{I,III}}} \frac{\partial^2 \psi^{\text{I,III}}}{\partial x^2} . \quad (1.2.6)$$

The physical requirement is that only the reflected wave exists at region I except for the incident wave, so the electron wave function in region I can be written:

$$\psi^{\text{I}}(x, t) = A^{\text{in}} \exp(ik_0^{\text{I}}x - iEt) + \sum_n B_n^{\text{I}} \exp[-ik_n^{\text{I}}x - i(E + n\omega)t] , \quad (1.2.7)$$

with  $B_n^{\text{I}}$  the amplitude of reflected wave. Also, only the transmitted wave exists in region III, thus the electron wave function in region III can be written:

$$\psi^{\text{III}}(x, t) = \sum_n A_n^{\text{III}} \exp[ik_n^{\text{III}}x - i(E + n\omega)t] , \quad (1.2.8)$$

with  $A_n^{\text{III}}$  the amplitude of the transmitted wave, here  $k_n^{\text{L}} = [2m_{\text{L}}(E + n\omega - V_0^{\text{L}})]^{1/2}$  and  $m_{\text{L}}$  is the effective mass of electron in L region,  $V_0^{\text{L}}$  the flat potential level in L region.

### 1.3 Boundary Condition

Using the continuity condition of the wave function and current at  $x=0$  and  $x=d$ , we have

$$\psi^I(x=0, t) = \psi^{II}(x=0, t)$$

$$\frac{1}{m_I} \frac{\partial}{\partial x} \psi^I(x=0, t) = \frac{1}{m_{II}(0)} \frac{\partial}{\partial x} \psi^{II}(x=0, t)$$

$$\psi^{II}(x=d, t) = \psi^{III}(x=d, t)$$

$$\frac{1}{m_{II}(d)} \frac{\partial}{\partial x} \psi^{II}(x=d, t) = \frac{1}{m_{III}} \frac{\partial}{\partial x} \psi^{III}(x=d, t) \quad (1.3.1)$$

Since the solution of wave function in each region can be expressed in time dependent components, each component should satisfy the boundary condition of Eq. (1.3.1). Thus, we obtain the following equations:

$$\sum_j f(j-n)[A_j^{II} \phi_j^a(0) + B_j^{II} \phi_j^b(0)] = A^{in} \delta_{n,0} + B_n^I,$$

$$\frac{1}{m_{II}(0)} \sum_j f(j-n)[A_j^{II} \phi_j^{\prime a}(0) + B_j^{II} \phi_j^{\prime b}(0)] = \frac{1}{m_I} ik_n^I (A^{in} \delta_{n,0} - B_n^I),$$

$$\sum_j f(j-n)[A_j^{II} \phi_j^a(d) + B_j^{II} \phi_j^b(d)] = A_n^{III} \exp(ik_n^{III} d),$$

$$\frac{1}{m_{II}(d)} \sum_j f(j-n)[A_j^{II} \phi_j^{\prime a}(d) + B_j^{II} \phi_j^{\prime b}(d)] = \frac{1}{m_{III}} ik_n^{III} A_n^{III} \exp(ik_n^{III} d), \quad (1.3.2)$$

with

$$f(j-n) = \sum_k [(V/\omega)^k / k!] [(-V^\dagger/\omega)^{j-n+k} / (j-n+k)!],$$

where  $\phi_j^\alpha$  is the derivative of  $\phi_j^\alpha$ ,  $\alpha = a, b$ . Eq. (1.3.2) consists a group of coupled equations, through which components of the wave function in different energy channels couple with each other through phonon emission and absorption. We can solve Eq. (1.3.2) to determine the  $A_n^{\text{II}}$  and  $B_n^{\text{II}}$ , and then obtain  $B_n^{\text{I}}$ , and  $A_n^{\text{III}}$ . By use of a serial substitution method to solve these equations, i. e., step by step to obtain  $\psi_E^{(0)}$ ,  $\psi_{E \pm \omega}^{(1)}$ ,  $\psi_E^{(2)}$ ,  $\psi_{E \pm 2\omega}^{(2)}$ ,  $\psi_{E \pm \omega}^{(3)}$ ,  $\psi_E^{(4)}$ , . . . , with sup-index ( $n$ ) corresponds the term  $\sim |V|^n$ , the order of phonon operators in each term is determined. The transmitted current at energy  $E + n\omega$  is

$$J_n^{\text{tran}} = (k_n^{\text{III}} / m_{\text{III}}) \langle A_n^{\text{III}\dagger} A_n^{\text{III}} \rangle, \quad (1.3.3)$$

and the reflected current at energy  $E + n\omega$  is

$$J_n^{\text{ref}} = (k_n^{\text{I}} / m_{\text{I}}) \langle B_n^{\text{I}\dagger} B_n^{\text{I}} \rangle, \quad (1.3.4)$$

where  $\langle \dots \rangle$  means the average over the phonon assemble (below the bottom of the barrier,  $k_n^{\text{L}}$  becomes imaginary, and  $J_n^{\text{tran(ref)}}$  is zero). Assuming phonons are in equilibrium at temperature  $T_L$ , we have

$$\langle V^\dagger V \rangle = \sum_q |M(q)|^2 n_q, \quad \langle V V^\dagger \rangle = \sum_q |M(q)|^2 (1 + n_q), \quad (1.3.5)$$

with the phonon occupation number  $n_q = [\exp(\omega/k_B T_L) - 1]^{-1}$ . Also, we can calculate the average value for the assemble of a product of  $V$ 's and  $V^\dagger$ 's. The transmission coefficient is given by

$$T_{\text{trans}} = \frac{\sum_n J_n^{\text{tran}}}{J^{\text{in}}}, \quad J^{\text{in}} = \frac{k_0^{\text{I}}}{m_{\text{I}}} |A^{\text{in}}|^2. \quad (1.3.6)$$

Current conservation is ensured, namely,

$$J^{\text{in}} = \sum_n (J_n^{\text{tran}} + J_n^{\text{ref}}) . \quad (1.3.7)$$

We emphasize that the above boundary conditions uniquely determine the solution of an electron tunneling wave function in the case with dissipation as well as in the case without dissipation. This key point was not properly considered in some previous works. In Ref. 5, for example, the wave function is described by  $\psi = e^{i(s_0 + s_1)}$ , where  $s_0$  is the action without phonons,  $s_1$  is the correction due to the phonon effect. In the equation for  $s_1$  authors neglect the terms  $\partial^2 s_1 / \partial x^2$  (WKB) and  $(\partial s_1 / \partial x)^2$  ( $\sim |V|^2$ ), and reduce the equation for  $s_1$  to a first order differential equation to  $x$ . They then arbitrarily impose the left hand boundary condition  $s_1(x=0, t)=0$ . This forces  $s_1$  to be zero for  $x < 0$ , so that one finds the incorrect result that there is no phonon correction to the reflected current. This correction is needed to obtain the proper physical results on the right hand side. By use of the WKB method with the neglect of the  $(\partial s_1 / \partial x)^2$  term they have lost one of the two solutions, hence can not impose the correct boundary conditions at both sides.<sup>14</sup> Moreover,  $(\partial s_1 / \partial x)^2$  is of order  $|V|^2$  and must be kept to retain this accuracy in the transmission, as discussed before.

#### 1.4 Results and Discussion

It is obvious from our approach that a process with emission (or absorption) of  $n$  phonons must involve the electron eigenfunctions up to the  $E \pm n\omega$  sidebands. Therefore, if a resonant state in a double-barrier structure appears at energy level  $\bar{E}$  in the case of elastic tunneling, a phonon-assisted resonant tunneling can appear when electron injects at energy  $\bar{E} + n\omega$ , since the resonant eigenfunction  $\phi_{\bar{E}}^a(x)$  and  $\phi_{\bar{E}}^b(x)$

are included in the expression of a wave function for electrons injected at  $\bar{E} + n\omega$  through electron-phonon coupling. We have calculated the transmission of electrons in an double barrier structure. Since we are interested in the phonon effect inside the double barrier region (as in Ref. 4), electron-phonon scattering is considered only inside the double-barrier region (although our approach allows region II to extend beyond the double barrier region). The calculation is made with accuracy up to  $|V|^2$  (one phonon processes). By neglecting  $V, V^\dagger$  in Eq. (1.2.5b), we can obtain the elastic solution  $\psi_E^{(0)}$  at  $E$  channel. substituting  $\psi_E^{(0)}$  into Eqs. (1.2.5a), (1.2.5c), and solving Eq. (1.3.2) at  $E \pm \omega$  channels, we obtain the  $J_{\pm 1}^{\text{tran(ref)}}$ , which represent the phonon effect at inelastic channels. We then go back to Eq. (1.2.5b) to calculate  $\psi_E^{(2)}$  ( $\sim |V|^2$ ), which represents the feedback effect of inelastic scattering on the elastic channel. Therefore, the transmitted current and the reflected current at each energy channel are obtained, and our results indicate that current conservation is exactly satisfied. In Fig. 2, we plot the total transmission coefficient of the electron,  $T_{\text{trans}}$ , in a square double-barrier structure as a function of the energy  $E$  of the incident electron. The structure parameters are for a GaAs well sandwiched between two  $\text{Al}_{0.3}\text{Ga}_{0.7}\text{As}$  barriers.<sup>13</sup> The optical phonon energy  $\omega$  is 36.2 meV. For comparison with Ref. 3, the electron-phonon coupling constant is taken as  $g = \sum_{\mathbf{q}} (|M(\mathbf{q})|/\omega)^2 = 0.1$ . At zero temperature, only a phonon assisted resonant peak appears at  $\bar{E} + \omega$ , since only emission of phonons is allowed. At  $T_L = 300$  K peaks at both  $\bar{E} \pm \omega$  appear. The amplitude of the resonant peak at incident energy  $\bar{E}$  decreases when electron-phonon scattering is included. The effects of inelastic scattering alone at  $T_L = 0$  K are displayed in curve C of Fig. 2, where peaks occur at incident energy  $\bar{E} + \omega$  and  $\bar{E}$ . From Eq. (1.2.5c), it is clear that the inelastic peak can

occur when either  $\phi_0(x)$  or  $\phi_{-1}(x)$  is an elastic resonant eigenfunction. In Fig. 3, we plot the transmission coefficient,  $T_{\text{trans}}$ , as a function of the potential drop of the applied electric field,  $V_a$ , in the same structure as that for Fig. 2, when incident electron is at energy  $E_0=70$  meV. We see the phonon assisted resonant peak appears at potential drop  $V_a=108$  meV, at which an elastic resonance occurs at energy  $E_0-\omega$ . The coupling constant  $g=0.03$  is more realistic for a GaAs/AlGaAs structure,<sup>3</sup> Fig. 3 shows that the peak position at  $g=0.03$  and  $g=0.1$  are the same, but the amplitude of the phonon assisted resonant peak decreases with decrease of  $g$ .

In conclusion, based on an independent boson model for electron-phonon interaction, we have proposed an approach for the study of phonon associated electron tunneling through an arbitrary barrier. The algebra in this approach is simple and straightforward. The correct boundary conditions and current conservation are ensured. Our results for double barrier tunneling show the presence at the sidebands of phonon assisted resonant tunneling, which has been shown in experiments<sup>15</sup>. Our model is good for phonons with long wavelength, but can only qualitatively describe the properties of a realistic device, where the three dimensional electron-phonon interaction, statistics and screening effect of electrons should be taken into account.

## Section 2: General Case via Green's Function

### 2.1 General Description of the Method

There are so few systems of physical interest for which exact solution can be found that approximation methods play an important part in application of the theory. Some models and approximate approaches for quantum mechanical transmission and reflection of electron at presence of inelastic scattering. These are: the Feynman path-integral method,<sup>2</sup> a model of two-state system,<sup>3</sup> scattering of electrons into a single resonant state,<sup>4</sup> WKB approximation,<sup>5</sup> a unitary one-phonon approximation,<sup>6</sup> a solvable model for a thin barrier<sup>7</sup> and a model of a time-modulated barrier.<sup>8</sup>

From previous section<sup>9</sup> we show a solvable model if electron-phonon interaction is assumed  $x$  independent in the interaction region. In that case, we can find a general solution of electron wave function solution with electron-phonon interaction in each region. Then we let them match at boundary in a perturbed expansion with incident wave and out-going scattering condition. Thus we can determine scattering current in each energy branch. Nevertheless, this method can not be applied to the case in which the electron-phonon interaction is  $x$  dependent. The reason is it is nearly impossible to find an exact electron wave function solution in interaction region, since variables  $x$  and  $t$  can not be separated in solving the Schrödinger equation. No systematic research has yet been done in this case to our knowledge. To avoid the long wave-length approximation a complete new technique is required.

In this section, we propose a method with Green function theory to calculate the electron-phonon inelastic scattering probabilities in one dimension. Since the rest of two dimension in most semiconductor devices can be considered as an uniform

potential, the one-dimensional Green's function can be easily developed to the three dimensional situation. The main difficulties we should overcome in Green's function method are:

1)How to get a steady state via a Green's function formula for inelastic scattering.

2)How to construct a unperturbed retarded Green's function for a non-uniform potential.

Mostly, the scattering current can be measured in a steady state if a steady incident wave maintains. For the situation of inelastic scattering such as electron-optical-phonon interaction, the electron current keeps emission and absorption phonons in a steady state and leads to multi-channel transmission and reflection. Thus, the steady state solution can be expressed in time dependent components

$e^{-\frac{i}{\hbar}Et}$ ,  $e^{-\frac{i}{\hbar}(E\pm\hbar\omega)t}$ ,  $e^{-\frac{i}{\hbar}(E\pm\hbar\omega)t}$  .... where  $\hbar\omega$  is optical phonon energy. We will first

derive the steady state of electron wave function. The way is we write down the electron wave function defined in whole region from a general Green Function formula.

Then we use iteration method to get electron wave function in a series expansion via the order of electron-phonon interaction potential, and an unperturbed electron wave function with certain incident energy from region I. Since electron-phonon interaction is time  $t$  dependent, so we keep time order in each term. By introducing electron-phonon interaction from  $t=-\infty$  we handle all integral over time and derive the electron steady state in each order of electron-phonon interaction via a unperturbed retarded Green's function and incident wave function.

The greatest difficulty in the Green's function method for tunneling problem is

how to construct a unperturbed retarded Green's function in a non-uniform potential case. For uniform space, since we can choose plane wave as a complete set, it is trivial to get retarded Green's function. For a non-uniform space we choose a complete set which is associated with scattering  $S$  matrix of lattice potential, with which we first construct unperturbed Green's function outside of interaction region. Then with a general solution of Green's function and its boundary conditions at material discontinuity, we construct the unperturbed retarded Green's function in whole region.

With the steady state and the unperturbed retarded Green's function in whole region, we can calculate the electron tunneling current and reflected current. Assuming optical phonons are in equilibrium at some lattice temperature  $T_L$ , we make an average over the phonon assemble to the currents and get a numerical result.

In sec.2.2 a Green's function method is presented and the derivation of steady state is given in sec.2.3. In sec.2.4 the characters of scattering  $S$  matrix is discussed, the complete set associated with  $S$  matrixed is given in sec.2.5. In sec.2.6 the technique of constructing unperturbed retarded Green's function is described. The numerical result and discussions is presented in sec.2.7.

## 2.2 Green's Function Formula

In scattering problems our attention is focused upon wave solutions which develop in time from initial conditions imposed in the remote past rather than on stationary energy eigenfunctions, that is standing waves. Characteristically given a wave packet which in the remote past represents a particle approaching a potential, one ask what the wave will look like in the remote future.

We start with the full Schr: \* odinger equation

$$i\hbar \frac{\partial}{\partial t} \Psi(x,t) = H \Psi(x,t) = [H_0(x) + V(x,t)] \Psi(x,t), \quad (2.2.1)$$

where  $H_0(x)$  is a unperturbed Hamiltonian of the particle which in our problem can be written

$$H_0(x) = -\frac{\hbar^2}{2} \frac{\partial}{\partial x} \frac{1}{m(x)} \frac{\partial}{\partial x} + V_0(x), \quad (2.2.2)$$

$V_0(x)$  is lattice potential which usually is the combination of barriers and wells in our problem,  $m(x)$  is the particle effective mass. For inelastic scattering  $V(x,t)$  is electron-phonon interaction.

Since Eq. (2.21) gives the first time derivative of  $\Psi(x,t)$  in terms  $\Psi(x,t)$  itself and higher time derivatives do not appear in the equation, the value of  $\Psi(x,t)$  for all  $x$  and one particular time  $t$  suffice to determine  $\Psi(x,t)$  for all  $x$  and all  $t$  (both earlier and later). Also, since the wave equation is linear in  $\Psi(x,t)$ , solutions can be superposed and the relation between  $\Psi(x,t)$  at different times must be linear. We turn to Huygens's principle for a convenient way of viewing this process. If the wave function  $\Psi(x',t')$  is known at one particular time  $t'$ , it may be found at any later time  $t$  by considering at time  $t'$  each point of space  $x'$  as a source of spherical waves which propagate outward from  $x$ . The strength of the wave amplitude arriving at point  $x$  at time  $t$  from point  $x'$  will be proportional to the original wave amplitude  $\Psi(x',t')$  the total wave arriving at the point  $x$  at time  $t$  will, by Huygens' principle, be

$$\Psi(x,t) = i \int dx' G(xt, x't') \Psi(x', t') \quad (2.2.3)$$

where the integration is over all space. This equation also serves to define  $G(xt, x't')$ , which is called the Green's function that corresponds to the Hamiltonian  $H(x,t)$ .

Eq. (2.2.3) does not make a distinction between forward propagation of  $\Psi(x,t)$  in time ( $t > t'$ ), and backward propagation ( $t < t'$ ) these two case. For forward propagation we define the retarded Green's function or propagator:

$$G^+(xt, x't') = \begin{cases} G(xt, x't') & \text{for } t > t' \\ 0 & \text{for } t < t' \end{cases} \quad (2.2.4)$$

We also introduce the unit step function  $\theta(\tau)$  defined by

$$\theta(\tau) = 1 \quad \text{for } \tau > 0 \quad \theta(\tau) = 0 \quad \text{for } \tau < 0 \quad (2.2.5)$$

Then the equation

$$\theta(t-t') \Psi(x,t) = i \int G^+(xt, x't') \Psi(x',t') dx' \quad (2.2.6)$$

is the trivial identity  $0=0$  for  $t < t'$  and is same as Eq. (2.2.3)

We must still give a complete formal definition of  $G(xt, x't')$ . So far we have only claimed its existence on the basis of physical arguments. Let us pursue these arguments further in order to develop a better understanding of the propagator approach. Consider first a solution of  $H_0(x)$ . Assuming the motion of  $H_0(x)$  is completely known, (we emphasize here  $H_0(x)$  is not necessarily limited of free particle) and it should not come as a surprise that the corresponding  $H_0(x)$  Green's function  $G_0(xt, x't')$  can be constructed explicitly. If we now introduce an interaction potential,  $G_0(xt, x't')$  should be modified. Let  $V(x_1, t_1)$  represent an interaction potential which is "turned on" for a very brief interval of time  $\Delta t_1$  at  $t < t_1 < t'$ . For times earlier than  $t_1$ , the wave function will be the solution of  $H_0(x)$ :  $\Psi_0(x, t)$ , and the corresponding propagator will be  $G_0(xt, x't')$ . However,  $V(x_1, t_1)$  acts a source of new waves according to the Schrödinger equation

$$\left[ i\hbar \frac{\partial}{\partial t_1} - H_0(x_1, t_1) \right] \Psi(x_1, t_1) = V(x_1, t_1) \Psi(x_1, t_1) \quad (2.2.7)$$

The right-hand side differs from zero in the interval  $\Delta t_1$ . It produces an additional change in  $\Psi(x_1, t_1)$  during  $\Delta t_1$  above that taking place in the absence  $V(x_1, t_1)$ . This additional wave  $\Delta\Psi(x_1, t_1)$  is found by integrating Eq. (2.2.7) to first order in  $\Delta t_1$ :

$$\Delta\Psi(x_1, t_1) = -iV(x_1, t_1)\Psi_0(x_1, t_1)\Delta t_1 \quad (2.2.8)$$

This added wave, by Huygens' principle and Eq. (2.2.3) leads at a future time  $t$  to a new contribution to  $\Psi(x, t)$ , which is

$$\Delta\Psi(x, t) = \int dx_1 G_0(xt, x_1t_1)V(x_1, t_1)\Psi_0(x_1, t_1)\Delta t_1 \quad (2.2.9)$$

Thus the wave  $\Psi(x, t)$  developing from an arbitrary packet  $\Psi_0(x, t)$  in the remote past is:

$$\begin{aligned} \Psi(x, t) &= \Psi_0(x, t) + \int dx_1 G_0(xt, x_1t_1)V(x_1, t_1)\Psi_0(x_1, t_1)\Delta t_1 \\ &= i \int dx' [G_0(xt, x't') + \int dx_1 \Delta t_1 G_0(xt, x_1t_1)V(x_1, t_1)G_0(x_1t_1, x't')] \Psi(x', t') \end{aligned} \quad (2.2.10)$$

comparing with Eq. (2.2.3) we see that the Green's function here is given by

$$G(xt, x't') = G_0(xt, x't') + \int dx_1 \Delta t_1 G_0(xt, x_1t_1)V(x_1, t_1)G_0(x_1t_1, x't') \quad (2.2.11)$$

If we turn on another potential  $V(x_2, t_2)$  for an interval  $\Delta t_2$  at time  $t < t_2 < t_1 < t'$ , the additional contribution to  $\Psi(x, t)$  for  $t > t_2$  is, in analogy to Eq .

(2.2.9)

$$\begin{aligned}\Delta\Psi(x, t) &= \int dx_2 G_0(xt, x_2t_2)V(x_2, t_2)\Psi(x_2, t_2)\Delta t_2 \\ &= i \int dx' dx_2 \Delta t_2 G_0(xt, x_2t_2)V(x_2, t_2) \times \\ &[G_0(x_2t_2, x't') + \int dx_1 \Delta t_1 G_0(x_2t_2, x_1t_1)V(x_1, t_1)G_0(x_1t_1, x't')] \Psi_0(x't') \quad (2.2.12)\end{aligned}$$

The total wave arriving at  $(x, t)$  is then built up by inserting Eq. (2.2.10) for  $\Psi(x_2, t_2)$  in the right hand side of Eq. (2.2.12) and adding the resulting  $\Delta\Psi$  to Eq. (2.2.10)

$$\begin{aligned}\Psi(x, t) &= \Psi_0(x, t) + \int dx_1 \Delta t_1 G_0(xt, x_1t_1)\Psi(x_1, t_1) + \int dx_2 \Delta t_2 G_0(xt, x_2t_2)\Psi_0(x't') \\ &+ \int dx_1 \Delta t_1 dx_2 \Delta t_2 G_0(xt, x_2t_2)V(x_2, t_2)G_0(x_2t_2, x_1t_1)V(x_1, t_1)\Psi(x_1, t_1) \quad (2.2.13)\end{aligned}$$

Without further ado, if there are  $n$  such time intervals when the potential  $V$  is turned on, the wave arriving at  $(x, t)$  will be

$$\begin{aligned}\Psi(x, t) &= \Psi_0(x, t) + \sum_i \int dx_i \Delta t_i G_0(xt, x_i t_i)V(x_i, t_i)\Psi_0(x_i, t_i) \\ &+ \sum_{i>j} \int dx_i \Delta t_i dx_j \Delta t_j V(x_i, t_i)G_0(x_i t_i, x_j t_j)\Psi_0(x_j, t_j) \\ &+ \sum_{i>j>t_k} \int dx_i \Delta t_i dx_j \Delta t_j dx_k \Delta t_k \times \\ &G_0(xt, x_i t_i)V(x_i, t_i)G_0(x_i t_i, x_j t_j)V(x_j, t_j)G_0(x_j t_j, x_k t_k)V(x_k, t_k)\Psi_0(x_k, t_k) + \dots \quad (2.2.14)\end{aligned}$$

By comparison with Eq. (2.2.11) and Eq. (2.2.12) the corresponding expression for the Green's function  $G(xt, x't')$  will be

$$G(xt, x't') = G_0(xt, x't') + \sum_{t_i} \int dx_i \Delta t_i G_0(xt, x't') V(x_i, t_i) G_0(x_i t_i, x't') \Psi_0(x', t')$$

$$+ \sum_{t_i < t_j} \int dx_i \Delta t_i dx_j \Delta t_j G_0(xt, x_i t_i) V(x_i, t_i) G_0(x_i t_i, x_j t_j) V(x_j, t_j) G_0(x_j t_j, x't') + \dots \quad (2.2.15)$$

We may lift the time ordering restrictions  $t_i > t_j$ , etc if we use unperturbed retarded Green's function

$$G_0^+(xt, x't') = \theta(t-t') G_0(xt, x't') \quad (2.2.16)$$

Physically this just means that no Huygens wavelets  $\Delta\Psi$  from the  $i$ th interaction (at time  $t_i$ ) appear until after  $t_i$ .

In the limit of a continuous interaction the sums over time intervals may be replaced by integrals over  $dt$  with the result

$$G^+(xt, x't') = G_0^+(xt, x't') + \int dx_1 dt_1 G_0^+(xt, x_1 t_1) V(x_1, t_1) G_0^+(x_1 t_1, x't')$$

$$+ \int dx_1 dt_1 dx_2 dt_2 G_0^+(xt, x_1 t_1) V(x_1, t_1) G_0^+(x_1 t_1, x_2 t_2) V(x_2, t_2) G_0^+(x_2 t_2, x't') + \dots \quad (2.2.17)$$

This multiple scattering series Eq. (2.2.17) is assumed to converge and may be summed formally to yield

$$G^+(xt, x't') = G_0^+(xt, x't') + \int dx_1 G_0^+(xt, x_1 t_1) V(x_1, t_1) G^+(x_1 t_1, x't') \quad (2.2.18)$$

Eq. (2.2.17) gives us an interaction procedure for finding  $G^+$  in terms of  $V$  and  $G_0^+$  and hence for constructing the wave function  $\Psi(x, t)$  if it is known at an earlier time. In particular, to solve the scattering problem, we must know the wave in the remote future, given a wave packet  $\Psi_0(x', t')$  representing a particle in the remote past approaching the interaction region. In order to define properly the scattering problem,

there should be no interaction at this initial time, so that  $\Psi_0$  is a solution of the Schrödinger equation associated with  $H_0$  which incorporates the required initial conditions.

A mathematically convenient way of accomplishing this is to localize the interaction in time by adiabatically turning off  $V(x, t)$  as  $t \rightarrow -\infty$ ; the exact solution  $\Psi(x, t)$  then approaches  $\Psi_0$  in the remote past and there is no scattered wave. In the future the wave  $\Psi(x, t)$  is given by

$$\Psi(x, t) = \lim_{t' \rightarrow -\infty} i \int dx' G^+(x, t, x', t') \Psi_0(x', t') \quad (2.2.19)$$

Expressing  $G^+$  in terms of  $G_0^+$  by Eq. (2.2.18), we see

$$\begin{aligned} \Psi(x, t) &= \lim_{t' \rightarrow -\infty} i \int dx' [G_0^+(x, t, x', t') + \int dx_1 G_0^+(x, t, x_1, t_1) V(x_1, t_1) G^+(x_1, t_1, x', t')] \Psi_0(x', t') \\ &= \Psi_0(x, t) + \int dx_1 G_0^+(x, t, x_1, t_1) V(x_1, t_1) \Psi(x_1, t_1) \end{aligned} \quad (2.2.20)$$

We have really not solved anything, since the unknown  $\Psi$  appears under the integral on the right. However, we do have a formulation which includes the desired boundary conditions and which affords an immediate approximation procedure if the perturbing potential  $V$  is weak. For example, to the second order the wave function  $\Psi$  can be written:

$$\begin{aligned} \Psi(x, t) &= \Psi_0(x, t) + \int_{-\infty}^t dx_1 dt_1 G_0^+(x, t, x_1, t_1) V(x_1, t_1) \Psi_0(x_1, t_1) \\ &+ \int_{-\infty}^t dx_2 dt_2 \int_{-\infty}^{t_2} dx_1 dt_1 G_0^+(x, t, x_2, t_2) V(x_2, t_2) G_0^+(x_2, t_2, x_1, t_1) V(x_1, t_1) \Psi_0(x_1, t_1) + \dots \end{aligned} \quad (2.2.21)$$

We can find the equation for  $G^+$  by operating on Eq. (2.2.6) with  $i\partial/\partial t - 1/\hbar H$ ,

where  $H$  is total Hamiltonian defined in Eq. (2.2.5). It is necessary to make use of the relation

$$\frac{d}{d\tau}\theta(\tau) = \delta(\tau) \quad (2.2.22)$$

which follows from Eq. (2.2.1). The result is

$$i\delta(t-t')\Psi(x, t) = i \int \left[ i\frac{\partial}{\partial t} - \frac{1}{\hbar}H \right] G^+(xt, x't') \Psi(x', t') dx' \quad (2.2.23)$$

where use has been made of Eq. (2.2.1). This equation shows that the right side must be proportional to  $\delta(t-t')$ , so that only  $\Psi(x', t')$  can be an arbitrary function of  $x'$  at any particular time  $t'$ , the rest of the integrand of the right side must be proportional to  $\delta(x-x')$ . We then conclude that

$$\left[ i\frac{\partial}{\partial t} - \frac{1}{\hbar}H(x, t) \right] G^+(xt, x't') = \delta(x-x') \delta(t-t') \quad (2.2.24)$$

The integral and differential equations for the Green's function, obtained above, can be written in a operator form that is instructive. Eq. (2.2.17) may be written:

$$G^+ = G_0^+ + \hbar^{-1}G_0^+VG_0^+ + \hbar^{-2}G_0^+VG_0^+VG_0^+ + \dots \quad (2.2.25)$$

In similar fashion, we may write Eq. (2.2.18) in the form

$$G^+ = G_0^+ + \hbar^{-1}G_0^+VG^+ \quad (2.2.26)$$

Again, the differential equation Eq. (2.2.24) may be written:

$$\left[ i\frac{\partial}{\partial t} - \frac{1}{\hbar}H \right] G^+ = 1 \quad (2.2.27)$$

On omitting the  $V$  term in  $H$ , we obtain in place of Eq. (2.2.27)

$$\left( i \frac{\partial}{\partial t} - \frac{1}{\hbar} H_0 \right) G_0^{\dagger} = 1 \quad (2.2.28)$$

### 2.3 Inelastic Steady State via Green's Function

In experiment, the tunneling current are usually measured in a steady state, that is, when maintaining a steady incident wave we measure the scattering wave which brings the information of the interaction inside of structure. For the situation of inelastic scattering such as electron-optical-phonon interaction, the carrier current keeps emission and absorption of phonons in a steady state, which leads to multi-channel transmission and reflection. Thus the steady state solution can be expressed in time dependent components

$$\Psi(x, t) = \sum_n \psi_n(x) e^{-\frac{i}{\hbar}(E \pm n\hbar\omega)t} \quad (2.3.1)$$

where  $E$  is carrier incident energy, (at present we assume a monochromatic incident wave, for a wave packet we need a integral over energy  $E$ )  $\hbar\omega$  is optical phonon and  $\psi(x)$  is only space dependent.

From Green's function formula given in sec. 2.2, the electron wave function can be written in integral form

$$\Psi(x, t) = \Psi_0(x, t) + \int_{-\infty}^t dt_1 \int dx_1 G_0^{\dagger}(x, t, x_1, t_1) V(x_1, t_1) \Psi(x_1, t_1) \quad (2.3.1)$$

where  $G_0^{\dagger}(x, t, x_1, t_1)$  is the unperturbed retarded Green's function that vanishes when  $t < t'$ . Here  $\Psi_0(x, t)$  is the unperturbed wave function with a steady incident wave from region I at energy  $E$ ,  $\Psi_0(x, t) = \psi_0(x) \exp(-\frac{i}{\hbar}Et)$ , and  $V(x, t)$  is the electron-phonon interaction potential. At present we assume a one dimensional optical deformation

interaction which can be written as:

$$V(x,t) = [V(x)e^{-i\omega t} + V(x)^\dagger e^{i\omega t}] \theta(x+d_l) \theta(d_r-x), \quad V(x) = \sum_q M(q) e^{iqx} a_q, \quad (2.3.2)$$

$\theta(x)$  is defined in Eq. (2.2.5),  $q$  is phonon momentum,  $M(q)$  is electron-optical-phonon interaction matrix and  $a_q$  is phonon creation operators.

We need to handle the integral over time in Eq. (2.2.21). Since the time dependence of interaction potential  $V$  and unperturbed electron wave function is clear, we only need to find what is time dependence of unperturbed retarded Green's function  $G_0^\pm(xt, x't')$ . Let's first study a general case. Supposing a complete and orthogonal set of eigenfunction associated with a given Hamiltonian  $H$  is known, we can write any state as

$$\Psi(x,t) = \sum_n A_n(t) \phi_n(x) \quad (2.3.3)$$

where  $\phi_n(x)$  is the  $n$ th eigenfunction of  $H(x)$  and  $A_n(t)$  satisfies

$$A_n(t) = \int dx \Psi(x,t) \phi_n(x) \quad (2.3.4)$$

We put Eq. (2.3.3) in Schrödinger equation associated with  $H$  and get:

$$i\hbar \frac{d}{dt} A_n(t) = E_n A_n(t)$$

which yields

$$A_n(t) = A_n(t') e^{-iE_n(t-t')/\hbar}$$

Thus, if  $\Psi(x,t)$  is known at time  $t=t'$ , the solution at any time  $t$  is given

$$\Psi(x,t) = \sum_n A_n(t') e^{-iE_n(t-t')/\hbar} \phi_n(x) \quad A_n(t') = \int dx' \Psi(x',t') \phi_n(x') \quad (2.3.5)$$

The wave function at time  $t$  can be written

$$\Psi(x,t) = \int dx' \left[ \sum_n \phi_n(x') \phi_n(x) e^{-iE_n(t-t')/\hbar} \right] \Psi(x',t') \quad (2.3.6)$$

From Green's function definition in Eq. (2.2.3), we can figure out

$$G(xt, x't') = -i \sum_n \phi_n^*(x') \phi_n(x) e^{-iE_n(t-t')/\hbar} \quad (2.3.7)$$

Remember that the summation should be taken over all the eigenstates of  $H$ . If we have continue states the summation should be changed to integral.

With the help of  $G(xt, x't')$  we can write retarded Green's function:

$$G^+(xt, x't') = \theta(t-t') G(xt, x't') = -i \theta(t-t') \sum_n \phi_n^*(x') \phi_n(x) e^{-iE_n(t-t')/\hbar} \quad (2.3.8)$$

Since the form above for  $G^+(xt, x't')$  resembles a Fourier expression in the time difference  $t-t'$ , the possibility of separating out the time dependence by expression  $\theta(t-t')$  as a Fourier expansion suggests itself. We now show that this has the form

$$\theta(\tau) = \lim_{\epsilon \rightarrow 0^+} -\frac{1}{2\pi i} \int_{-\infty}^{\infty} e^{-i\omega\tau} \frac{d\omega}{\omega+i\epsilon} \quad (2.3.9)$$

We know first that the derivative of this with respect to  $\tau$  is

$$\frac{1}{2\pi} \int_{-\infty}^{\infty} e^{-i\omega\tau} d\omega$$

which is equal to  $\delta(\tau)$ . This result is independent of whether the denominator of the integrand in Eq. (2.3.9) is chosen to be  $\omega+i\epsilon$  or  $\omega-i\epsilon$ , that is, whether the pole in the integrand is below or above the contour of integration, which is along the real axis. However, the two choices corresponds to a pole at  $-i\epsilon$ . For  $\tau < 0$ , this contour may be

completed with an infinite semicircle in the positive imaginary half plane, since the exponential becomes vanishingly small there and contributes nothing to the integral; then  $\theta(\tau)=0$ . For  $\tau>0$ , the contour may be completed with an infinite semicircle in the negative imaginary half plane, and the integral is equal to  $-2\pi i$  times the residue of the integrand at the only pole ( $\omega=-i\epsilon$ ) that lies within the contour. Then, in the limit  $\epsilon\rightarrow 0^+$ ,  $\theta(\tau)=1$ . Substituting Eq. (2.3.9) in Eq. (2.3.8) we can write outgoing Green's function in Fourier integral form as:

$$G_0^+(x, t, x', t') = \frac{1}{2\pi} \int_{-\infty}^{\infty} dE G_0^+(x, x', E) e^{-\frac{i}{\hbar}E(t-t')}, \quad G_0^+(x, x', E) = \lim_{\epsilon \rightarrow 0^+} \sum_{k, \alpha} \frac{\Phi_{k\alpha}^*(x') \Phi_{k\alpha}(x)}{E - E_k + i\epsilon}, \quad (2.3.10)$$

where  $\Phi_{k\alpha}(x)$  is a complete, orthogonal set of eigenfunction associated with the Hamiltonian  $H_0(x)$  and  $k = \sqrt{2mE_k}/\hbar$ , whose value goes from zero to positive infinity,  $m$  is the constant electron effective mass in regions I and III,  $\alpha$  indexes the possibly two degenerate modes at each eigenvalue  $E_k$ , for one dimension case and  $V_0(x)=0$  at  $x \rightarrow \pm\infty$ , this degeneracy is at most two.

Applying the iteration method to Eq. (2.3.1) we can develop the electron wave function as a power expansion in the electron-phonon interaction potential:

$$\Psi(x, t) = \Psi_0(x, t) + \Psi_1(x, t) + \Psi_2(x, t) + \dots \quad (2.3.11)$$

Since that  $G_0^+(xt, x_1t_1)$  vanishes when  $t < t_1$ , thus we can let upper limit  $t$  in Eq. (2.3.1) go to infinity. The first order electron wave function is then:

$$\Psi_1(x, t) = e^{-\frac{i}{\hbar}(E+\hbar\omega)t} \int dx_1 G_0^+(x, x_1, E+\hbar\omega) V(x_1) \Psi_0(x_1)$$

$$+ e^{-\frac{i}{\hbar}(E-\hbar\omega)t} \int dx_1 G_0^+(x, x_1, E-\hbar\omega) V^\dagger(x_1) \psi_0(x_1) . \quad (2.3.12)$$

The first term above stands for the electron absorption of a phonon followed by a jump to an upper sideband from the incident energy level, the second term stands for electron emission of a phonon followed by drop to a lower sideband from the incident energy level. The second order electron wave function can be obtained in the same way as:

$$\begin{aligned} \Psi_2(x, t) = & e^{-\frac{i}{\hbar}(E+2\hbar\omega)t} \int dx_2 G_0^+(x, x_2, E+2\hbar\omega) V(x_2) \int dx_1 G_0^+(x_2, x_1, E+\hbar\omega) V(x_1) \psi_0(x_1) \\ & + e^{-\frac{i}{\hbar}Et} \int dx_2 G_0^+(x, x_2, E) V(x_2) \int dx_1 G_0^+(x_2, x_1, E+\hbar\omega) V^\dagger(x_1) \psi_0(x_1) \\ & + e^{-\frac{i}{\hbar}Et} \int dx_2 G_0^+(x, x_2, E) V^\dagger(x_2) \int dx_1 G_0^+(x_2, x_1, E-\hbar\omega) V(x_1) \psi_0(x_1) \\ & + e^{-\frac{i}{\hbar}(E-2\hbar\omega)t} \int dx_2 G_0^+(x, x_2, E-2\hbar\omega) V^\dagger(x_2) \int dx_1 G_0^+(x_2, x_1, E-\hbar\omega) V^\dagger(x_1) \psi_0(x_1) . \end{aligned} \quad (2.3.13)$$

The first term stands for two phonon absorption with a jump to the  $E+2\hbar\omega$  sideband. The second and third terms stand for absorption (emission) a phonon, jumping (dropping) to  $E \pm \hbar\omega$  sideband, then returning to the original state via emission (absorption). The last term stands for two phonon emission with a drop to the  $E-2\hbar\omega$  sideband.

#### 2.4 Scattering $S$ Matrix of Lattice Potential $V_0$

For the one dimensional scattering problem (elastic scattering), the particle could be incident either from the right or from the left. The solution of the Schrödinger equation are now oscillatory in both region I and region III; hence to each value of the

energy correspond two linearly independent, degenerate eigenfunctions. We can write the solution in a composition of plane wave in these two regions as:

$$\phi(x) = \begin{cases} A e^{ikx} + B e^{-ikx} & \text{if } x \leq -d_l \\ F e^{ikx} + G e^{-ikx} & \text{if } x \geq d_r \end{cases} \quad (3.4.1)$$

where  $\hbar k = \sqrt{2mE}$ ,  $m$  is electron effective mass in region I and region III. The four coefficients  $A$ ,  $B$ ,  $F$  and  $G$  are determined by boundary conditions together with incident source. An equivalent representation expresses the coefficients  $B$  and  $F$  of the outgoing waves in terms of the coefficients  $A$  and  $G$  of the incoming waves by the  $S$  matrix relation

$$\begin{bmatrix} B \\ F \end{bmatrix} = - \begin{bmatrix} S_{11} & S_{12} \\ S_{21} & S_{22} \end{bmatrix} \begin{bmatrix} A \\ G \end{bmatrix} \quad (3.4.2)$$

The representation in terms of the scattering  $S$  matrix is readily generalized to three-dimensional situations, and the symmetry properties are best formulated in terms of the  $S$  matrix.

In one-dimensional stationary state the probability current density must be independent of  $x$

$$\frac{\partial j(x)}{\partial x} = 0 \quad j(x) = \frac{\hbar}{2mi} \left[ \phi^* \frac{d\phi}{dx} - \frac{d\phi^*}{dx} \phi \right] \quad (3.4.3)$$

where  $\phi$  is a stationary solution of Schrödinger equation. Applying expression above to Eq. (3.4.1), we obtain:

$$|A|^2 - |B|^2 = |F|^2 - |G|^2 \quad \text{or} \quad |B|^2 + |F|^2 = |A|^2 + |G|^2 \quad (3.4.4)$$

as expected, since  $|A|^2$  and  $|F|^2$  measure the probability flow to the right, while

$|B|^2$  and  $|G|^2$  measure the flow in the opposite direction. Using matrix notation, we can write this as

$$[B^* \ F^*] \begin{bmatrix} B \\ F \end{bmatrix} = [A^* \ G^*] \tilde{S}^* S \begin{bmatrix} A \\ G \end{bmatrix} = [A^* \ G^*] \begin{bmatrix} A \\ G \end{bmatrix} \quad (3.4.5)$$

where  $\tilde{S}$  denotes the transpose matrix of  $S$ , and  $S^*$  the complex conjugate. It follows that  $S$  must obey the condition

$$\tilde{S}^* S = I \quad (3.4.6)$$

with  $I$  denoting the unit matrix in two dimensions. If the Hermitian conjugate  $S^+$  of a matrix  $S$  is defined by

$$S^+ = \tilde{S}^* = \begin{bmatrix} S_{11}^* & S_{12}^* \\ S_{21}^* & S_{22}^* \end{bmatrix} \quad (3.4.7)$$

Eq. (3.4.6) implies the statement that the inverse of  $S$  must be the same as its Hermitian conjugate. Such a matrix is said to be unitary.

The elements of the matrix  $S$  are therefore subject to the following constraints:

$$|S_{11}| = |S_{22}| \quad \text{and} \quad |S_{12}| = |S_{21}| \quad (3.4.8)$$

$$|S_{11}|^2 + |S_{12}|^2 = 1 \quad (3.4.8)$$

and

$$S_{11} S_{12}^* + S_{21} S_{22}^* = 0 \quad (3.4.9)$$

Since the potential is real, the Schrödinger equation has the time-reversed solution

$$i\hbar \frac{\partial \phi^*(x, -t)}{\partial t} = -\frac{\hbar^2}{2m} \frac{\partial^2}{\partial x^2} \phi^*(x, -t) + V_0 \phi(x, -t) \quad (3.4.10)$$

The behavior of the wave equation exhibited by Eq. (3.4.10) is called its invariance under time reversal. For a stationary wave function, invariance under time reversal implies that if  $\phi(x)$  is a stationary wave function,  $\phi^*(x)$  is also one. Hence, it follows that, if  $\phi(x)$  is a nondegenerate solution,  $\phi(x)$  must be real, except for an arbitrary constant complex factor.

According to Eq. (3.4.1) we can write its time-reversed solution

$$\phi_1(x) = \begin{cases} A^* e^{-ikx} + B^* e^{ikx} & \text{if } x \leq -d_l \\ F^* e^{-ikx} + G^* e^{ikx} & \text{if } x \geq d_r \end{cases} \quad (3.4.11)$$

Comparison of this solution with Eq. (3.4.1) shows that effectively the directions of motion have been reversed and the coefficient  $A$  has been interchanged with  $B^*$ , and  $F$  with  $G^*$ . Hence, in Eq. (3.4.2) we may make the replacements  $A \leftrightarrow B^*$  and  $F \leftrightarrow G^*$ , and obtain an equally valid equation

$$\begin{bmatrix} A^* \\ G^* \end{bmatrix} = - \begin{bmatrix} S_{11} & S_{12} \\ S_{21} & S_{22} \end{bmatrix} \begin{bmatrix} B^* \\ F^* \end{bmatrix} \quad (3.4.12)$$

Eq. (3.4.12) and Eq. (3.4.2) can be combined to yield the condition

$$S^* S = I \quad (3.4.13)$$

This condition in conjunction with the unitarity relation Eq. (3.4.6) implies that the  $S$  matrix must be symmetric as a consequence of time reversal symmetry. Since that  $k$  appears in the Schrödinger equation only quadratically, with the same method of deriving Eq. (3.4.6) we have

$$S(k)S(-k) = I \quad (3.4.14)$$

If the potential is an even function of  $x$ , another solution is obtained by replacing  $x$  in Eq. (3.4.1) by  $-x$ . The substitution gives

$$\phi_2(x) = \begin{cases} A e^{-ikx} + B e^{ikx} & \text{if } x > d_l \\ F e^{-ikx} + G e^{ikx} & \text{if } x < -d_r \end{cases} \quad (3.4.15)$$

If  $Ge^{ikx}$  is the wave incident on the barrier from the left,  $Be^{ikx}$  is the transmitted and  $Fe^{-ikx}$  the reflected wave in Eq. (3.4.15).  $Ae^{-ikx}$  is incident from the right. Hence, in Eq. (3.4.2) we may make the replacements  $A \leftrightarrow G$  and  $B \leftrightarrow F$ , and obtain

$$\begin{bmatrix} F \\ B \end{bmatrix} = - \begin{bmatrix} S_{11} & S_{12} \\ S_{21} & S_{22} \end{bmatrix} \begin{bmatrix} G \\ A \end{bmatrix} \quad (3.4.16)$$

## 2.5 Complete Set via $S$ matrix

In order to construct a complete and orthogonal set of  $H_0(x)$  via  $S$  matrix, we define a new matrix  $U$

$$S = U \times U = U^2 = e^{-2\Delta} \quad (2.5.1)$$

From  $S$  matrix properties in Sec.2.4 we have  $U$  matrix properties:

$$U^+ U = I \quad U^* U = I \quad U(-k)U(k) = I \quad (2.5.2)$$

We construct a complete eigenfunction set of  $H_0(x)$  at a given energy  $E_k$ , via  $U$  matrix elements

$$\Phi_{k\alpha}(x) = \begin{cases} \frac{1}{\sqrt{2\pi}} [U_{l\alpha}^*(k)e^{ikx} - U_{\alpha l}(k)e^{-ikx}] & \text{if } x \leq -d_l \\ A_{k\alpha} \phi_{E_k}^1(x) + B_{k\alpha} \phi_{E_k}^2(x) & \text{if } -d_l < x < d_r \\ \frac{1}{\sqrt{2\pi}} [U_{r\alpha}^*(k)e^{-ikx} - U_{\alpha r}(k)e^{ikx}] & \text{if } x \geq d_r \end{cases} \quad (2.5.3)$$

$$U = \begin{bmatrix} U_{ll} & U_{lr} \\ U_{rl} & U_{rr} \end{bmatrix}, \quad (2.5.4)$$

where  $\phi_{E_k}^1(x)$ , and  $\phi_{E_k}^2(x)$  are two independent solutions of  $H_0(x)$  in  $-d_l < x < d_r$ .  $A_{k\alpha}$  and  $B_{k\alpha}$  are two  $k$  (energy) dependent coefficients which are determined by matching the wave function at  $x=d_r$ . At present, we limit ourselves to the absence of a true bound state case. Thus, the  $S$  matrix is analytic in the upper  $k$  plane.<sup>11</sup> With the help of analytic properties of  $S$  matrix, It is easy to show the completeness and orthogonality in the form:

$$\sum_{\alpha} \int_0^{\infty} dk \Phi_{k\alpha}^*(x') \Phi_{k\alpha}(x) = \delta(x-x'), \quad \int_{-\infty}^{\infty} dx \Phi_{k'\alpha'}^*(x) \Phi_{k\alpha}(x) = \delta_{\alpha'\alpha} \delta(k'-k). \quad (2.5.5)$$

## 2.6 Unperturbed Retarded Green's Function

The greatest difficulty in Green Function method is how to construct a  $G_0^+(x, x', E_0)$  with out-going boundary condition, in a non uniform space. For uniform space, since we can choose plane wave as our complete set, it is obvious that there are two poles in Eq.(2.3.10), one slightly above the real axis near  $k$  and the other is a little bellow real axis near  $k$ . These two singularities are easy to handle by choosing some contour path in complex  $k$  space. For one dimensional case we can write

$$G_0^+(x, x', E_k) = \frac{1}{2\pi} \frac{2m}{\hbar^2} \int_{-\infty}^{\infty} dk' \frac{e^{ik'(x-x')}}{k^2 - k'^2 + i\epsilon} \quad (2.6.1)$$

Since

$$\int_{-\infty}^{\infty} dk' \frac{e^{ik'(x-x')}}{k^2 - k'^2 + i\epsilon} = -\frac{1}{2k} \int_{-\infty}^{\infty} dk' e^{ik'(x-x')} \left( \frac{1}{k'-k-i\epsilon} - \frac{1}{k'+k+i\epsilon} \right)$$

the integral path contour above may be completed with an infinite semicircle in the

positive imaginary half plane if  $x > x'$  and opposite if  $x < x'$ , which results

$$G_0^+(x, x', E_k) = -\frac{im}{\hbar^2 k} e^{ik|x-x'|} \quad (2.6.2)$$

With the same method, the three dimensional retarded Green's function can be written

$$G_0^+(\mathbf{R}, \mathbf{R}', E_k) = -\frac{m}{2\pi\hbar^2} \frac{e^{ik|\mathbf{R}-\mathbf{R}'|}}{|\mathbf{R}-\mathbf{R}'|} \quad (2.6.3)$$

where  $\mathbf{R}$  is three dimensional coordinate.

Dealing with non uniform space requires care for it is not easy to discuss the analytic properties in Eq.(2.3.10) before the integral over  $k$  is carried out. Taking the combination of barriers as an example, we will have some functions like  $q = \sqrt{E^2 - V}$  which contributes cut in complex  $k$  plane. For more complicated case, such as with applied electric field, the electron wave function should be Airy function and it is also not easy to handle with when we carry out the integral over  $k$  in Eq.(2.3.10). For some special potential with only numerical electron wave function solution, it looks nearly impossible to discuss the analytic properties of Eq.(2.3.10).

Our method to construct the retarded unperturbed Green's function in a non uniform potential is as follow:

We first use the complete set given in Eq. (2.5.3) to construct  $G_0^+(x, x', E)$  for both  $x$  and  $x'$  are outside of interaction region. Since the  $S$  matrix is analytic in the upper half complex  $k$  plane, so we can directly carry out integral over  $k$  in Eq. (2.3.10) and get  $G_0^+(x_I, x'_I, E)$  and  $G_0^+(x_{III}, x'_{III}, E)$  in analytic expression. Second, we use two independent solution of Hamiltonian  $H_0(x)$  at each energy level  $E_k$  to construct a general Green's function in which there are two coordinate dependent coefficients being determined later. Third, we match the general Green's function expression at the

boundary with the Green's function outside of interaction region and fix all coefficients.

Let us first calculate unperturbed retarded Green's function for both  $x$  and  $x'$  at region III. In order to carry out integral in Eq. (2.3.10), we need summation over degeneracy  $\alpha$  which yields

$$\sum_{\alpha} \Psi_{k\alpha}^*(x'_{III}) \Psi_{k\alpha}(x_{III}) = \frac{1}{2\pi} \left[ e^{-ik(x_{III}-x'_{III})} + e^{ik(x_{III}-x'_{III})} - S_{rr}(k) e^{ik(x_{III}+x'_{III})} - S_{rr}^*(k) e^{-ik(x_{III}+x'_{III})} \right] \quad (2.6.4)$$

then, we analytically expand to  $-k$  space and get:

$$G_0^+(x_{III}, x'_{III}, E) = \frac{1}{2\pi} \int_{-\infty}^{\infty} dk' \frac{e^{ik'(x_{III}-x'_{III})}}{E-E_{k'}+i\epsilon} - \frac{1}{2\pi} \int_{-\infty}^{\infty} dk' \frac{S_{rr}(k) e^{ik'(x_{III}+x'_{III})}}{E-E_{k'}+i\epsilon} \quad (2.6.5)$$

Using the analytic property of  $S(k)$ , we can get

$$G_0^+(x_{III}, x'_{III}, E) = -\frac{im}{\hbar^2 k} \left[ e^{ik|x_{III}-x'_{III}|} - S_{rr}(k) e^{ik(x_{III}+x'_{III})} \right] \quad x_{III}, x'_{III} \geq d_r. \quad (2.6.6)$$

The first term above is the Green's function expression in uniform space compared with that in Eq. (2.6.2). The second term comes from non-uniform potential contribution, which is  $x_{III}+x'_{III}$  dependent. With the same method, we can get unperturbed retarded Green's function for both  $x$  and  $x'$  at region I

$$\hat{G}_0^+(x_I, x'_I, E) = -\frac{im}{\hbar^2 k} \left[ e^{ik|x_I-x'_I|} - S_{ll}(k) e^{-ik(x_I+x'_I)} \right] \quad x_I, x'_I \leq -d_l. \quad (2.6.7)$$

In order to get the unperturbed retarded Green's function in whole region, we need a general expression of  $G_0^+(x, x', E)$ . Since  $G_0^+(x, x', E)$  satisfies:

$$\hat{L}(x) G_0^+(x, x', E) = \delta(x-x'), \quad \hat{L}(x) = E - H_0(x) + i\epsilon, \quad (2.6.8)$$

the Green's function can also be written as:<sup>12</sup>

$$G_0^+(x, x', E) = \begin{cases} a_E^1(x') \phi_E^1(x) + a_E^2(x') \phi_E^2(x) & \text{if } x > x' \\ b_E^1(x') \phi_E^1(x) + b_E^2(x') \phi_E^2(x) & \text{if } x < x' \end{cases} \quad (2.6.9)$$

where  $\phi_E^1(x)$  and  $\phi_E^2(x)$  are any two independent solutions of Hamiltonian  $H_0(x)$ . There are four  $x'$  dependent functions  $a_E^1(x')$ ,  $a_E^2(x')$ ,  $b_E^1(x')$  and  $b_E^2(x')$ . Two of them are determined by the conditions of Green's function continuity at  $x=x'$  and the appropriate derivative discontinuity<sup>12</sup> at  $x=x'$ , which is shown as follows.

The unperturbed retarded Green's function itself should be continuity everywhere, so we have

$$\lim_{\varepsilon \rightarrow 0^+} G_0^+(x'+\varepsilon, x', E) = \lim_{\varepsilon \rightarrow 0^+} G_0^+(x'-\varepsilon, x', E) \quad (2.6.10)$$

Because of Delta function source at right in Eq. (2.6.8), the unperturbed retarded Green's function also satisfies

$$\lim_{\varepsilon \rightarrow 0^+} \frac{\hbar^2}{2} \left[ \frac{1}{m(x)} \frac{\partial}{\partial x} G_0^+(x, x', E) \Big|_{x=x'+\varepsilon} - \frac{1}{m(x)} \frac{\partial}{\partial x} G_0^+(x, x', E) \Big|_{x=x'-\varepsilon} \right] = 1 \quad (2.6.11)$$

With these two equations we can fix  $a_E^1(x')$  and  $a_E^2(x')$  and get

$$G_0^+(x, x', E) = \begin{cases} b_E^1(x') \phi_E^1(x) + b_E^2(x') \phi_E^2(x) + \frac{1}{\Pi_E(x')} [\phi_E^2(x') \phi_E(x) - \phi_E^1(x') \phi_E^2(x)] & \text{if } x > x' \\ b_E^1(x') \phi_E^1(x) + b_E^2(x') \phi_E^2(x) & \text{if } x < x' \end{cases} \quad (2.6.12)$$

where

$$\Pi_E(x') = \frac{\hbar^2}{2m(x')} \begin{bmatrix} \phi_E^1(x')' & \phi_E^2(x')' \\ \phi_E^1(x') & \phi_E^2(x') \end{bmatrix},$$

$\phi_E^i(x')$  is derivative at  $x'$ . The remaining two  $x'$  coefficients  $b_E^1(x')$  and  $b_E^2(x')$  are determined by the boundary condition at the points of material discontinuity. Since the conjugate Green's function obeys:

$$\hat{L}^*(x') G_0^{+*}(x, x', E) = \delta(x - x'), \quad (2.6.13)$$

we can construct  $G_0^+(x, x', E)$  for  $x > d_r$ ,  $x' < d_r$  in terms of the conjugate of the eigenfunctions in Eq (2.6.13):

$$G_0^+(x_{III}, x'_{II}, E) = f_E^1(x_{III}) \phi_E^{1*}(x'_{II}) + f_E^2(x_{III}) \phi_E^{2*}(x'_{II}) \quad x_{III} > d_r, x'_{II} < d_r. \quad (2.6.14)$$

where  $f_E^1(x_{III})$  and  $f_E^2(x_{III})$  are determined when we match Eq. (2.6.6) and Eq. (2.6.14) at  $x'_{III} = x'_{II} = d_r$ , in value and mass-normalized derivatives:

$$G_0^+(x_{III}, x'_{II}, E) \big|_{x'_{II}=d_r^-} = G_0^+(x_{III}, x'_{III}, E) \big|_{x'_{III}=d_r^+} \quad (2.6.15)$$

$$\frac{1}{m(x')} \frac{\partial}{\partial x'} G_0^+(x_{III}, x'_{II}, E) \big|_{x'_{II}=d_r^-} = \frac{1}{m(x')} \frac{\partial}{\partial x'} G_0^+(x_{III}, x'_{III}, E) \big|_{x'_{III}=d_r^+} \quad (2.6.16)$$

above two equations yields:

$$G_0^+(x_{III}, x'_{II}, E) = \frac{im}{\hbar^2 k} e^{ikx_{III}} [\xi_E^2 \phi_E^{1*}(x'_{II}) - \xi_E^1 \phi_E^{2*}(x'_{II})], \quad (2.6.17)$$

where

$$\xi_E^i = -[e^{-ikd_r} h_-^{i*}(E) + e^{ikd_r} h_+^{i*}(E) S_{rr}(E)], \quad h_{\pm}^i(E) = \frac{i\tilde{k}\phi_E^i(d_r) \pm \phi_E^i(d_r)'}{\Delta_E},$$

$$\Delta_E = \begin{bmatrix} \phi_E^1(d_r)' & \phi_E^2(d_r)' \\ \phi_E^1(d_r) & \phi_E^2(d_r) \end{bmatrix},$$

where  $\tilde{k} = k \frac{m_{II}(d_r)}{m}$  and  $\phi_E^i(d_r)'$  is derivative at  $x = d_r$ . Finally we use Eq. (2.6.12) as

$G_0^+(x_{II}, x'_{II}, E)$  for both  $x, x'$  in region II. By matching Eq. (2.6.12) and Eq. (2.6.17) and their mass-normalized derivatives at  $x_{II} = x_{III} = d_r$ :

$$G_0^+(x_{II}, x'_{II}, E) \Big|_{x_{II}=d_r^-} = G_0^+(x_{III}, x'_{II}, E) \Big|_{x_{III}=d_r^+} \quad (2.6.18)$$

$$\frac{1}{m(x)} \frac{\partial}{\partial x} G_0^+(x_{II}, x'_{II}, E) \Big|_{x_{II}=d_r^-} = \frac{1}{m(x)} \frac{\partial}{\partial x} G_0^+(x_{III}, x'_{II}, E) \Big|_{x_{III}=d_r^+} \quad (2.6.19)$$

thus, we determine the remaining two  $x'$  dependent functions in Eq. (2.6.12). The final result is:

$$G_0^+(x_{II}, x'_{II}, E) = \begin{cases} G_0^+(d_r, x'_{II}, E) [h_-^2(E) \phi_E^1(x_{II}) - h_-^1(E) \phi_E^2(x_{II})] & x_{II} > x'_{II} \\ G_0^+(d_r, x'_{II}, E) [h_-^2(E) \phi_E^1(x_{II}) - h_-^1(E) \phi_E^2(x_{II})] + F & x_{II} < x'_{II} \end{cases} \quad (2.6.20)$$

$$F = \frac{m_{II}(d_r)}{m} \frac{2ik}{\Delta_E} [\phi_E^2(x'_{II}) \phi_E^1(x_{II}) - \phi_E^1(x'_{II}) \phi_E^2(x_{II})]$$

With the same method, we can construct  $G_0^+(x_I, x_{II}, E)$ . Thus we determine the unperturbed retarded Green's function everywhere. Our present unperturbed retarded Green's function is limited to the situation which there is no true bound state (a true bound state requires the presence of one pole on the real axis of  $k$  in Eq. (2.3.10). The Green's function would then be summed over those poles).

For the 3D case, since the  $y$ - $z$  plane in many devices can be treated uniformly, we can choose a plane wave for the  $y$ - $z$  dependence multiplied by Eq. (2.5.3) as a new complete set to construct 3D unperturbed retarded Green's function which involve an integral over transverse momentum.<sup>6</sup>

## 2.7 Results and Discussion

As a first application, we calculate electron tunneling through a double barrier to second order in the optical-deformation potential. The current (including transmitted and reflected) is summed over three energy channels:  $E$  and  $E \pm \hbar\omega$  to maintain unitarity. The incident energy channel  $E$  is modified by the cross term  $\Psi_0 \Psi_2$ , a feed-back mechanism. Assuming optical phonons are in equilibrium at the lattice temperature  $T_L$  with phonon occupation number

$$N = [\exp(\hbar\omega/k_B T_L) - 1]^{-1} . \quad (2.7.1)$$

We should make an average over the phonon assemble to obtain the current:

$$\langle j \rangle = \frac{\hbar^2}{2mi} \left\langle \Psi^* \frac{d\Psi}{dx} - \frac{d\Psi^*}{dx} \Psi \right\rangle = \langle \Psi^+ \Psi \rangle \quad (2.7.2)$$

So we need calculate from Eq. (2.3.12) and Eq. (2.3.13)

$$\langle V^+(x') V(x) \rangle = \sum_q |M(q)|^2 e^{iq(x-x')} N \quad (2.7.3)$$

For the optical-deformation potential, we assume  $M(q)$  of Eq (2.) is  $q$  independent for simplicity. Thus we have

$$\langle V^+(x') V(x) \rangle = |M|^2 N \frac{L}{2\pi} \frac{2\sin\left(\frac{\pi(x-x')}{a}\right)}{x-x'} \quad (2.7.4)$$

where

$$L = d_l + d_r$$

Since the ratio of the length of region II  $L$  and the lattice constant  $a$  is large, the summation over all phonon modes of  $e^{iq(x-x')}$  can be approximated as a delta function.

Thus we get:

$$\langle V(x_1)V^\dagger(x_2) \rangle \approx [ |M|^2 N(d_r+d_l) \delta(x_1-x_2) ], \quad (2.7.5)$$

$$\langle V^\dagger(x_1)V(x_2) \rangle \approx [ |M|^2 (N+1)(d_r+d_l) ] \delta(x_1-x_2). \quad (2.7.6)$$

There is then only one integral over  $x_1$  in calculating the current. Our result for the transmission  $T_{\text{trans}}$  is shown in Fig. 4: the structure parameters are for a GaAs well sandwiched between two  $\text{Al}_{0.3}\text{Ga}_{0.7}\text{As}$  barriers<sup>13</sup>, (with well width 4.5 nm, barrier thickness 2.8 nm, the lattice constant is  $5.65\text{\AA}$ , and optical phonon energy  $\omega$  is 36.2 meV.) The electron-optical-deformation coupling constant is taken as  $g \equiv (|M|/\hbar\omega)^2 = 5.6 \times 10^{-3}$ . At room temperature, phonon assisted resonant peaks appear at  $E_0 \pm \hbar\omega$  with an intensity reduced compared to that of the long wave length approximation.

In conclusion, by use of the steady state and unperturbed retarded Green's function  $G_0^+(x, x', E)$  constructed above, we can calculate electron tunneling in the presence of inelastic scattering. We emphasize that our present formula can be applied to a real phonon system and generalized to the 3D case.

## **Part II: Nonequilibrium transport of an electron-phonon-hole system in a semiconductor quantum well**

### **1 INTRODUCTION**

There has recently been a great deal of interest in the dynamics of the photoexcited electron-hole plasma system in the two-dimensional semiconductor quantum well.<sup>1</sup> A series of recent experiments<sup>2-5</sup> made a good determination of the transport of carriers. The experiment<sup>3</sup> is performed by injection of minority electrons in *p*-doped GaAs layers by the use of picosecond photoexcitation under an arbitrarily applied electric field. They show that the distribution of electrons at high field is found to be "hot" in contrast to that of holes which remains close to room temperature. The energy loss rate of electrons is much larger in the presence of a hole plasma than that of a pure electron system. The weak field mobility of electrons is found to be about  $1500 \text{ cm}^2/\text{V sec}$ . These results provide strong evidence that the electron-hole interaction is important in addition to electron-phonon and hole-phonon interactions. The energy and momentum relaxation rates would be determined by carrier-phonon and electron-hole interactions if rapid thermalization of electrons and holes are assumed<sup>3</sup> by electron-electron and hole-hole collisions. The effects of carrier-phonon interaction have been extensively studied, but until now, few theoretical calculations have been made for an electron-phonon-hole system in a semiconductor quantum well, a quasi-two-dimensional (2D) system.

In this paper, recently developed techniques<sup>6,7</sup> for coupling 2D carriers with phonons are applied to the system of coexisting electrons and holes in GaAs-Ga<sub>1-x</sub>Al<sub>x</sub>As heterojunctions. In such a case, carrier-carrier physical interaction is influenced by all kinds of carriers; thus the renormalized interaction potentials for electron-electron, hole-hole, and electron-hole interaction are derived in the ring diagram approximation. The coupled carrier-carrier potential equations are solved. As far as electron-lattice interaction is concerned, optical phonons dominate above room temperature. The phonons are coupled with quasi-2D electrons via the Fröhlich electron-optical-phonon interaction. The lattice-hole interaction is a little more complicated. This is because of the anisotropy of the valence band structure of GaAs, compared with the sphericity of the conduction band structure. The anisotropic band structure would make not only the polar optical phonons involved in hole scatterings (*s* wave), but also nonpolar optical phonons would induce the hole collisions (*p* wave). Since both electrons and holes “screen” electron-lattice and hole-lattice interactions, we derive these two renormalized potentials in the ring diagram approximation. Using the Liouville equation for the density matrix, we derive the kinetic equations both for the electrons and holes to second order of carrier-carrier and carrier-phonon interactions in the presence of an applied electric field. As suggested by experiments,<sup>2-5</sup> the electron and hole distribution functions are described by the displaced velocity temperature model, for frequent electron-electron and hole-hole collisions establish instant thermalization, which is expressed as electron and hole temperatures  $T_e$  and  $T_h$ . The force and energy balance equations are constructed using the kinetic equations of the carrier density matrix. The force and energy balance equations are solved simultaneously (numerically) in the steady state, which yields  $T_e$ ,  $T_h$ ,  $v_e$ , and  $v_h$  as

functions of the applied electric field. We found that the drift velocity of electrons increases almost linearly with field with a low-field mobility of about  $1700 \text{ cm}^2/\text{V sec}$  due to the extra momentum relaxation to high-density hole plasma via Coulomb scattering. The mobility of holes remains constant at about  $250 \text{ cm}^2/\text{V sec}$  within a wide range up to  $10 \text{ kV/cm}$ . The temperatures  $T_e$  and  $T_h$ , which depend on input power, show that the electrons are more heated by the electric field. In contrast, the holes seem to stay cool, close to room temperature. These results are in reasonable agreement with the experimental measurement.<sup>3</sup> At  $5 \text{ kV/cm}$  or higher, there is a quantitative deviation between our result and experimental data, which indicates that the single subband calculation would be not available for strong electric field.

In Sec.II all kinds of interactions in two dimensions, including electron-hole, electron-phonon, hole-phonon, and carrier-impurity interactions are given. These renormalized potentials are derived by solving the coupled ring diagram approximation equations. In Sec.III, force and energy balance equations of electrons and holes are obtained by use of the Liouville formula for the density operator. The solution of these balance equations is used to evaluate the mobility of carriers and carrier temperature dependence on applied electric field. The detailed results with a brief discussion are presented in Sec.IV.

## 2 SCATTERING MECHANISM

Choosing the complete set of wave functions of electron and hole as:

$$\Psi_{n\mathbf{k}}^e(\mathbf{R}) = \frac{1}{\sqrt{A}} e^{i\mathbf{k}\cdot\mathbf{r}} \xi_n(z) , \quad (2.1)$$

$$\Psi_{mp}^h(\mathbf{R}) = \frac{1}{\sqrt{A}} e^{i\mathbf{p}\cdot\mathbf{r}} \zeta_m(z), \quad (2.2)$$

where  $A$  is the area of the sample,  $\mathbf{R} = (\mathbf{r}, z)$  is the 3D coordinate,  $\mathbf{k}$  and  $\mathbf{p}$  are, respectively, the momentum of electron and hole in the  $x$ - $y$  plane, and  $\xi_n(z)$ ,  $\zeta_m(z)$  are envelope wave functions of the electron and hole in the  $z$  direction. The bare electron-electron, hole-hole, and electron-hole Coulomb interactions in two dimensions can be expressed in matrices  $V_{ee}$ ,  $V_{hh}$ , and  $V_{eh}$ . Their elements are given by:

$$V_{ee}^{n'n,m'm}(q) = \frac{2\pi e^2}{\kappa_0 q A} F_{ee}^{n'n,m'm}(q), \quad (2.3)$$

$$F_{ee}^{n'n,m'm}(q) = \int_{-\infty}^{\infty} dz \int_{-\infty}^{\infty} dz' e^{-q|z-z'|} \xi_n^*(z) \xi_n(z) \xi_m^*(z') \xi_m(z'), \quad (2.4)$$

$$V_{hh}^{n'n,m'm}(q) = \frac{2\pi e^2}{\kappa_0 q A} F_{hh}^{n'n,m'm}(q), \quad (2.5)$$

$$F_{hh}^{n'n,m'm}(q) = \int_{-\infty}^{\infty} dz \int_{-\infty}^{\infty} dz' e^{-q|z-z'|} \zeta_m^*(z) \zeta_m(z) \zeta_n^*(z') \zeta_n(z'), \quad (2.6)$$

$$V_{eh}^{n'n,m'm}(q) = -\frac{2\pi e^2}{\kappa_0 q A} F_{eh}^{n'n,m'm}(q), \quad (2.7)$$

$$F_{eh}^{n'n,m'm}(q) = \int_{-\infty}^{\infty} dz \int_{-\infty}^{\infty} dz' e^{-q|z-z'|} \xi_n^*(z) \xi_n(z) \zeta_m^*(z') \zeta_m(z'), \quad (2.8)$$

where  $\kappa_0$  is the static dielectric constant, and  $\mathbf{Q} = (q, q_z)$  is the 3D momentum exchange.

The renormalization interaction potentials should include screening factors coming both from electrons and holes. The simple physical picture is that each carrier-carrier interaction is influenced by all kinds of carriers for they are all Coulomb in nature. Thus the interactions are coupled, which can be seen in Fig. 1 in the random

phase approximation (RPA).

Using Fig.1, we can write coupled potential matrices as follows:

$$\tilde{V}_{ee} = V_{ee} + V_{ee}\Pi_e\tilde{V}_{ee} + V_{eh}\Pi_h\tilde{V}_{he} , \quad (2.9)$$

$$\tilde{V}_{hh} = V_{hh} + V_{hh}\Pi_h\tilde{V}_{hh} + V_{he}\Pi_e\tilde{V}_{eh} , \quad (2.10)$$

$$\tilde{V}_{eh} = V_{eh} + V_{ee}\Pi_e\tilde{V}_{eh} + V_{eh}\Pi_h\tilde{V}_{hh} , \quad (2.11)$$

$$\tilde{V}_{he} = V_{he} + V_{hh}\Pi_h\tilde{V}_{he} + V_{he}\Pi_e\tilde{V}_{ee} , \quad (2.12)$$

where  $\tilde{V}_{ee}$ ,  $\tilde{V}_{hh}$ , and  $\tilde{V}_{eh}$  are renormalized interaction potentials defined in the  $(\mathbf{q}, \omega)$  representation. Defining:

$$\tilde{V} = \begin{bmatrix} \tilde{V}_{ee} & \tilde{V}_{eh} \\ \tilde{V}_{he} & \tilde{V}_{hh} \end{bmatrix}, \quad V = \begin{bmatrix} V_{ee} & V_{eh} \\ V_{he} & V_{hh} \end{bmatrix}, \quad \Pi = \begin{bmatrix} \Pi_e & 0 \\ 0 & \Pi_h \end{bmatrix},$$

Eqs. (2.9)–(2.12) can be changed to a simple matrix formula:

$$\tilde{V} = V + V\Pi\tilde{V} . \quad (2.13)$$

Thus the carrier-carrier renormalized potentials are solved:

$$\tilde{V} = (1 - V\Pi)^{-1} V . \quad (2.14)$$

In the case that only lowest subbands are occupied, it can be straightforwardly written:

$$\tilde{V} = \frac{1}{\Delta} \begin{bmatrix} (1 - V_{hh}\Pi_h)V_{ee} + V_{eh}\Pi_h V_{he} & V_{eh} \\ V_{he} & (1 - V_{ee}\Pi_e)V_{hh} + V_{he}\Pi_e V_{eh} \end{bmatrix}, \quad (2.15)$$

with

$$\Delta = (1 - V_{ee}\Pi_e)(1 - V_{hh}\Pi_h) - V_{eh}\Pi_h V_{he}\Pi_e ,$$

where  $\Pi_e$ ,  $\Pi_h$  are the polarizability functions of 2D electron and hole gases.<sup>15</sup> In the RPA their forms are given by:

$$\Pi_{n'n}^e(\mathbf{q}, \omega) = 2 \sum_{\mathbf{k}} \frac{f_{n'\mathbf{k}-\mathbf{q}} - f_{n\mathbf{k}}}{\hbar\omega + E_{n'\mathbf{k}-\mathbf{q}} - E_{n\mathbf{k}} + i\delta}, \quad (2.16)$$

$$\Pi_{m'm}^h(\mathbf{q}, \omega) = 2 \sum_{\mathbf{k}} \frac{g_{m'\mathbf{p}-\mathbf{q}} - g_{m\mathbf{p}}}{\hbar\omega + E_{m'\mathbf{p}-\mathbf{q}} - E_{m\mathbf{p}} + i\delta}, \quad (2.17)$$

where  $f_{n\mathbf{k}}$  and  $g_{m\mathbf{p}}$  are electron and hole distribution functions in the states, respectively,  $(n, \mathbf{k})$  and  $(m, \mathbf{p})$ ,  $E_{n\mathbf{k}} = E_n + \hbar^2 k^2 / 2m_e$ ,  $E_{m\mathbf{p}} = E_m + \hbar^2 p^2 / 2m_h$ , and  $E_n$ ,  $E_m$  stand for the electron and hole subband energy levels associated with the confinement potential.  $\hbar\omega$  is the energy exchange in the corresponding scattering process. It is easy to see that if the hole density was zero, interaction potentials would revert back to the form for a pure electron system.

So far as carrier-lattice interaction is concerned, the optical phonon (OP) dominates at room temperature and above. The electron-OP interaction can only occur via polar phonons. Using the Fröhlich continuum model,<sup>11</sup> we have the electron-OP interaction expression:

$$\hat{V}_{e-L} = \frac{1}{\sqrt{A}} \sum_{n',n} \sum_{\mathbf{k},\mathbf{k}'} \sum_Q [b_Q^L \delta_{\mathbf{k}',\mathbf{k}+\mathbf{q}} V_{e-L}^{n'n}(\mathbf{q}, q_z) + b_Q^{L\dagger} \delta_{\mathbf{k},\mathbf{k}-\mathbf{q}} V_{e-L}^{n'n*}(\mathbf{q}, q_z)] \hat{a}_{n'\mathbf{k}'}^\dagger \hat{a}_{n\mathbf{k}}, \quad (2.18)$$

with

$$V_{e-L}^{n'n} = M_{e-L}(\mathbf{q}, q_z) G_{n'n}^e(\mathbf{q}, q_z), \quad M_{e-L}(\mathbf{q}, q_z) = \frac{i\alpha}{Q}, \quad (2.19)$$

where L represents longitudinal optical phonon,  $\alpha$  is the Fröhlich electron-L coupling constant,  $\alpha = [2\pi e^2 \hbar \omega_L (1/\kappa_\infty - 1/\kappa_0)]^{1/2}$ , and

$$G_{n'n}^e(\mathbf{q}, q_z) = \frac{1}{\sqrt{L}} \int_{-\infty}^{\infty} dz \xi_n^*(z) \xi_n(z) e^{iq_z z} . \quad (2.20)$$

Both polar and nonpolar optical phonons produce hole-lattice interactions for the anisotropic valence band structure of GaAs.<sup>8,12,13</sup> The choice of nonpolar optical potential (deformation potential) parameters and their meanings have been discussed in detail<sup>12,13</sup> and will not be repeated in this paper. Here the hole-L interaction term can be written:

$$\begin{aligned} \hat{V}_{h-L} = & \frac{1}{\sqrt{A}} \sum_{m',m} \sum_{p',p} \sum_Q [\hat{b}_Q^L \delta_{p',p+q} V_{h-L}^{m'm}(\mathbf{q}, q_z) \\ & + \hat{b}_Q^{L\dagger} \delta_{p',p-q} V_{h-L}^{m'm*}(\mathbf{q}, q_z)] \hat{d}_{m'p}^\dagger \hat{d}_{mp} , \end{aligned} \quad (2.21)$$

where

$$V_{h-L}^{m'm} = M_{h-L}(\mathbf{q}, q_z) G_{m'm}^h(\mathbf{q}, q_z) , \quad M_{h-L}(\mathbf{q}, q_z) = -iK_p^{1/2} \frac{\alpha}{Q} + \frac{\hbar(D_t K)}{(2\rho_0 \hbar \omega_L)^{1/2}} , \quad (2.22)$$

with

$$G_{m'm}^h(\mathbf{q}, q_z) = \frac{1}{\sqrt{L}} \int_{-\infty}^{\infty} dz \zeta_{m'}^*(z) \zeta_m(z) e^{iq_z z} . \quad (2.23)$$

$D_t K = (\frac{3}{2})^{1/2} d_0 / a_0$ , with  $d_0$  the phenomenological optical deformation potential constant,  $a_0$  the lattice constant,  $\rho_0$  the mass density of the crystal, and  $K_p$  the correction factor due to  $p$ -type wave function for holes and existence of light holes.<sup>13</sup> Coupling between the hole and transverse phonon (T) can only occur via the nonpolar optical deformation potential interaction.<sup>14</sup> The size of the effects which are observed suggests that T and L phonons are of roughly comparable importance<sup>13</sup> in  $p$ -doped GaAs. The hole-T term can be written as:

$$\begin{aligned} \hat{V}_{h-T} &= \frac{1}{\sqrt{A}} \sum_{m',m} \sum_{p',p} \sum_Q [b_Q^T \delta_{p',p+q} V_{h-T}^{m'm}(\mathbf{q}, q_z) + b_Q^{T\dagger} \delta_{p,p-q} V_{h-T}^{m'm*}(\mathbf{q}, q_z)] \hat{d}_{m'p}^\dagger \hat{d}_{mp}, \\ V_{h-T} &= \frac{1}{\sqrt{A}} \sum_{m',m} \sum_{p',p} \sum_Q [b_Q \delta_{p',p+q} V_{h-T}^{m'm}(\mathbf{q}, q_z) + b_Q^\dagger \delta_{p,p-q} V_{h-T}^{m'm*}(\mathbf{q}, q_z)] d_{m'p}^\dagger d_{mp}, \end{aligned} \quad (2.24)$$

with

$$V_{h-T}^{m'm} = M_{h-T}(\mathbf{q}, q_z) G_{m'm}^h(\mathbf{q}, q_z), \quad M_{h-T}(\mathbf{q}, q_z) = \frac{\hbar(D_t K)}{(2\rho_0 \hbar \omega_T)^{1/2}}. \quad (2.25)$$

The renormalized carrier-phonon interaction potentials are coupled with each other via the self-consistent carrier-carrier coupling. The ring diagram approximation for carrier-lattice interactions is shown in Fig. 2. The potentials can be written:

$$\begin{bmatrix} \tilde{V}_{ep} \\ \tilde{V}_{hp} \end{bmatrix} = \begin{bmatrix} 1 + \tilde{V}_{ee}\Pi_e & \tilde{V}_{eh}\Pi_h \\ \tilde{V}_{he}\Pi_e & 1 + \tilde{V}_{hh}\Pi_h \end{bmatrix} \begin{bmatrix} V_{ep} \\ V_{hp} \end{bmatrix}. \quad (2.26)$$

Inserting the previously evaluated  $\tilde{V}_{ee}$ ,  $\tilde{V}_{hh}$ ,  $\tilde{V}_{eh}$ , and  $\tilde{V}_{he}$  we get the coupled equations (in the lowest subband approximation):

$$\tilde{V}_{ep} = \frac{1}{\Delta} [(1 - V_{hh}\Pi_h)V_{ep} + V_{eh}\Pi_h V_{hp}], \quad (2.27)$$

$$\tilde{V}_{hp} = \frac{1}{\Delta} [(1 - V_{ee}\Pi_e)V_{hp} + V_{he}\Pi_e V_{ep}]. \quad (2.28)$$

This coupling is to be expected since the carrier-lattice interactions are all basically Coulomb interactions.

One more interaction to be included is the elastic scattering by two sets of ionized impurities: the remote impurities a distance  $s$  into the  $\text{Ga}_{1-x}\text{Al}_x\text{As}$  barrier with a total area density  $n_o$  and the background charged impurities existing in the GaAs region with a small area density  $n_i$ . Both electrons and holes would be scattered by impurities. The coupled potentials are:

$$\tilde{V}_{e\text{-imp}} = \frac{1}{\Delta} [(1 - V_{hh}\Pi_h)V_{e\text{-imp}} + V_{eh}\Pi_h V_{h\text{-imp}}] , \quad (2.29)$$

$$\tilde{V}_{h\text{-imp}} = \frac{1}{\Delta} [(1 - V_{ee}\Pi_e)V_{h\text{-imp}} + V_{he}\Pi_e V_{e\text{-imp}}] . \quad (2.30)$$

The bare carrier-impurity interactions in two dimensions have been previously given.<sup>9</sup>

### 3 TWO-DIMENSIONAL BALANCE EQUATIONS

We consider an electron-hole-lattice system in GaAs heterojunctions, which consists of  $N_e$  electrons and  $N_h$  holes confined in a quasi-2D plane by a potential normal in direction to the interface. Electrons and holes are subject to an applied uniform electric field in the plane and are coupled with 3D phonons. The motion of electrons and holes can be separated into center-of-mass and relative motions. We define center-of-mass momenta  $\hat{P}_e$  and  $\hat{P}_h$  and coordinate variables  $\hat{R}_e$  and  $\hat{R}_h$  as well as relative momentums and coordinate variables  $\hat{p}'_{ei}$ ,  $\hat{p}'_{hi}$ ,  $\hat{r}'_{ei}$ , and  $\hat{r}'_{hi}$  by:

$$\hat{P}_e = \sum_{i=1}^{N_e} \hat{p}_{ei} , \quad \hat{R}_e = \frac{1}{N_e} \sum_{i=1}^{N_e} \hat{r}_{ei} , \quad (3.1)$$

$$\hat{P}_h = \sum_{i=1}^{N_h} \hat{p}_{hi} , \quad \hat{R}_h = \frac{1}{N_h} \sum_{i=1}^{N_h} \hat{r}_{hi} , \quad (3.2)$$

$$\hat{p}'_{ei} = \hat{p}_{ei} - \frac{1}{N_e} \hat{P}_e , \quad \hat{r}'_{ei} = \hat{r}_{ei} - \hat{R}_e , \quad (3.3)$$

$$\hat{p}'_{hi} = \hat{p}_{hi} - \frac{1}{N_h} \hat{P}_h , \quad \hat{r}'_{hi} = \hat{r}_{hi} - \hat{R}_h , \quad (3.4)$$

which satisfy the following commutation rules:

$$[\hat{\mathbf{R}}_{e,\alpha}, \hat{\mathbf{P}}_{e,\beta}] = i\hbar \delta_{\alpha,\beta}, \quad [\hat{\mathbf{R}}_{h,\alpha}, \hat{\mathbf{P}}_{h,\beta}] = i\hbar \delta_{\alpha,\beta}, \quad (3.5)$$

$$[\hat{\mathbf{r}}'_{ei,\alpha}, \hat{\mathbf{p}}'_{ej,\beta}] = i\hbar \delta_{\alpha,\beta} \left[ \delta_{i,j} - \frac{1}{N_e} \right], \quad [\hat{\mathbf{r}}'_{hi,\alpha}, \hat{\mathbf{p}}'_{hj,\beta}] = i\hbar \delta_{\alpha,\beta} \left[ \delta_{i,j} - \frac{1}{N_h} \right]. \quad (3.6)$$

The remaining commutators are zero.

The Hamiltonian of the electron-hole-lattice system in an applied field can be written as:

$$\hat{H} = \hat{H}_0 + \hat{V}, \quad (3.7)$$

$$\hat{H}_0 = \hat{H}_e + \hat{H}_h + \hat{H}_p, \quad (3.8)$$

$$\begin{aligned} \hat{V} = & \hat{V}_{ee} + \hat{V}_{hh} + \hat{V}_{pp} \\ & + \hat{V}_{ep} + \hat{V}_{hp} + \hat{V}_{eh} + \hat{V}_{e\text{-imp}} + \hat{V}_{h\text{-imp}}. \end{aligned} \quad (3.9)$$

Since the applied electric field acts only on the center of mass of electrons and holes, the expression of  $\hat{H}_e$  and  $\hat{H}_h$  can be written:

$$\hat{H}_e = \frac{\hat{\mathbf{P}}_e^2}{2M_e} - eN_e \mathbf{E} \cdot \hat{\mathbf{R}}_e + \hat{H}'_e, \quad (3.10)$$

$$\hat{H}_h = \frac{\hat{\mathbf{P}}_h^2}{2M_h} + eN_h \mathbf{E} \cdot \hat{\mathbf{R}}_h + \hat{H}'_h, \quad (3.11)$$

where  $\hat{H}'_e$  and  $\hat{H}'_h$  are Hamiltonians describing the relative motions of free electrons and holes whose expressions in the occupation number representation are:

$$\hat{H}'_e = \sum_{n,\mathbf{k}} E_{nk} \hat{a}_{nk}^\dagger \hat{a}_{nk}, \quad (3.12)$$

$$\hat{H}'_h = \sum_{m,p} E_{mp} \hat{a}_{mp}^\dagger \hat{a}_{mp} , \quad (3.13)$$

where spin indices have been omitted.  $\hat{H}_p$  is the 3D optical phonon Hamiltonian:

$$\hat{H}_p = \sum_Q (\hbar\omega_L \hat{b}_Q^{L\dagger} \hat{b}_Q^L + \hbar\omega_T \hat{b}_Q^{T\dagger} \hat{b}_Q^T) . \quad (3.14)$$

The nonequilibrium state of electron-hole-phonon system is described by the density matrix  $\hat{\rho}(t)$  whose time evolution is governed by the quantum-mechanical Liouville equation:

$$i\hbar \frac{\partial \hat{\rho}(t)}{\partial t} = [\hat{H}, \hat{\rho}(t)] . \quad (3.15)$$

Using Bogoliubov's<sup>16,17</sup> description of the quantum kinetic equation for the nonequilibrium state, we introduce a set of kinetic macroscopic observables:

$$M(t) = \{f_{n\mathbf{k}}(t) , g_{m\mathbf{p}}(t) , \mathbf{v}_e(t) , \mathbf{v}_h(t)\} , \quad (3.16)$$

where  $f_{n\mathbf{k}}(t)$  ,  $g_{m\mathbf{p}}(t)$  are the electron and hole distribution functions in their relative coordinates, and  $\mathbf{v}_e$  ,  $\mathbf{v}_h$  are drift velocities of electrons and holes, which satisfy:

$$M(t) = \text{Tr}\{\hat{M}\hat{\rho}(t)\} , \quad (3.17)$$

where  $\hat{M}(t)$  are corresponding operators of  $M(t)$  such as:

$$f_{n\mathbf{k}}(t) = \text{Tr}[\hat{a}_{n\mathbf{k}}^\dagger \hat{a}_{n\mathbf{k}} \hat{\rho}(t)] , \quad g_{m\mathbf{p}}(t) = \text{Tr}[\hat{a}_{m\mathbf{p}}^\dagger \hat{a}_{m\mathbf{p}} \hat{\rho}(t)] . \quad (3.18)$$

Their explicit time evolution is governed by:

$$i\hbar \frac{\partial M(t)}{\partial t} = \text{Tr}\{[\hat{M}(t), \hat{H}] \hat{\rho}(t)\} . \quad (3.19)$$

To second order in the interaction potential  $V$  we get:

$$\begin{aligned} \frac{\partial M(t)}{\partial t} &= \frac{i}{\hbar} \text{Tr}\{[\hat{H}_0, \hat{M}(t)]\hat{\rho}_0(t)\} + \frac{i}{\hbar} \text{Tr}\{[\hat{V}, \hat{M}(t)]\hat{\rho}_0(t)\} \\ &+ \left(\frac{i}{\hbar}\right)^2 \lim_{\epsilon \rightarrow 0^+} \int_{-\infty}^0 d\tau e^{\epsilon\tau} \text{Tr}\{[\hat{V}(\tau), [\hat{V}, \hat{M}(t)]]\hat{\rho}_0(t)\}, \end{aligned} \quad (3.20)$$

where

$$\hat{V}(\tau) = \exp\left[\frac{i\hat{H}_0\tau}{\hbar}\right] \hat{V} \exp\left[\frac{-i\hat{H}_0\tau}{\hbar}\right],$$

and  $\hat{\rho}_0(t)$  is the quasistationary value of  $\hat{\rho}(t)$ , chosen to guarantee the irreversible character<sup>16,17</sup> of time evolution of  $M(t)$ :

$$\hat{\rho}_0(t) = \frac{1}{Z} \exp\left[-\sum_i B_i(M(t))\hat{M}_i\right], \quad (3.21)$$

$Z$  is a normalization constant and the function  $B_i$  is determined by the requirement:

$$M_i(t) = \text{Tr} \hat{M}_i \hat{\rho}_0(t) \quad (3.22)$$

that the macroscopic variables assume their appropriate values. Equation (3.21) describes a quasiequilibrium state for the operators  $\hat{M}_i(t)$ ; subject to “slowly varying” external forces.

Using Eq. (3.20), we derive the kinetic equation of the electron distribution function in a straightforward way:

$$\frac{\partial f_{n\mathbf{k}}(t)}{\partial t} = \left(\frac{\partial f_{n\mathbf{k}}(t)}{\partial t}\right)_{\text{ch}} + \left(\frac{\partial f_{n\mathbf{k}}(t)}{\partial t}\right)_{\text{e-L}} + \left(\frac{\partial f_{n\mathbf{k}}(t)}{\partial t}\right)_{\text{e-imp}} + \left(\frac{\partial f_{n\mathbf{k}}(t)}{\partial t}\right)_{\text{ee}}, \quad (3.23)$$

with

$$\left[ \frac{\partial f_{n\mathbf{k}}(t)}{\partial t} \right]_{\text{eh}} = \frac{2\pi}{\hbar} \sum_{n',m',m} \sum_{\mathbf{k}',\mathbf{p}',\mathbf{p}} \sum_{\mathbf{q}} [f_{n'\mathbf{k}'} (1-f_{n\mathbf{k}})g_{m'\mathbf{p}'} (1-g_{m\mathbf{p}}) - f_{n\mathbf{k}} (1-f_{n'\mathbf{k}'})g_{m\mathbf{p}} (1-g_{m'\mathbf{p}'})]$$

$$| \tilde{V}_{\text{eh}}^{n'n,m'm}(\mathbf{q}) |^2 \times \delta_{\mathbf{k}',\mathbf{k}-\mathbf{q}} \delta_{\mathbf{p}',\mathbf{p}+\mathbf{q}} \delta(E_{n'\mathbf{k}'}+E_{m'\mathbf{p}'}-E_{n\mathbf{k}}-E_{m\mathbf{p}}-\hbar\mathbf{q}\cdot(\mathbf{v}_e-\mathbf{v}_h)). \quad (3.24)$$

The first term in the square brackets describes a transition from the electron state with subband energy level  $E_{n'}$  and momentum  $\mathbf{k}'$  into band level  $E_n$  with momentum  $\mathbf{k}$  after collision with a hole. The second term describes the opposite transition. The collision process is governed by momentum and energy conservation. Since we write the energy in the center-of-mass system,  $\mathbf{v}_e$ ,  $\mathbf{v}_h$  will appear in the energy conservation law. The scattering by the electron-phonon interaction contains four considerations (emission, absorption, and the reverse transitions):

$$\left[ \frac{\partial f_{n\mathbf{k}}(t)}{\partial t} \right]_{\text{e-L}} = \frac{4\pi}{\hbar A} \sum_{\mathbf{q}} \sum_{q_z} \sum_{n',\mathbf{k}'} \tilde{V}_{\text{e-L}}^{n'n*}(\mathbf{q}, q_z) \tilde{V}_{\text{e-L}}^{n'n}(\mathbf{q}, q_z) (\{f_{n'\mathbf{k}'}(t)[1-f_{n\mathbf{k}}(t)]\delta_{\mathbf{k}',\mathbf{k}+\mathbf{q}} \delta(E_{n'\mathbf{k}'}-E_{n\mathbf{k}}-\hbar\omega_L)-f_{n\mathbf{k}}(t)[1-f_{n'\mathbf{k}'}(t)]\delta_{\mathbf{k}',\mathbf{k}-\mathbf{q}} \delta(E_{n\mathbf{k}}-E_{n'\mathbf{k}'}-\hbar\omega_L)\} [1+n^L(T_c)] + \{f_{n'\mathbf{k}'}(t)[1-f_{n\mathbf{k}}(t)]\delta_{\mathbf{k}',\mathbf{k}-\mathbf{q}} \delta(E_{n'\mathbf{k}'}-E_{n\mathbf{k}}+\hbar\omega_L) -f_{n\mathbf{k}}(t)[1-f_{n'\mathbf{k}'}(t)]\delta_{\mathbf{k}',\mathbf{k}+\mathbf{q}} \delta(E_{n\mathbf{k}}-E_{n'\mathbf{k}'}+\hbar\omega_L)\} n^L(T_c)), \quad (3.25)$$

where  $n^L(T_c)$  is the equilibrium occupation number of L-type phonons and  $T_c$  is crystal temperature. In the present calculation we assume phonons are in equilibrium at lattice temperature. The hole equation can be written:

$$\begin{aligned} \frac{\partial g_{mp}(t)}{\partial t} = & \left[ \frac{\partial g_{mp}(t)}{\partial t} \right]_{\text{he}} + \left[ \frac{\partial g_{mp}(t)}{\partial t} \right]_{\text{h-L}} + \left[ \frac{\partial g_{mp}(t)}{\partial t} \right]_{\text{h-T}} \\ & + \left[ \frac{\partial g_{mp}(t)}{\partial t} \right]_{\text{h-imp}} + \left[ \frac{\partial g_{mp}(t)}{\partial t} \right]_{\text{hh}} . \end{aligned} \quad (3.26)$$

The explicit expression of each term in (3.26) can be obtained in the same way as we have done for electrons, so they are not repeated here. The terms of electron-electron and hole-hole collisions  $(\partial f_{n\mathbf{k}}(t)/\partial t)_{\text{ee}}$ ,  $(\partial g_{mp}(t)/\partial t)_{\text{hh}}$  are not specified here, since their effects are approximately represented by the displaced velocity temperature model.

The equations of motions for the center of mass of the electrons and holes are:

$$M_e \frac{\partial \mathbf{v}_e}{\partial t} = -eN_e \mathbf{E} + \mathbf{F}_{\text{e-L}} + \mathbf{F}_{\text{eh}} + \mathbf{F}_{\text{e-imp}} , \quad (3.27)$$

$$M_h \frac{\partial \mathbf{v}_h}{\partial t} = eN_h \mathbf{E} + \mathbf{F}_{\text{h-L}} + \mathbf{F}_{\text{h-T}} + \mathbf{F}_{\text{he}} + \mathbf{F}_{\text{h-imp}} , \quad (3.28)$$

where  $M_e, M_h$  are total mass of electrons and holes.  $\mathbf{F}_{\text{e-L}}, \mathbf{F}_{\text{e-h}}, \mathbf{F}_{\text{e-imp}}$ , and corresponding hole terms are the frictional forces due to the carrier-lattice, carrier-impurity, and carrier-carrier interactions. Using (3.24) and (3.25) we define:

$$\Gamma_{\text{e-L}} = \frac{2\pi}{\hbar} \sum_{n',n} \sum_{q_z} \tilde{V}_{\text{e-L}}^{n'n*}(\mathbf{q}, q_z) \tilde{V}_{\text{e-L}}^{n'n}(\mathbf{q}, q_z) \{ I_{n'n}^{(+)}(\mathbf{q}, \omega) [1+n^L(T_c)] - I_{n'n}^{(-)}(\mathbf{q}, \omega) n^L(T_c) \} , \quad (3.29)$$

$$\Gamma_{\text{h-L}} = \frac{2\pi}{\hbar} \sum_{m',m} \sum_{q_z} \tilde{V}_{\text{h-L}}^{m'm*}(\mathbf{q}, q_z) \tilde{V}_{\text{h-L}}^{m'm}(\mathbf{q}, q_z) \{ J_{m'm}^{(+)}(\mathbf{q}, \omega) [1+n^L(T_c)] - J_{m'm}^{(-)}(\mathbf{q}, \omega) n^L(T_c) \} , \quad (3.30)$$

$$\Gamma_{h-T} = \frac{2\pi}{\hbar} \sum_{m',m} \sum_{q_z} \tilde{V}_{h-T}^{m'm*}(\mathbf{q}, q_z) \tilde{V}_{h-T}^{m'm}(\mathbf{q}, q_z) \{J_{m'm}^{(+)}(\mathbf{q}, \omega) [1+n^T(T_c)] - J_{m'm}^{(-)}(\mathbf{q}, \omega) n^T(T_c)\}, \quad (3.31)$$

with

$$J_{n'n}^{(\pm)}(\mathbf{q}, \omega) = \frac{2}{A} \sum_{\mathbf{K}} \sum_{\mathbf{k}} f_{n\mathbf{k}}(t) [1-f_{n'\mathbf{k}'}(t)] \delta_{\mathbf{k}', \mathbf{k}+\mathbf{q}} \delta(E_{n\mathbf{k}} - E_{n'\mathbf{k}'} \pm \hbar\omega_L \mp \hbar\mathbf{q} \cdot \mathbf{v}_e), \quad (3.32)$$

$$J_{m'm}^{(\pm)}(\mathbf{q}, \omega) = \frac{2}{A} \sum_{\mathbf{P}'} \sum_{\mathbf{P}} g_{m\mathbf{P}}(t) [1-g_{m'\mathbf{P}'}(t)] \delta_{\mathbf{P}', \mathbf{P}+\mathbf{q}} \delta(E_{m\mathbf{P}} - E_{m'\mathbf{P}'} \pm \hbar\omega \mp \hbar\mathbf{q} \cdot \mathbf{v}_h). \quad (3.33)$$

Then,  $\mathbf{F}_{e-L}$ ,  $\mathbf{F}_{h-L}$ , and  $\mathbf{F}_{h-T}$  are expressed as:

$$\mathbf{F}_{e-L} = -\sum_q \hbar\mathbf{q} \Gamma_{e-L}, \quad (3.34)$$

$$\mathbf{F}_{h-L} = -\sum_q \hbar\mathbf{q} \Gamma_{h-L}, \quad (3.35)$$

$$\mathbf{F}_{h-T} = -\sum_q \hbar\mathbf{q} \Gamma_{h-T}. \quad (3.36)$$

$\mathbf{F}_{eh}$ ,  $\mathbf{F}_{e-imp}$ , and  $\mathbf{F}_{h-imp}$  can be directly obtained from (3.24) :

$$\mathbf{F}_{e-h} = \frac{2\pi}{\hbar} \sum_{n',n,m',m} \sum_{\mathbf{K},\mathbf{k},\mathbf{P}',\mathbf{P}} \sum_q \hbar\mathbf{q} f_{n'\mathbf{K}'}(t) [1-f_{n\mathbf{k}}(t)] g_{m'\mathbf{P}'}(t) [1-g_{m\mathbf{P}}(t)] |\tilde{V}_{eh}^{n'n,m'm}(\mathbf{q})|^2$$

$$\times \delta_{\mathbf{K}', \mathbf{k}-\mathbf{q}} \delta_{\mathbf{P}', \mathbf{P}+\mathbf{q}} \delta(E_{n'\mathbf{K}'} + E_{m'\mathbf{P}'} - E_{n\mathbf{k}} - E_{m\mathbf{P}} - \hbar\mathbf{q} \cdot (\mathbf{v}_e - \mathbf{v}_h)),$$

(3.37)

$$\mathbf{F}_{e-imp} = \sum_q \hbar\mathbf{q} \Gamma_{e-imp}, \quad (3.38)$$

$$\mathbf{F}_{\text{h-imp}} = \sum_{\mathbf{q}} \hbar \mathbf{q} \Gamma_{\text{h-imp}} , \quad (3.39)$$

with

$$\Gamma_{\text{e-imp}} = \frac{2\pi}{\hbar} \sum_{n',n} \sum_{\mathbf{k}',\mathbf{k}} f_{n'\mathbf{k}'}(t)[1-f_{n\mathbf{k}}(t)] \tilde{U}_{\text{e-imp}}^{n'n}(\mathbf{q}) \delta_{\mathbf{k}',\mathbf{k}-\mathbf{q}} \delta(E_{n'\mathbf{k}'} - E_{n\mathbf{k}} - \hbar \mathbf{q} \cdot \mathbf{v}_e) , \quad (3.40)$$

$$\Gamma_{\text{h-imp}} = \frac{2\pi}{\hbar} \sum_{m',m} \sum_{\mathbf{p}',\mathbf{p}} g_{m'\mathbf{p}'}(t)[1-g_{m\mathbf{p}}(t)] \tilde{U}_{\text{h-imp}}^{m'm}(\mathbf{q}) \delta_{\mathbf{p}',\mathbf{p}-\mathbf{q}} \delta(E_{m'\mathbf{p}'} - E_{m\mathbf{p}} - \hbar \mathbf{q} \cdot \mathbf{v}_h) , \quad (3.41)$$

where

$$\tilde{U}_{\text{e-imp}}^{n'n}(\mathbf{q}) = \int d\mathbf{R}_a n_i(\mathbf{R}_a) |V_{\text{e-imp}}^{n'n}(\mathbf{q}, \mathbf{R}_a)|^2 ,$$

$$\tilde{U}_{\text{h-imp}}^{m'm}(\mathbf{q}) = \int d\mathbf{R}_a n_i(\mathbf{R}_a) |V_{\text{h-imp}}^{m'm}(\mathbf{q}, \mathbf{R}_a)|^2 .$$

Here  $n_i(\mathbf{R}_a)$  is the density of ionized impurities. The energy loss rates of electrons and holes in their center of mass system are:

$$\frac{\partial E_e^c(t)}{\partial t} = \left[ \frac{\partial E_e^c(t)}{\partial t} \right]_{\text{eh}} + \left[ \frac{\partial E_e^c(t)}{\partial t} \right]_{\text{e-L}} + \left[ \frac{\partial E_e^c(t)}{\partial t} \right]_{\text{e-imp}} + \left[ \frac{\partial E_e^c(t)}{\partial t} \right]_{\text{ee}} , \quad (3.42)$$

$$\frac{\partial E_h^c(t)}{\partial t} = \left[ \frac{\partial E_h^c(t)}{\partial t} \right]_{\text{he}} + \left[ \frac{\partial E_h^c(t)}{\partial t} \right]_{\text{h-L}}$$

$$+ \left[ \frac{\partial E_h^c(t)}{\partial t} \right]_{\text{h-T}} + \left[ \frac{\partial E_h^c(t)}{\partial t} \right]_{\text{h-imp}} + \left[ \frac{\partial E_h^c(t)}{\partial t} \right]_{\text{hh}} . \quad (3.43)$$

The explicit form of each energy-loss rate can be obtained as we have done for the force term. The results are:

$$\left( \frac{\partial E_e^c}{\partial t} \right)_{e-L} = -\sum_q (\hbar\omega_L - \hbar\mathbf{q}\cdot\mathbf{v}_e)\Gamma_{e-L}, \quad (3.44)$$

$$\left( \frac{\partial E_h^c}{\partial t} \right)_{h-L} = -\sum_q (\hbar\omega_L - \hbar\mathbf{q}\cdot\mathbf{v}_h)\Gamma_{h-L}, \quad (3.45)$$

$$\left( \frac{\partial E_h^c}{\partial t} \right)_{h-T} = -\sum_q (\hbar\omega_T - \hbar\mathbf{q}\cdot\mathbf{v}_h)\Gamma_{h-T}, \quad (3.46)$$

$$\left( \frac{\partial E_e^c}{\partial t} \right)_{e-h} = \frac{2\pi}{\hbar} \sum_{n',n,m',m} \sum_{\mathbf{K},\mathbf{k},\mathbf{p}',\mathbf{p}} \sum_q (E_{n\mathbf{k}} - E_{n'\mathbf{K}}) f_{n'\mathbf{K}}(t) [1 - f_{n\mathbf{k}}(t)] g_{m'\mathbf{p}'}(t) [1 - g_{m\mathbf{p}}(t)]$$

$$|\tilde{V}_{ch}^{n'n,m'm}(\mathbf{q})|^2 \times \delta_{\mathbf{K},\mathbf{k}-\mathbf{q}} \delta_{\mathbf{p}',\mathbf{p}+\mathbf{q}} \delta(E_{n'\mathbf{K}} + E_{m'\mathbf{p}'} - E_{n\mathbf{k}} - E_{m\mathbf{p}} - \hbar\mathbf{q}\cdot(\mathbf{v}_e - \mathbf{v}_h)), \quad (3.47)$$

$$\left( \frac{\partial E_h^c}{\partial t} \right)_{h-e} = -\frac{2\pi}{\hbar} \sum_{n',n,m',m} \sum_{\mathbf{K},\mathbf{k},\mathbf{p}',\mathbf{p}} \sum_q [E_{n\mathbf{k}} - E_{n'\mathbf{K}} - \hbar\mathbf{q}\cdot(\mathbf{v}_e - \mathbf{v}_h)]$$

$$\times f_{n'\mathbf{K}}(t) [1 - f_{n\mathbf{k}}(t)] g_{m'\mathbf{p}'}(t) [1 - g_{m\mathbf{p}}(t)] |\tilde{V}_{ch}^{n'n,m'm}(\mathbf{q})|^2$$

$$\times \delta_{\mathbf{K},\mathbf{k}-\mathbf{q}} \delta_{\mathbf{p}',\mathbf{p}+\mathbf{q}} \delta(E_{n'\mathbf{K}} + E_{m'\mathbf{p}'} - E_{n\mathbf{k}} - E_{m\mathbf{p}} - \hbar\mathbf{q}\cdot(\mathbf{v}_e - \mathbf{v}_h)). \quad (3.48)$$

Since the impurities are assumed fixed, the elastic collision with carriers in the center of mass are:

$$\left( \frac{\partial E_e^c}{\partial t} \right)_{e-imp} = \sum_q \hbar\mathbf{q}\cdot\mathbf{v}_e \Gamma_{e-imp}, \quad (3.49)$$

$$\left( \frac{\partial E_h^c}{\partial t} \right)_{h\text{-imp}} = \sum_{\mathbf{q}} \hbar \mathbf{q} \cdot \mathbf{v}_h \Gamma_{h\text{-imp}} . \quad (3.50)$$

At room temperature and above, electrons and holes can be treated as nondegenerate gases. The distribution functions of electrons and holes are taken as Maxwellian. For the lowest subband Eqs. (3.32) and (3.33) can be reduced to:

$$I_{00}^{(\pm)}(\mathbf{q}, \omega) = \left( \frac{m_e \beta_e}{2\pi} \right)^{1/2} \frac{n_e}{\hbar q} e^{-\eta_{\pm}} ,$$

$$\eta_{\pm} = \frac{m_e \beta_e}{2\hbar^2 q^2} \left[ \hbar \omega \pm \frac{\hbar^2 q^2}{2m_e} - \hbar \mathbf{q} \cdot \mathbf{v}_e \right]^2 , \quad \beta_e = \frac{1}{K_B T_e} , \quad (3.51)$$

$$J_{00}^{(\pm)}(\mathbf{q}, \omega) = \left( \frac{m_h \beta_h}{2\pi} \right)^{1/2} \frac{n_h}{\hbar q} e^{-\mu_{\pm}} ,$$

$$\mu_{\pm} = \frac{m_h \beta_h}{2\hbar^2 q^2} \left[ \hbar \omega \pm \frac{\hbar^2 q^2}{2m_h} - \hbar \mathbf{q} \cdot \mathbf{v}_h \right]^2 , \quad \beta_h = \frac{1}{K_B T_h} . \quad (3.52)$$

The hole summation part in the electron-hole interaction term can be reduced to:

$$\sum_{\mathbf{p}, \mathbf{p}'} g_{0\mathbf{p}'} (1 - g_{0\mathbf{p}}) \delta_{\mathbf{p}', \mathbf{p} + \mathbf{q}} \delta(E_{0\mathbf{k}'} + E_{0\mathbf{p}'} - E_{0\mathbf{k}} - E_{0\mathbf{p}} - \hbar \mathbf{q} \cdot (\mathbf{v}_e - \mathbf{v}_h)) = A n_h \left( \frac{m_h \beta_h}{2\pi} \right)^{1/2} \frac{e^{-\chi_0}}{\hbar q} , \quad (3.53)$$

where

$$\chi_0 = \frac{\beta_h m_h}{2\hbar^2 q^2} \left[ \frac{\hbar^2 \mathbf{k}' \cdot \mathbf{q}}{m_e} + \frac{\hbar^2 q^2}{2m_e} + \frac{\hbar^2 q^2}{2m_h} + \hbar \mathbf{q} \cdot (\mathbf{v}_e - \mathbf{v}_h) \right]^2 .$$

The electron polarizability function (2.16) can be simplified to:

$$\begin{aligned} & \text{Re } \Pi_{00}^e(\mathbf{q}, \omega) \\ &= An_e \frac{(2\beta_e m_e)^{1/2}}{\hbar q} \left[ \int_0^{|\mathbf{v}_-|} dx \text{sgn}(\mathbf{v}_-) e^{-(\mathbf{v}_-^2 - x^2)} - \int_0^{|\mathbf{v}_+|} dx \text{sgn}(\mathbf{v}_+) e^{-(\mathbf{v}_+^2 - x^2)} \right], \end{aligned} \quad (3.54)$$

$$\text{Im } \Pi_{00}^e(\mathbf{q}, \omega) = An_e \left[ \frac{\pi\beta_e m_e}{2} \right]^{1/2} \frac{1}{\hbar q} (e^{-\mathbf{v}_+^2} - e^{-\mathbf{v}_-^2}), \quad (3.55)$$

where

$$\mathbf{v}_\pm = \left[ \frac{m_e \beta_e}{2\hbar^2 q^2} \right]^{1/2} \left[ \hbar\omega - \hbar\mathbf{q} \cdot \mathbf{v}_e \pm \frac{\hbar^2 q^2}{2m_e} \right].$$

#### 4 RESULTS AND DISCUSSION

The four equations (3.27), (3.28), (3.42), and (3.43) should be equal to zero simultaneously in the steady state. We solve these equations numerically in the presence of an applied electric field. The approximations we have made in our calculation are: (i) both electron and hole distribution functions are taken as displaced Maxwellian and the lattice temperature is set at 300 K; (ii) electrons and holes are assumed to occupy their lowest subbands. The solution of the four balance equations in the steady state produce the physical quantities  $T_e$ ,  $T_h$ ,  $\mathbf{v}_e$ , and  $\mathbf{v}_h$  as functions of electric field  $E$ . The parameters we have used in calculation are same as in ref 3. The reference sample structure is:  $d_1 = 90 \text{ \AA}$  (GaAs),  $d_2 = 54 \text{ \AA}$  ( $\text{Ga}_{1-x}\text{Al}_x\text{As}$   $p$  doped with Be to  $2 \times 10^{18} \text{ cm}^{-3}$ ), and  $d_3 = 323 \text{ \AA}$  (undoped  $\text{Ga}_{1-x}\text{Al}_x\text{As}$  between the two layers).

The drift velocities of electrons (solid curve) and holes (dot-dashed curve) are plotted in Fig. 3 as functions of the applied electric field in comparison with experimental data. Our calculation shows that the drift velocities of electrons increase

almost linearly with field with a low-field mobility of about  $1700 \text{ cm}^2/\text{V sec}$  and reaches  $10^7 \text{ cm/sec}$  near electric field  $5 \text{ kV/cm}$ . The drift velocity of the hole only reaches  $1.25 \times 10^6 \text{ cm/sec}$  and it increases linearly in  $E$  with a constant mobility  $250 \text{ cm}^2/\text{V sec}$ . In the no-hole case, the drift velocity of electrons (dash curve) is enhanced much faster with increasing electric field and an electron mobility of about  $5800 \text{ cm}^2/\text{V sec}$ . This indicates that the presence of a high density hole plasma causes strong momentum relaxation by electron-hole Coulomb scattering.

The carrier temperatures as functions of electric field  $E$  are plotted in Fig. 4. It shows that both electron and hole temperatures are close to the lattice temperature at very low field, less than  $2 \text{ kV/cm}$ . After the electric field reaches  $4 \text{ kV/cm}$  the minority electrons are more heated than holes. The hole temperature is close to the lattice one even until the electric field reaches  $8 \text{ kV/cm}$ . The difference of two temperatures would be  $300 \text{ K}$  more at high field. The reason for this is that hole-lattice scattering occurs in a spread region of large  $q$  (due to the large effective mass of the heavy hole) and, hence, the sum over  $q$  in Eqs. (3.45) and (3.46) should be performed in a much larger phase space than that of electrons. Also, there is an extra optical deformation potential for coupling with holes. These make the relaxation time of holes 1 order of magnitude smaller than that of the electrons.<sup>18</sup> At high electric fields, there is a quantitative discrepancy between our result and experimental data. This is because: (i) the single subband calculation would not be enough since both electrons and holes could have sufficient kinetic energy gained from the applied electric field to be excited to their upper subband level and other valleys; and (ii) hot phonon effects<sup>19,20</sup> should be considered. These two factors would involve much more complicated calculation and will be discussed in our next work.

The net energy loss rate per electron is plotted in Fig. 5. It can be seen that besides electron-phonon scattering, the energy transfer between electrons and holes is substantial within the temperature range considered in our calculation. The strength of electron-hole coupling depends on the distribution of carriers. At room temperature or above, both electron and hole plasmas can be treated nondegenerately. Thus a large number of electrons and holes contribute to scattering among themselves. The experiment<sup>5</sup> done by Polland, Rühle, Kuhl, Ploog, Fujiwara, and Nakayama shows that electron-hole energy transfer is strongly reduced at low temperature below 40 K due to the degeneracy of the electron plasma. In their case, only a small number of electrons collide with holes. On the other hand, we should mention that electron-hole energy transfer is sensitive to the choice of the bound states of electrons and holes in the  $z$  direction. Stern<sup>9</sup> gave a beautiful method (self-consistent result) of determining the wave function and bound energy in GaAs-Ga<sub>1-x</sub>Al<sub>x</sub>As heterojunctions for the pure electron system. His results show that due to the electrostatic potential and effective potential associated with heterojunction discontinuity, the electron is roughly confined in a small range (less than 50 Å) near each barrier at the high electron density ( $> 5 \times 10^{10}/\text{cm}^2$ ). In the case that minority electrons and majority holes coexist, the electrons can only be bound by the quantum well structure, whereas the hole is bound by self-consistent heterojunction well.<sup>19</sup> Using the variational function<sup>9</sup> with the parameters listed in Ref.3, we estimate that the peak of the lowest band wave function (hole) is located at about the middle of the quantum well. Therefore the wave function of an infinite square well potential would be a good approximation for holes in this case. Under the assumption of infinite square well structure the form factors (2.4), (2.6), and (2.8) have the same structure.

In our calculation we assume the frequencies of longitudinal and transverse optical phonons are dispersionless. A detailed calculation using the phonon-plasmon coupling mode in an electron gas has been presented by Das Sarma *et al.*<sup>21</sup> Their result shows that the coupling effect is significant at low carrier temperatures and densities. When electrons and holes coexist, the phonon Green's functions renormalized by the electron and hole polarizability functions induce a mixing between longitudinal and transverse phonons. This effect has not been considered in this work. Since the frequency difference between the "bare" longitudinal and transverse phonons is small, the frequencies of the new modes mixed then should not change much from their "bare" values. In this near degenerate case, the total carrier-phonon scattering rate will be nearly the same whether "bare" or mixed modes are used, according to the principle of spectroscopic stability.<sup>22</sup> We conjecture that the phonon mixed modes should not qualitatively change our result. However, a quantitative estimate of the importance of the mixing effect is reserved for further work.

## **Part III: Quasianalytical simulation of ultrafast relaxation of photoexcited electrons in a semiconductor**

### **1 INTRODUCTION**

The generation of ultrafast pulses has led to laser-probe techniques<sup>1-7</sup> in studying the relaxation of photoexcited electrons on a subpicosecond time scale. Important information about carrier-carrier interaction, carrier-phonon interaction, and multivalley interaction has been obtained from ultrafast processes. In this time scale the distribution function of electrons differs from a thermal distribution described by an electron temperature, typically, by peaks appearing at some special energy levels. The photoexcited electrons are concentrated in an energy level, which is determined by the frequency of laser pumping and the energy gap between conduction and valence bands. In the relaxation processes of the excited electrons, it is also possible that other peaks appear, for example due to phonon cascade emissions or the existence of subbands. In this case the analytical method that uses a simple electron-temperature model is no longer valid. Most theoretical analyses of ultrafast processes rely on Monte Carlo simulation.<sup>8-11</sup>

It is desirable to have an approach that fills the gap between the Monte Carlo numerical method and the analytic carrier temperature model.<sup>12,13</sup> In the case of weak laser pumping (excited electrons are a small fraction of background electrons), Esipov and Levinson<sup>14-16</sup> have used analytical methods to study the effects of the electron-

electron and electron-phonon scattering, mainly, for steady-state processes. In the present work, we propose an analytical function approach for the time dependent relaxation of a strong laser pumping excited electrons into the semiconductor quantum wells. The distribution function is assumed approximately isotropic during the relaxation process and consists of two parts: (i) Gauss-type energy functions to simulate the nonthermal photoexcited electrons with possible peaks appearing during the relaxation process. (ii) A Maxwell-Boltzmann-type function parametrized by an electron temperature to describe the background electrons. The two-dimensional electron-electron scattering is introduced via a screened Coulomb interaction. At room temperature and above, longitudinal-optical (LO) phonons dominate and contribute to the relaxation of both the carrier distribution and carrier energy. The amplitudes and widths of the time dependent Gauss-type functions and the "electron temperature" are deduced using the Boltzmann equation from a certain initial condition. The merits of this approach are as follows. (1) Some related integrals in the calculation can be analytically worked out or be expressed by a standard integral. Thus only an integral over  $q$  in the Boltzmann equation remains to be numerically handled, greatly reducing the computation time. (2) The evolution of the distribution of electrons is described by the evolution of several parameters. It is convenient for analysis of the results, especially, because the distribution of electrons approaches that of the temperature model after a few picoseconds of laser pumping. (3) This approach may be more suitable for including, for example, dynamical screening effect and so on.

We use the above approach for the case of low-energy photoexcited electrons (close to the band edge, 20 meV). Since the mean energy of these photoexcited electrons in the present calculation is less than the longitudinal-optical-phonon energy,

the carrier-carrier scattering is the primary mechanism in the thermalization processes. Because of the large mass of the heavy hole, the main contribution to relaxation of electrons is through electron-electron scattering with inelastic electron-hole scattering playing a small role, which was pointed out by Goodnick and Lugli.<sup>11</sup> If the mass of the hole is considered as approximately infinite,<sup>10</sup> the electron-hole scattering is elastic. The chief effect of such elastic scattering is to relax the nonisotropic portion of the distribution. Since we have already imposed an isotropic distribution of the electrons, it is appropriate to omit electron-hole scattering in the present paper. This is particularly appropriate for comparison with Monte Carlo simulations that use an infinite hole mass. For the finite (but large) mass case, small inelastic exchange of energy between electrons and holes will have a cumulative effect that will become important at larger times than considered here. Therefore, we omit electron-hole interaction for simplicity. For low-energy photoexcitation with well length about 100 Å, the most electrons occupy the lowest subband state. So we did not include multisubband and multivalley scattering in the present paper. We find that the peak of photoexcited electrons decreases monotonically and the width of the Gauss-type function, which gives the expansion of the nonthermal photoexcited electrons in  $k$  space, increases. Sixty percent of the photoexcited electrons are converted to background electrons within the first 100 fs via the strong electron-electron interaction at low-density excitation ( $2 \times 10^{10} \text{ cm}^{-2}$ ) with background electron density ( $6 \times 10^{10} \text{ cm}^{-2}$ ). Our estimate for the relaxation of photoexcited electrons is qualitatively in agreement with the experiment<sup>1</sup> and the result of Monte Carlo calculation.<sup>10</sup>

The paper is organized as follows. In Sec.II, a form of analytic distribution is assumed. A set of equations for the evolution of relative parameters is derived from the

Boltzmann equation for two-dimensional electrons, including electron-electron and electron-LO-phonon collisions. The detailed results with a brief discussion are presented in Sec.III.

## 2 APPROACH

Laser-probe techniques can create photoexcited electrons sharply peaked in a special energy region within a few femtoseconds. The distribution of electrons can be considered approximately isotropic in the two-dimensional momentum space  $\mathbf{k}$ , if an external electric field is not applied. The energy of the electron in an  $(n, \mathbf{k})$  state is written as  $E_{n, \mathbf{k}} = \mathbf{k}^2/2m_e + E_n$  with  $m_e$  the effective mass of the electron, and  $E_n$  the subband energy. We choose Gauss-type functions in energy space to simulate the peaks at  $E_{n,i}$  for  $i=0,1,2,\dots$  of nonthermal electrons in the  $n$ th subband:

$$f_{n, \mathbf{k}}^1(t) = \sum_i b_{n,i}(t) \exp[-\sigma_{n,i}(t)(E_{n, \mathbf{k}} - E_{n,i})^2]. \quad (2.1)$$

The peak with subindex  $i=0$  represents the directly photoexcited electrons at energy  $E_{n,0}$ . The peaks with  $i=1,2,\dots$  represent peaks produced by cascading phonon emissions. Here  $E_{n,i}$  is the energy level of the  $i$ th peak in  $n$ th subband and  $E_{n,i} = E_{n,0} - i\hbar\omega_{LO}$  with  $\omega_{LO}$  the LO-phonon energy;  $b_{n,i}(t)$  is the amplitude of the  $i$ th peak in  $n$ th subband;  $\sigma_{n,i}$  determines the full width at half height of the peak to be

$$\Delta E_{n,i} = 2 [(\ln 2)/\sigma_{n,i}]^{1/2}, \quad (2.2)$$

The parameters  $b_{n,i}(t)$  and  $\sigma_{n,i}(t)$  are determined by the time-evolution equations. In addition to the photoexcited distribution, we include an equilibrium Maxwell-Boltzmann background distribution of electrons, which is initially small for undoped devices, but is large for  $n$ -doped devices. The expression for this part of electron distribution can be

written as

$$f_{n,\mathbf{k}}^0(t) = a_n(t) \exp[-\beta_e(t)E_{n,\mathbf{k}}] , \quad (2.3)$$

where  $a_n(t)$  determines the density of background electrons in the  $n$ th subband and  $T_e = 1/(k_B\beta_e)$  is the "temperature" of background electrons. The total distribution is normalized to the total electron density:

$$N_e = 2 \sum_{n,\mathbf{k}} f_{n,\mathbf{k}}(t) = 2 \sum_{n,\mathbf{k}} [f_{n,\mathbf{k}}^0(t) + f_{n,\mathbf{k}}^1(t)] . \quad (2.4)$$

Here we neglect the change of electron density due to electron-hole recombination since the typical relaxation time for this process is more than 1 ns.

One of the important scattering mechanisms on the picosecond time scale is electron-electron interaction. For simplicity, we use the static screened electron-electron Coulomb interaction in a two-dimensional heterojunction, which can be expressed in wave-vector space as<sup>13</sup>

$$V_{e-e}^{n'n,m'm}(q) = \frac{2\pi e^2}{\kappa_0(q + q_0)A} F_{e-e}^{n'n,m'm}(q) . \quad (2.5)$$

Here the  $q$  is the momentum exchange in the scattering; the form factor  $F_{e-e}^{n'n,m'm}(q)$  is given by

$$F_{e-e}^{n'n,m'm}(q) = \int_{-\infty}^{\infty} dz dz' e^{-q|z-z'|} \\ \times \xi_{n'}^*(z) \xi_n(z) \xi_m^*(z') \xi_m(z') , \quad (2.6)$$

with  $\xi_n(z)$  the envelope function of the electron in the  $z$  direction which can be generally derived by a variational method.<sup>17,18</sup> The subband energy levels  $E_n$ , for  $n = 0$  and  $n = 1$ , have been given elsewhere<sup>18,19</sup> for a GaAs-Al<sub>x</sub>Ga<sub>1-x</sub>As heterojunction. The

two-dimensional Fermi-Thomas dielectric constant  $q_0 = 2e^2 m_e / \kappa_0 \hbar^2$  (see Ashcroft and Mermin<sup>20</sup>) and  $\kappa_0$  is the static dielectric constant. As far as carrier-lattice interaction is concerned, the electron-LO-phonon scattering dominates at room temperature and above. The electron-LO-phonon scattering is treated as a Coulomb interaction between the electron charge density and the divergence of the polarization associated with a polaron. Using the Fröhlich continuum model,<sup>13</sup> the electron-LO-phonon interaction expression is then given by

$$V_{e-LO}(\mathbf{Q}) = M_{e-LO}(\mathbf{q}, q_z) G_{n'n}(\mathbf{q}, q_z), \quad M_{e-LO}(\mathbf{q}, q_z) = i\alpha/Q, \quad (2.7)$$

where  $\mathbf{Q}(\mathbf{q}, q_z)$  is the 3D LO-phonon momentum, and  $\alpha$  is the Fröhlich electron-LO-phonon coupling constant,  $\alpha = [2\pi e^2 \hbar \omega_{LO} (1/\kappa_\infty - 1/\kappa_0)]^{1/2}$ , with  $\kappa_\infty$  the high-frequency dielectric constant,

$$G_{n'n}(\mathbf{q}, q_z) = \frac{1}{\sqrt{L}} \int_{-\infty}^{\infty} dz \xi_n^*(z) \xi_n(z) e^{iq_z z}. \quad (2.8)$$

The time derivative of the electron distribution can be obtained by using the Boltzmann equation<sup>12,13</sup> with a collision term:

$$\frac{\partial f_{n\mathbf{k}}(t)}{\partial t} = \left[ \frac{\partial f_{n\mathbf{k}}(t)}{\partial t} \right]_{e-e} + \left[ \frac{\partial f_{n\mathbf{k}}(t)}{\partial t} \right]_{e-LO}. \quad (2.9)$$

The first term on the right side due to electron-electron scattering is given by

$$\left[ \frac{\partial f_{n\mathbf{k}}(t)}{\partial t} \right]_{e-e} = \frac{2\pi}{\hbar} \sum_{n', m', m} \sum_{\mathbf{k}', \mathbf{p}', \mathbf{p}} \sum_{\mathbf{q}} [f_{n'\mathbf{k}'} (1-f_{n\mathbf{k}}) f_{m'\mathbf{p}'} (1-f_{m\mathbf{p}})]$$

$$\begin{aligned}
 & - f_{n\mathbf{k}} (1-f_{n'\mathbf{k}'}) f_{m\mathbf{p}} (1-f_{m'\mathbf{p}'}) |V_{e-e}^{n'n, m'm}(\mathbf{q})|^2 \\
 & \times \delta_{\mathbf{k}', \mathbf{k}-\mathbf{q}} \delta_{\mathbf{p}', \mathbf{p}+\mathbf{q}} \delta(E_{n'\mathbf{k}'} + E_{m'\mathbf{p}'} - E_{n\mathbf{k}} - E_{m\mathbf{p}}). \quad (2.10)
 \end{aligned}$$

The first term in the square brackets describes a transition from the electron state with subband energy level  $E_{n'}$  and momentum  $\mathbf{k}'$  into band level  $E_n$  with momentum  $\mathbf{k}$  after collision with another electron. The second term describes the opposite transition. The collision process is governed by momentum and energy conservation. We omit the effects of exchange in the present study. The second term on the right side of Eq.(2.9), due to electron-LO-phonon scattering, is given by

$$\begin{aligned}
 & \left( \frac{\partial f_{n\mathbf{k}}(t)}{\partial t} \right)_{e\text{-LO}} = \frac{4\pi}{\hbar A} \sum_{\mathbf{q}} \sum_{q_z} \sum_{n', \mathbf{k}'} |V_{e\text{-LO}}^{n'n}(\mathbf{q}, q_z)|^2 \\
 & \times \{ f_{n'\mathbf{k}'}(t) [1-f_{n\mathbf{k}}(t)] \delta_{\mathbf{k}', \mathbf{k}+\mathbf{q}} \delta^- - f_{n\mathbf{k}}(t) [1-f_{n'\mathbf{k}'}(t)] \delta_{\mathbf{k}', \mathbf{k}-\mathbf{q}} \delta^+ \} [1+n^{\text{LO}}(T_L)] \\
 & + \{ f_{n'\mathbf{k}'}(t) [1-f_{n\mathbf{k}}(t)] \delta_{\mathbf{k}', \mathbf{k}-\mathbf{q}} \delta^+ - f_{n\mathbf{k}}(t) [1-f_{n'\mathbf{k}'}(t)] \delta_{\mathbf{k}', \mathbf{k}+\mathbf{q}} \delta^- \} n^{\text{LO}}(T_L), \quad (2.11)
 \end{aligned}$$

where

$$\delta^+ = \delta(E_{n'\mathbf{k}'} - E_{n\mathbf{k}} + \hbar\omega_{\text{LO}})$$

and

$$\delta^- = \delta(E_{n'\mathbf{k}'} - E_{n\mathbf{k}} - \hbar\omega_{\text{LO}}).$$

Here  $n^{\text{LO}}(T_L)$  is the LO-phonon occupation number and is assumed in equilibrium at

lattice temperature  $T_L$ . The hot-phonon effect is neglected here since the nonequilibrium phonons are not yet excited on a subpicosecond time scale. The total electron-energy loss due to electron-LO-phonon emission can be expressed as

$$\left( \frac{dE_e}{dt} \right)_{e-LO} = - \sum_{\mathbf{q}} \hbar \omega_{LO} \Gamma_{e-LO} , \quad (2.12)$$

$$\Gamma_{e-LO} = \frac{2\pi}{\hbar} \sum_{n',n} \sum_{q_z} |V_{e-LO}^{n'n}(\mathbf{q}, q_z)|^2 \times \{ I_{n'n}^{(+)}(\mathbf{q}, \omega) [1 + n^{LO}(T_L)] - I_{n'n}^{(-)}(\mathbf{q}, \omega) n^{LO}(T_L) \} , \quad (2.13)$$

and

$$I_{n'n}^{(\pm)}(\mathbf{q}, \omega) = \frac{2}{A} \sum_{\mathbf{k}'} \sum_{\mathbf{k}} f_{n\mathbf{k}}(t) [1 - f_{n'\mathbf{k}'}(t)] \times \delta_{\mathbf{k}', \mathbf{k} + \mathbf{q}} \delta(E_{n\mathbf{k}} - E_{n'\mathbf{k}'} \pm \hbar \omega_{LO}) , \quad (2.14)$$

In the following calculation, the above approach is applied to the case of high electron density. Peaks due to cascading phonon emission are then suppressed by the strong electron-electron scattering. For simplicity, the electrons are assumed to occupy the lowest subband only. With these assumptions our formulas can be simplified. The integral over  $\mathbf{k}'$  and  $\mathbf{p}$  in Eq. (2.10) can be completed or reduced to a known special function. Only the final integral over  $\mathbf{q}$  requires numerical calculation. By using the dimensionless variables

$$y = \beta_0 \frac{\hbar^2 k^2}{2m_e} , z = \beta_0 \frac{\hbar^2 q^2}{2m_e} , y_0 = \beta_0 E_{0,0} ,$$

$$\rho(t) = \frac{\beta_e(t)}{\beta_0} , \gamma(t) = \frac{\sigma_{0,0}(t)}{\beta_0^2} , \omega_0 = \beta_0 \hbar \omega , \quad (2.15)$$

where  $\beta_0$  is the scaling factor with dimension of  $1/(k_B T)$ , and defining

$$f_{n,\mathbf{k}}(t) \approx \delta_{n,0} f(y,t), \quad F_{e-e}^{00,00}(\mathbf{q}) = F_{e-e}^0(z), \quad (2.16)$$

Eq. (2.10) can be reduced to

$$\begin{aligned} \left( \frac{\partial f(y,t)}{\partial t} \right)_{e-e} &= \frac{2m_e}{\pi \hbar^3} \left( \frac{e^2}{\kappa_0} \right)^2 \\ &\times \int_0^\infty dz \int_0^\pi d\phi \left[ \frac{F_{e-e}^0(z)}{z+z_0} \right]^2 \\ &\times [b_{0,0}^2(t) (2/\gamma^{1/4}) \{ \exp[-\gamma(\eta-y_0)^2] D_1(\mu_-) - \exp[-\gamma(y-y_0)^2] D_1(\mu_+) \} \\ &+ a_0(t) b_{0,0}(t) (\sqrt{\pi/\rho} \{ \exp[-\gamma(\eta-y_0)^2 - \rho z_-^2] - \exp[-\gamma(y-y_0)^2 - \rho z_+^2] \} \\ &+ (2/\gamma^{1/4}) [ \exp(-\rho\eta) D_1(\mu_-) - \exp(-\rho y) D_1(\mu_+) ] )], \end{aligned} \quad (2.17)$$

where

$$D_1(x) = \int_0^\infty d\eta \exp[-(x+\eta^2)^2], \quad (2.18)$$

and

$$z_\pm = \frac{\omega_0 \pm z}{2z^{1/2}}, \quad \mu_\pm = \gamma^{1/2} (z_\pm^2 - y_0),$$

with

$$\omega_0 = y - 2y^{1/2}x^{1/2}\cos\phi,$$

$$\eta = y + x - 2y^{1/2}x^{1/2}\cos\phi .$$

The first term in the bold square brackets ( [ ] ) of Eq. (2.17) represents the contribution from electron-electron scattering among photoexcited electrons. The second term in [ ] stands for the scattering between photoexcited and background electrons. The scattering among background electrons cancels on the whole since these electrons are in equilibrium with each other. The electron distribution Eq. (2.11) can be reduced to

$$\left[ \frac{\partial f(y,t)}{\partial t} \right]_{e-LO} = \frac{\alpha^2}{\hbar^2 \pi} (2m_e \beta_0)^{1/2}$$

$$\times (\{ f(y+w,t) [1-f(y,t)] [1+n^{LO}(T_L)] - f(y,t) [1-f(y+w,t)] n^{LO}(T_L) \} \Phi^+(y,w)$$

$$- \{ f(y-w,t) [1-f(y,t)] [1+n^{LO}(T_L)] - f(y,t) [1-f(y-w,t)] n^{LO}(T_L) \} \Phi^-(y,w) ) , \quad (2.19)$$

where

$$\Phi^\pm(y,w) = \int_0^{\theta^\pm} \frac{dz}{\sqrt{2\theta^{\pm 2} - z^2}} \times \left[ \frac{F_{e-e}^0(\delta_1^\pm + z^2)}{\sqrt{\delta_1^\pm + z^2}} + \frac{F_{e-e}^0(\delta_2^\pm - z^2)}{\sqrt{\delta_2^\pm - z^2}} \right] , \quad (2.20)$$

with

$$\theta^\pm = 2^{1/2} [y(y \pm w)]^{1/4} , \quad w = \beta_0 \hbar \omega_{LO} ,$$

$$\delta_1^\pm = 2y \pm w - \theta^{\pm 2} , \quad \delta_2^\pm = 2y \pm w + \theta^{\pm 2} . \quad (2.21)$$

The Eq. (2.12) can be simplified to

$$\left[ \frac{dE_e(t)}{dt} \right]_{e-LO} = -\frac{A\hbar\omega_{LO}}{2\beta_0^{1/2}\pi^2} \left[ \frac{2m_e}{\hbar^2} \right]^{3/2} \frac{\alpha^2}{2\hbar} \times \int_0^\infty dz \frac{F_{e-e}^0(z)}{z} \times (\Delta E_1 + \Delta E_2), \quad (2.22)$$

where  $F_{e-e}^0(z)$  is defined in Eq. (2.16),

$$\Delta E_1 = \frac{a_0(t)}{2} \left[ \frac{\pi}{\rho} \right]^{1/2} \exp(-\rho z_+^2) \times \{ [1+n^{LO}(T_L)] - n^{LO}(T_L) \exp(\rho w) \}, \quad (2.23)$$

and

$$\Delta E_2 = \frac{b_{0,0}(t)}{\gamma^{1/4}} \{ D_1(\mu_-) [1+n^{LO}(T_L)] - D_1(\mu_+) n^{LO}(T_L) \} \quad (2.24)$$

are, respectively, the contributions due to background electron-phonon scattering and photoexcited electron-phonon scattering. On the other hand, the time derivatives of electron-energy loss and electron distribution as well as of the total electron density can be written via the time differential of parameters  $a_0(t)$ ,  $b_{0,0}(t)$ ,  $\gamma(t)$ , and  $\rho(t)$  as

$$\frac{dE(t)}{dt} = \frac{\partial E(t)}{\partial b_{0,0}} \dot{b}_{0,0} + \frac{\partial E(t)}{\partial \gamma} \dot{\gamma} + \frac{\partial E(t)}{\partial \rho} \dot{\rho} + \frac{\partial E(t)}{\partial a} \dot{a}, \quad (2.25)$$

$$\frac{\partial f(y,t)}{\partial t} = \frac{\partial f(y,t)}{\partial b_{0,0}} \dot{b}_{0,0} + \frac{\partial f(y,t)}{\partial \gamma} \dot{\gamma} + \frac{\partial f(y,t)}{\partial \rho} \dot{\rho} + \frac{\partial f(y,t)}{\partial a_0} \dot{a}_0, \quad (2.26)$$

$$0 = \frac{\partial n_e}{\partial b_{0,0}} \dot{b}_{0,0} + \frac{\partial n_e}{\partial \gamma} \dot{\gamma} + \frac{\partial n_e}{\partial \rho} \dot{\rho} + \frac{\partial n_e}{\partial a_0} \dot{a}_0, \quad (2.27)$$

In our approximation, there are four independent variables which should be determined by Eqs. (2.25), (2.26), and (2.27). Here we choose the values of  $\partial f(y,t)/\partial t$  in Eq. (2.26) at two special  $y$  points, which correspond to the peak position and the half-width position of a Gauss-type peak in order to obtain information sensitive to the height and width parameters,  $b_{0,0}$  and  $\gamma$ . Thus the change of parameters in each time step can be

obtained by solving four linear equations with given initial condition.

### 3 RESULTS AND DISCUSSION

The time interval we choose in solving the difference equations is 0.1 fs. The result shows no significant change if an interval less than 0.1 fs is used. The initial conditions used in the present calculation are as follows: the temperature of the background electrons is set at lattice temperature  $T_e = T_L = 300$  K; the peak position of photoexcited electrons is located at 0.02 eV above the conduction-band edge; the width of the peak is chosen as 0.02 eV, which is comparable with that found in the time luminescence experiments.<sup>1</sup> The amplitude  $b_{0,0}(0)$  is chosen such that the density of photoexcited electrons is  $2 \times 10^{10} \text{ cm}^{-2}$ . The effective mass of an electron in GaAs is  $0.067m_0$ , with  $m_0$  the free mass of an electron. The energy of a LO-phonon,  $\hbar\omega_{LO}$ , is 36.8 meV, with  $\kappa_0 = 10.91$  and  $\kappa_\infty = 12.91$ . On a VAX-780 running Berkeley 4.3 UNIX, it takes 5 s (CPU) to calculate each time interval of 0.1 fs. So within 1.4 h we can reach 100 fs.

The electron distribution is plotted in Fig. 1 as a function of the energy of the electrons at different times. The photoexcited electron density is chosen as  $2 \times 10^{10} \text{ cm}^{-2}$  with a background electron density  $6 \times 10^{10} \text{ cm}^{-2}$ . The sharp peak of photoexcited electrons decreases and expands monotonically. The amplitude of the Gauss-type function decreases to about 40% of its initial value in the first 100 fs and then tends to vanish at about 200 fs. After 200 fs a Maxwellian-like shape which can be described by a temperature model appears. The result of Bailey *et al.*<sup>10</sup> Monte Carlo calculation is also shown in Fig. 1. Our result is in reasonable agreement with that of the Monte Carlo calculation. A detailed comparison indicates that the thermalization process in our

present model is a little faster than that of Monte Carlo simulation. In particular, the electron occupation with low energy in our result increases faster compared with that of the Monte Carlo simulation. The electron distribution with low background density ( $10^9 \text{ cm}^{-2}$ ) at the same excitation density is plotted in Fig. 2. The small amount of background electrons decreases the thermalization rate. The amplitude of the Gauss-type function decreases to about 51% of its initial value in the first 100 fs and then tends to vanish at about 280 fs.

The temperature  $T_e$  of the background electrons as a function of time is plotted in Fig. 3 with background density  $6 \times 10^{10} \text{ cm}^{-2}$  and excitation density  $2 \times 10^{10} \text{ cm}^{-2}$ . It is set at 300 K at the initial time and then it increases for the first 30 fs because in this period the dominant process is energy transfer from the photoexcited electrons to background electrons. At about 40 fs  $T_e$  arrives at a maximum value, then decreases mainly via electron-phonon interaction and approaches the lattice temperature after 350 fs.

In summary, we have proposed a simplified model to describe the complex nonequilibrium relaxation of photo-electrons in a semiconductor quantum well. As a first application we have calculated the relaxation of low-energy photoexcited pumping by use of an approach including only four parameters. In contrast to the approach by Esipov and Levinson,<sup>14</sup> our method does not require that the excited electrons be a small fraction of the background electrons. Since the electron-electron collisions among excited electrons are properly considered, our approach can be used for an arbitrary proportion of excited electrons and background electrons. We also use the generally available electron-phonon scattering matrix for a quasi-two-dimensional quantum well.

In our present model we use four parameters, which permits a description of the chief physical properties of the ultrafast process. In our model, nonphotoexcited electrons were assumed to be directly thermalized. As a result the electron occupation of low energy in our present model approaches the Maxwell-Boltzmann distribution faster than that of Monte-Carlo simulation. We have imposed a Gaussian peak, which prevents unsymmetrical decay from occurring. Since energy absorption and emission is necessarily nonsymmetric, this must be compensated for by using nonsymmetric basis function, or more simply by using more symmetric ones. At present in introducing the new technique, we restrict ourselves to try to describe the ultrafast process.

One interesting question is to determine how low the density of excited electrons should be for peaks associated with cascade LO-phonon emission to be visible. As shown in the formulation of this paper, the cascade problem can be studied by using our approach with more parameters. Numerical computation is in progress. Further work including dynamical screening is under consideration.

## **Part IV: Resonant level lifetime in GaAs/AlGaAs double-barrier structures with consideration of $\Gamma$ -X mixing**

### **1 INTRODUCTION**

Recently, there has been considerable interest in  $\text{Ga}_{1-x}\text{Al}_x\text{As-GaAs-Ga}_{1-x}\text{Al}_x\text{As}$  double-barrier structures because of their technological importance to high speed devices. These structures exhibit a number of interesting features, some of which are concerned with the evidence of  $\Gamma$  and  $X$  transfer in resonant tunneling in single and double barriers.<sup>1-4</sup> The experiments done by Mendez and his co-workers<sup>1</sup> show that the existence of confined states in  $\text{Ga}_{1-x}\text{Al}_x\text{As}$  at the  $X$  point gives a new resonant tunneling peak in some structures. Their results were explained by a quasi-bound state associated with the  $X$ -point band. Osbourn and Smith<sup>5</sup> have discussed  $\Gamma$ - $X$  transmission using the empirical tight-binding approximation in 1979. Later, Mailhot, Smith and McGill<sup>6</sup> studied the effect of  $\Gamma$ - $L$  mixing. Recent discussions of  $\Gamma$ - $X$  mixing are referred in Ref 7-10.

The conduction-band edge profiles for both  $\Gamma$  and  $X$  minima of  $\text{Al}_x\text{Ga}_{1-x}\text{As}$  were discussed by Batey and Wright<sup>11</sup> and in the review paper<sup>12</sup> written by Adachi. Their results show that, at some doping, the  $X$ -band minimum (conduction) can be lower than the  $\Gamma$ -band minimum (conduction) in  $\text{Ga}_{1-x}\text{Al}_x\text{As}$  and also lower than the  $X$ -band minimum in GaAs as shown in Fig. 1. This structure will induce a bound state for  $X$ -electrons confined in the double-barrier region, while the  $\Gamma$ -electrons form a quasi-

bound state and can leak out with some probability, if the GaAs substrate outside the double-barrier region is thick enough. General speaking, when electrons are photo-excited to the  $\Gamma$  valley conduction band inside a quantum well, the electrons will have a certain probability to transfer to  $X$  valley conduction band. Since a momentum change is required in the  $\Gamma$ - $X$  transfer, the intervalley scatterings appear only at the interfaces in the intrinsic tunneling case, and can be described by intervalley transfer potentials  $V_{\Gamma X}$  and  $V_{X\Gamma}$ . This  $\Gamma$ - $X$  transfers will effect the leakage rate of electrons out of the double-barrier region. In some design devices where the quasi-bound  $\Gamma$  energy level is close to some  $X$  energy level, a resonance of  $\Gamma$ - $X$  transfers may occur and induce a dramatic change of leakage rate of electrons. It is interesting to study the effect on the lifetime of electrons due to the  $\Gamma$ - $X$  coupling in such a energy level region.

In this paper, we present a quantitative model which gives a quantum mechanical calculation of the resonant level lifetime in the presence of  $\Gamma$ - $X$  coupling. Our results show that when the  $\Gamma$ -like energy level is not degenerate with an  $X$ -like energy level, the lifetime of  $\Gamma$  state is exponentially proportional to the thickness of  $\text{Ga}_{1-x}\text{Al}_x\text{As}$ . This is in agreement with the experiment done by Tsuchiya and his co-workers<sup>13</sup> and the theoretical calculation of Thomas *et al.*<sup>14</sup> However, for the case that the  $\Gamma$  energy levels become degenerate with the  $X$  energy levels, the lifetime dramatically changes and can be several orders longer than that of a pure  $\Gamma$  system.

The paper is organized as follows: in Sec.II a quantum mechanical model is described and the matrix is found, the vanishing of whose determinant yields the complex eigenvalues. Detailed results and a brief discussion are presented in Sec.III.

## 2 MODEL

We employ the following theoretical model which introduces a coupling between  $\Gamma$  and  $X$  minima within the effective mass envelope function approach: 1) Quasi-bound state theory is applied to our problem, so that the eigenvalue of the Hamiltonian becomes complex. The real part of the eigenvalue stands for the energy level of the state and the imaginary part relates to the lifetime of state. 2) Since the transfer between  $\Gamma$  and  $X$  is assumed to occur only at a heterointerface, for simplicity, we introduce a delta function potential to describe  $\Gamma$ - $X$  coupling, as was done by Liu<sup>9</sup>. 3) A spinor-like matrix formula is used with the upper component describing the  $\Gamma$  wave function, while the lower component describes the  $X$  wave function.

The Schrodinger equation can be written as:

$$H\Psi = E\Psi , \quad (2.1)$$

$$H = T + V , \quad (2.2)$$

where

$$E = e - i\frac{\hbar\gamma}{2} , \quad (2.3)$$

$e$  is the energy level of the state and  $\gamma$  is its the reciprocal lifetime,  $T$  is the kinetic energy operator,  $T$  can be expressed as:

$$T = \begin{bmatrix} -\frac{\hbar^2}{2} \frac{\partial}{\partial z} \frac{1}{m_{\Gamma}(z)} \frac{\partial}{\partial z} & 0 \\ 0 & -\frac{\hbar^2}{2} \frac{\partial}{\partial z} \frac{1}{m_X(z)} \frac{\partial}{\partial z} \end{bmatrix} \quad (2.4)$$

where  $m_{\Gamma}(z)$  and  $m_X(z)$  are the effective masses for the  $\Gamma$  point and  $X$  point,

respectively.  $V$  is the potential energy:

$$V = \begin{bmatrix} V_{\Gamma}(z) & V_I(z) \\ V_I(z) & V_X(z) \end{bmatrix}, \quad (2.5)$$

the diagonal elements  $V_{\Gamma}(z)$  and  $V_X(z)$  represent pure  $\Gamma$  and pure  $X$  band profiles, which can be written as:

$$V_{\Gamma}(z) = \begin{cases} 0 & \text{if } l \geq |z| \\ V_{\Gamma 0} & \text{if } l+b > |z| > l, \\ 0 & \text{if } |z| \geq l+b \end{cases} \quad (2.6)$$

$$V_X(z) = \begin{cases} V_{X0} & \text{if } l \geq |z| \\ V_{X1} & \text{if } l+b > |z| > l. \\ V_{X0} & \text{if } |z| \geq l+b \end{cases} \quad (2.7)$$

The potential heights  $V_{\Gamma 0}$ ,  $V_{X0}$  and  $V_{X1}$  depend on doping as discussed in detail in Ref. 9 and Ref. 10. The off-diagonal elements stand for the  $\Gamma$  and  $X$  interaction potentials:

$$V_I(z) = \alpha [\delta(|z| - l) + \delta(|z| - (l+b))], \quad (2.8)$$

where  $\alpha$  is a coupling parameter, and  $\delta$  is the Dirac-delta function. The off-diagonal terms quantify the intervalley transfer potentials. In general, the parameter  $\alpha$  could be a complex number, but we use a real one for simplicity. Under this assumption, there is only one parameter to be determined by experiment.

$\Psi$  is a two-component wave function:

$$\Psi = \begin{bmatrix} \Psi_{\Gamma} \\ \Psi_X \end{bmatrix}, \quad (2.9)$$

Using the Hamiltonian given above, we can write down the quasi-bound state wave function in the space  $z > 0$  (even state)

$$\Psi_{\Gamma}(z) = \begin{cases} A \cos(gz) & \text{if } 0 \leq z \leq l \\ B e^{g_1 z} + C e^{-g_1 z} & \text{if } l < z < l+b, \\ D e^{igz} & \text{if } z \geq l+b \end{cases} \quad (2.10)$$

with

$$g = \left[ \frac{2m_{\Gamma 0} E}{\hbar^2} \right]^{1/2}, \quad g_1 = \left[ \frac{2m_{\Gamma 1} (V_{\Gamma 0} - E)}{\hbar^2} \right]^{1/2},$$

where  $m_{\Gamma 0}$  and  $m_{\Gamma 1}$  are, respectively, the electron masses in the GaAs and  $\text{Ga}_{1-x}\text{Al}_x\text{As}$   $\Gamma$  valleys.

$$\Psi_X(z) = \begin{cases} A_1 (e^{qz} + e^{-qz}) & \text{if } 0 \leq z \leq l \\ B_1 e^{iq_1 z} + C_1 e^{-iq_1 z} & \text{if } l < z < l+b, \\ D_1 e^{-qz} & \text{if } z \geq l+b \end{cases} \quad (2.11)$$

where

$$q = \left[ \frac{2m_{X0} (V_{X0} - E)}{\hbar^2} \right]^{1/2}, \quad q_1 = \left[ \frac{2m_{X1} (E - V_{X1})}{\hbar^2} \right]^{1/2},$$

where  $m_{X0}$  and  $m_{X1}$  are, respectively, the electron masses in GaAs and  $\text{Ga}_{1-x}\text{Al}_x\text{As}$  of X valley. The boundary conditions at the interfaces can be written as:

$$\begin{bmatrix} \Psi_{\Gamma} \\ \Psi_X \end{bmatrix}_{z=l^+} = \begin{bmatrix} \Psi_{\Gamma} \\ \Psi_X \end{bmatrix}_{z=l^-}, \quad (2.12)$$

$$\begin{bmatrix} \Psi_{\Gamma} \\ \Psi_X \end{bmatrix}_{z=l+b^+} = \begin{bmatrix} \Psi_{\Gamma} \\ \Psi_X \end{bmatrix}_{z=l+b^-}, \quad (2.13)$$

$$-\left[ \frac{\hbar^2}{2} \frac{1}{m_{\Gamma 1}} \frac{\partial \Psi_{\Gamma}}{\partial z} \right]_{z=l^+} + \left[ \frac{\hbar^2}{2} \frac{1}{m_{\Gamma 0}} \frac{\partial \Psi_{\Gamma}}{\partial z} \right]_{z=l^-} + \alpha \Psi_X(l) = 0 \quad (2.14)$$

$$-\left[ \frac{\hbar^2}{2} \frac{1}{m_{X1}} \frac{\partial \psi_X}{\partial z} \right]_{z=l^+} + \left[ \frac{\hbar^2}{2} \frac{1}{m_{X0}} \frac{\partial \psi_X}{\partial z} \right]_{z=l^-} + \alpha \psi_\Gamma(l) = 0 \quad (2.15)$$

$$-\left[ \frac{\hbar^2}{2} \frac{1}{m_{\Gamma 0}} \frac{\partial \psi_\Gamma}{\partial z} \right]_{z=l+b^+} + \left[ \frac{\hbar^2}{2} \frac{1}{m_{\Gamma 1}} \frac{\partial \psi_\Gamma}{\partial z} \right]_{z=l+b^-} + \alpha \psi_X(l+b) = 0 \quad (2.16)$$

$$-\left[ \frac{\hbar^2}{2} \frac{1}{m_{X0}} \frac{\partial \psi_X}{\partial z} \right]_{z=l+b^+} + \left[ \frac{\hbar^2}{2} \frac{1}{m_{X1}} \frac{\partial \psi_X}{\partial z} \right]_{z=l+b^-} + \alpha \psi_\Gamma(l+b) = 0. \quad (2.17)$$

Therefore we have eight homogeneous equations with unknown coefficients  $A$ ,  $B$ ,  $C$ ,  $D$ ,  $A_1$ ,  $B_1$ ,  $C_1$  and  $D_1$ . For obtaining a nontrivial solution we require the determinant of the coefficient matrix to be zero and get the complex eigenvalue.

### 3 RESULTS AND DISCUSSION

Exact solution of the eight complex boundary equations (2.12-2.17) gives the complex eigenvalue  $E$  as a functions of GaAs quantum well width and  $\text{Ga}_{1-x}\text{Al}_x\text{As}$  barrier thickness. For the decoupled system, the energy level of the  $\Gamma$  state mainly depends on the width of the quantum well and is not sensitive to the thickness of  $\text{Ga}_{1-x}\text{Al}_x\text{As}$  except for the case in which the  $\text{Ga}_{1-x}\text{Al}_x\text{As}$  is very thin (the condition for a quasi-bound state is then not valid). In contrast, the  $X$  energy level mainly depends on the thickness of the  $\text{Ga}_{1-x}\text{Al}_x\text{As}$  barrier.

Fig. 2 shows the energy levels of ground state as function of  $b/l$ , the ratio of  $\text{Ga}_{1-x}\text{Al}_x\text{As}$  thickness  $b$  to GaAs well half width  $l$ , in the presence of  $\Gamma$ - $X$  coupling. The results of decoupling are also plotted in the same figure: dotted-line for  $X$  and dashed-line for  $\Gamma$ . The two solutions in the presence of coupling behave differently around the mixing point ( $b/l = \lambda = 2.022$ ):  $E_1$  changes from  $X$ -like to  $\Gamma$ -like after passing through mixing point, whereas  $E_2$  changes from  $\Gamma$ -like to  $X$ -like. In the mixing region,

these two solutions anticross and are neither  $\Gamma$ -like nor  $X$ -like.

The lifetimes  $\tau_1$ ,  $\tau_2$  which relate to the imaginary parts of the eigenvalues of these two solutions in the presence of coupling are plotted in Fig. 3. The lifetime of a pure  $\Gamma$  state depends exponentially on the thickness of the  $\text{Ga}_{1-x}\text{Al}_x\text{As}$  barrier. The latter is also shown in Fig. 3 (dashed line) for comparison. The lifetime of a pure  $X$  state is infinite. It is a true bound state because the potential in the well is below that at infinity.  $\tau_1$  changes from  $X$ -like to  $\Gamma$ -like when passing through the mixing point. Near the mixing point,  $\tau_1$  changes sharply and can be several orders larger than that of a pure  $\Gamma$  system. Meanwhile  $\tau_2$  changes smoothly from  $\Gamma$ -like to  $X$ -like. The peak position is not sensitive to the value of coupling strength.

To understand the solution with the long life time, the  $E_1, \tau_1$  state, we also calculated the wave function of that solution. We see that when  $b/l \ll \lambda$ , the solution can be distinguished as  $X$ -like, so the  $X$ -component wave function is large and the  $\Gamma$ -component wave function is rather small. On the other hand ( $b/l \gg \lambda$ ), the solution can be recognized as  $\Gamma$ -like, the  $X$ -component wave function is rather small and  $\Gamma$ -component wave function is large. Only when  $b/l \approx \lambda$ , are both  $\Gamma$ -component and  $X$ -component wave functions large. See Fig. 4. In this case the coupling between  $\Gamma$ -component and  $X$  component plays an important role, which permits the  $\Gamma$ -component amplitude  $D$  in region  $z \geq l+b$  (see Eq. (2.10)) to dramatically decrease (see Fig. 5) which shows consistency with Fig. 3. Thus, the life time becomes very long because the electron wave-function hardly leaks out.

To observe experimentally the effect of  $\Gamma$ - $X$  coupling on electron escape time in  $\text{GaAs}/\text{AlAs}$  double barrier structure, we plan to use picosecond time-resolved photoluminescence experiments on a sample. Since it is not easy to control the barrier

thickness, we suggest two possible methods: 1) Applying a small electric field to the sample whose lowest  $\Gamma$  energy level and  $X$  energy level are close to each other. 2) Application of hydrostatic pressure to change the relative positions of  $\Gamma$  - and  $X$ - point barrier.<sup>15</sup>

The electron-hole recombination time is determined by radiative and non-radiative lifetimes. The radiative lifetime is about  $100ns$  for low concentration ( $10^{16}cm^{-3}$ ) at room temperature,<sup>16-17</sup> the non-radiative lifetime is sample dependent, with a range from  $45$  to  $650ns$ .<sup>18-19</sup> The sharp life time peak in Fig. 3 should be reduced if the recombination time is taken into consideration. Assuming the radiative and non-radiative lifetimes are  $100ns$  and approximately independent of barrier thickness for simplicity, we calculate  $\tilde{\tau}_1$  by  $1/\tilde{\tau}_1 = 1/\tau_1 + 1/\tau_r$  where  $\tau_r$  is the total recombination time and  $\tau_1$  is shown in Fig. 3. We plot  $\tilde{\tau}_1$  in Fig. 6, which shows a large reduction of peak compared to that in Fig. 3, yet a visible peak can still be obtained.

In conclusion, we have presented a model to study the effect of the  $\Gamma$ - $X$  intervalley coupling on the lifetime of a quasi-bound state in a GaAlAs-GaAs-GaAlAs structure. We find that the lifetime of a photo-excited electron at some quasi-bound state in a GaAs well can be several orders longer than that of a pure  $\Gamma$  system if the energy level of this state is nearly equal to the energy level of the  $X$  state.

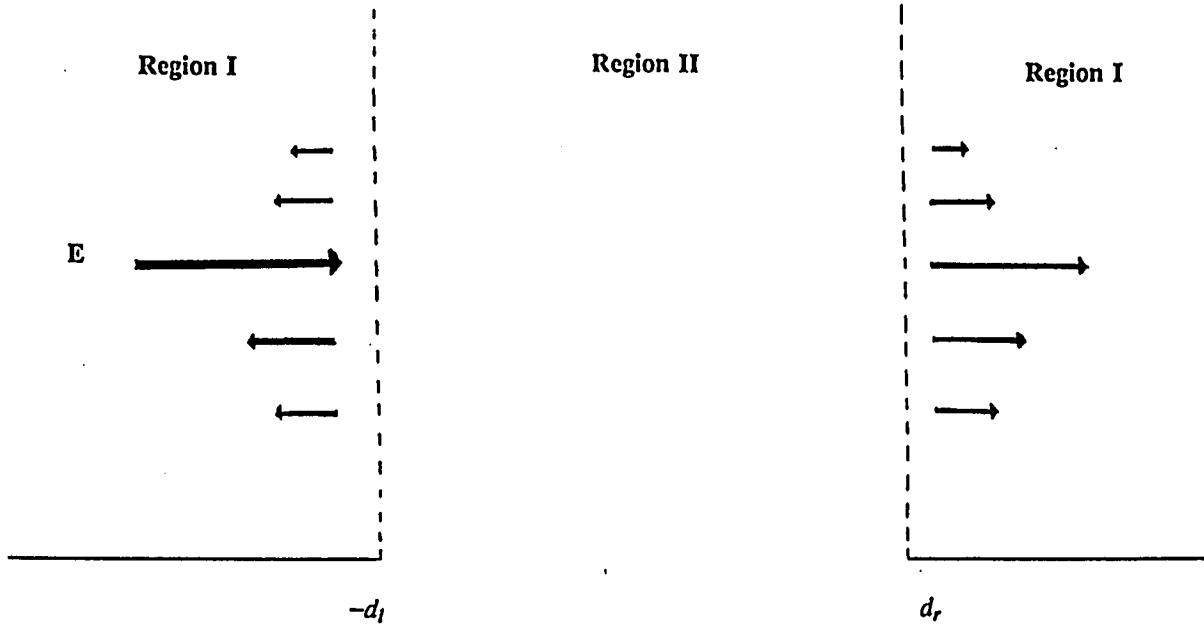


FIG. 1

Part I

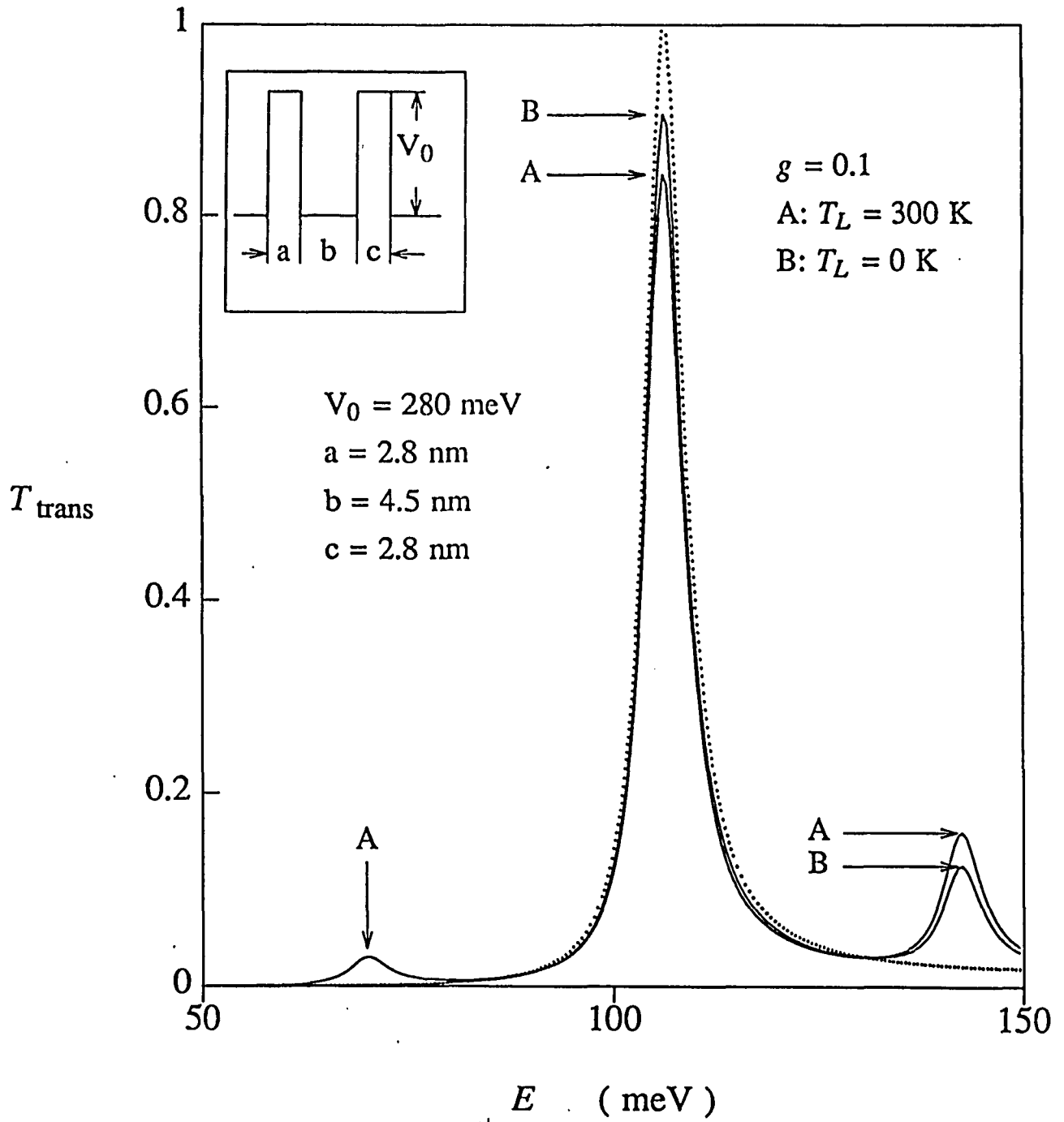


FIG. 2

Part I

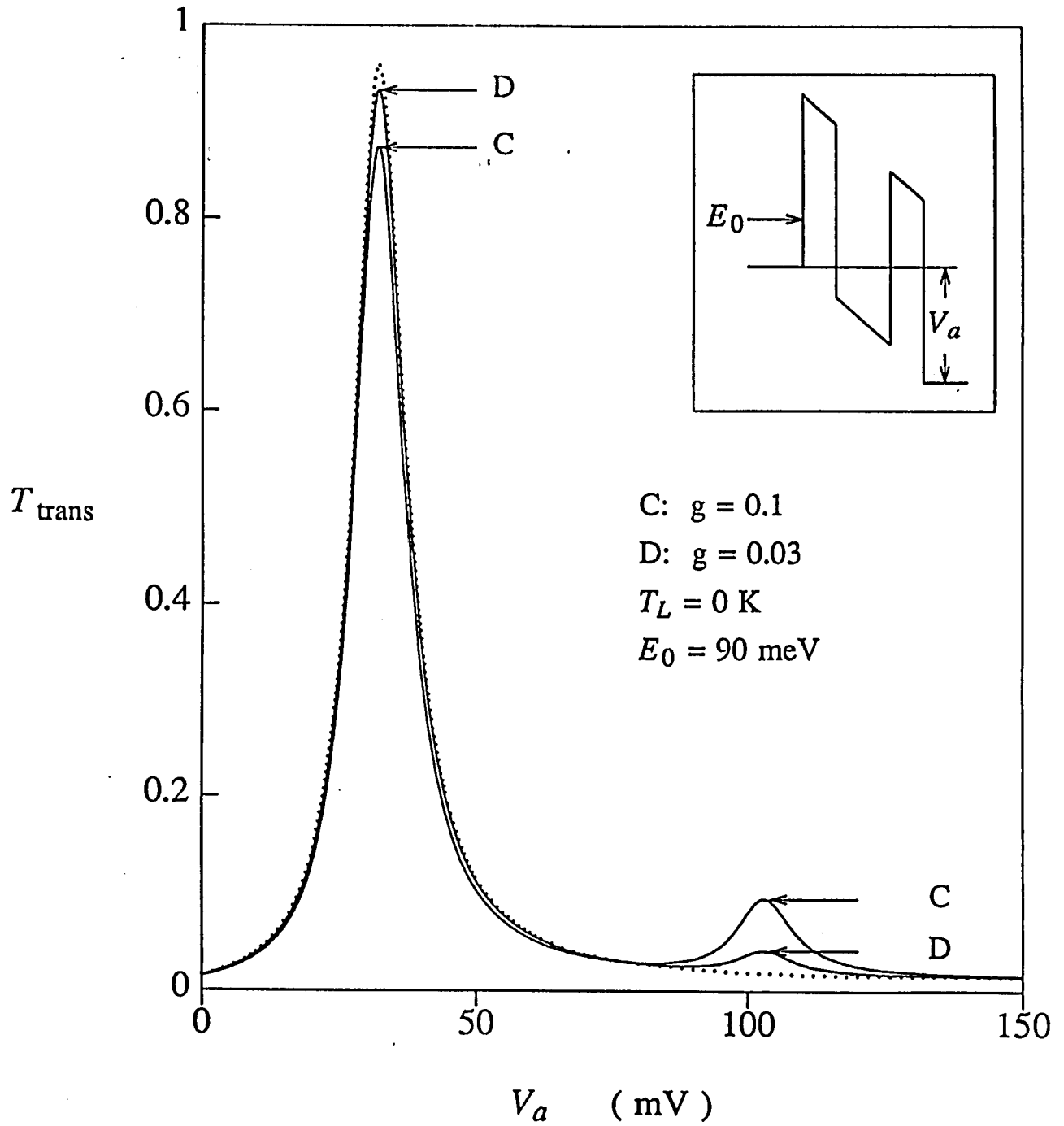


FIG. 3

Part I

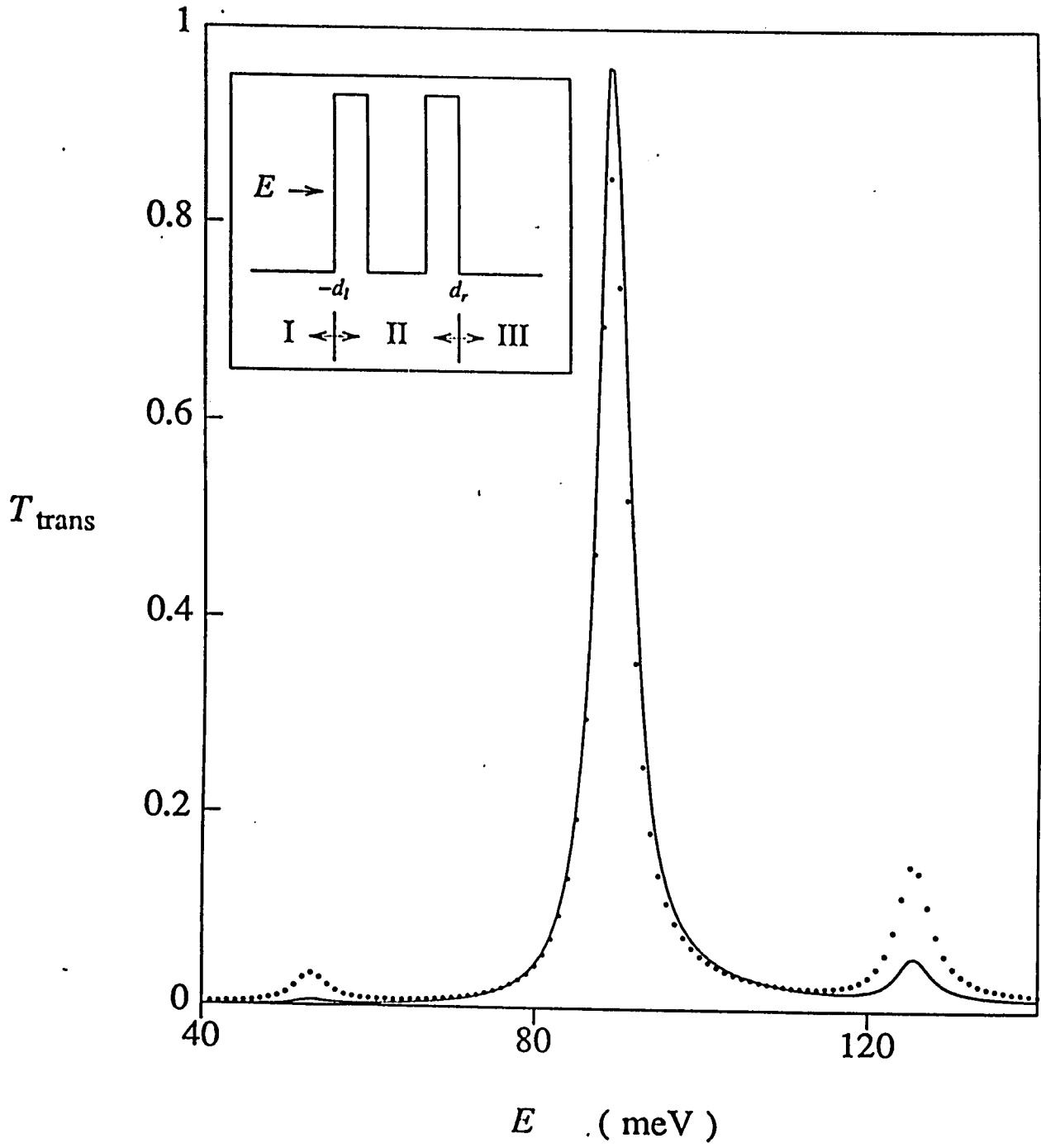


FIG. 4

Part I

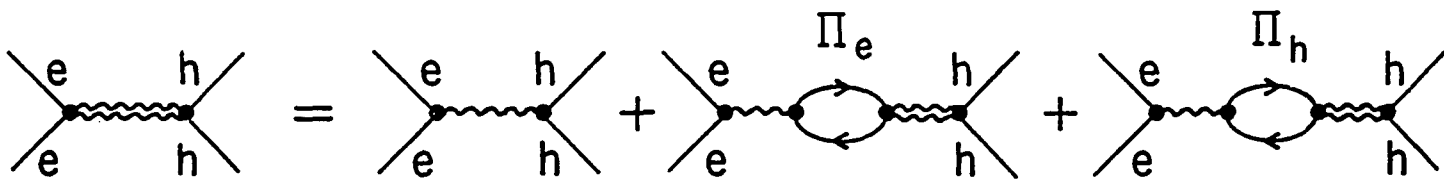
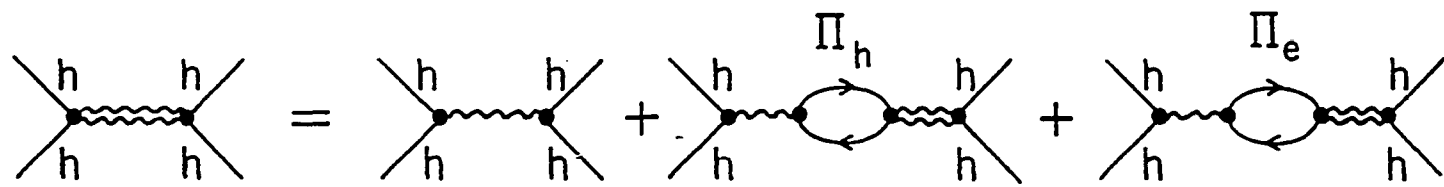
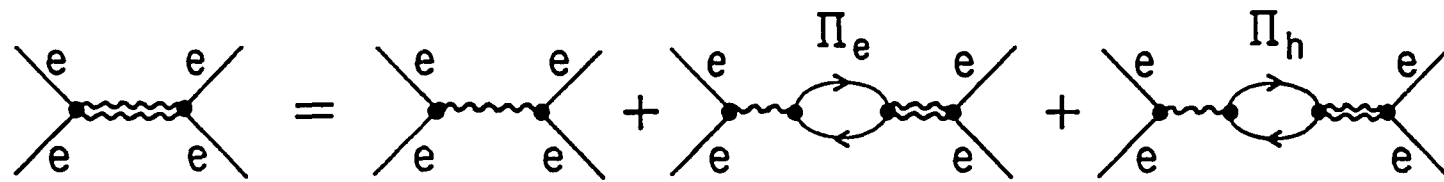


FIG. 1

Part II

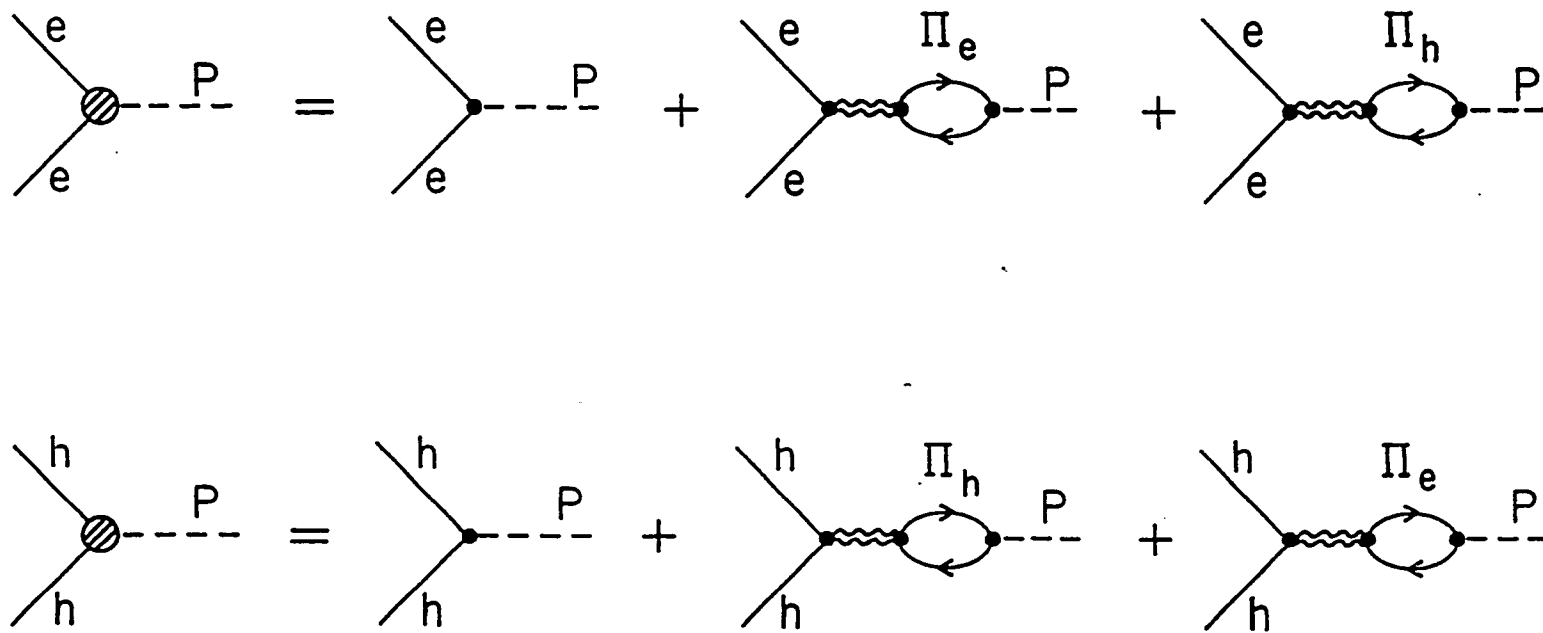


FIG. 2

Part II

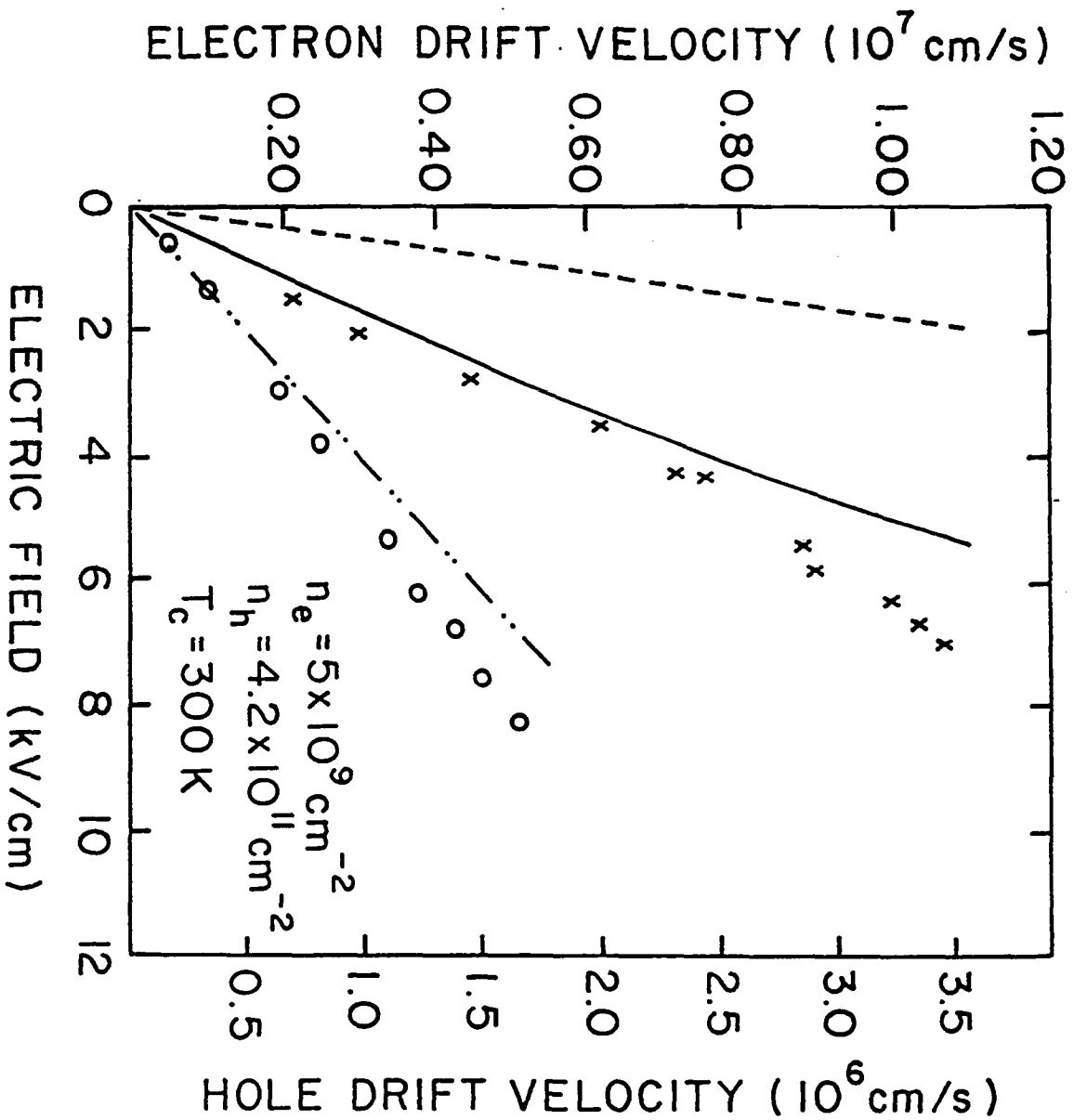


FIG. 3

Part II

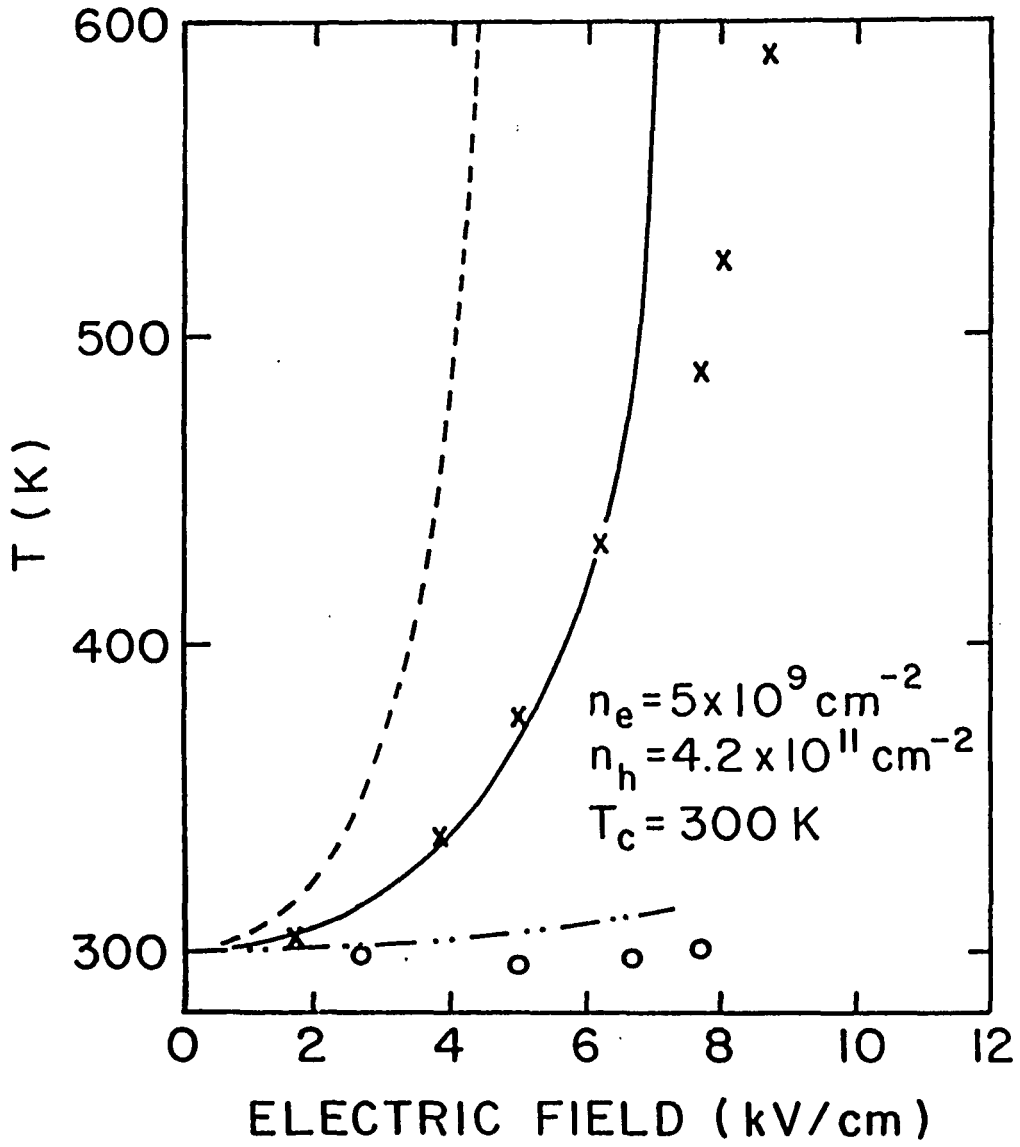


FIG. 4

Part II

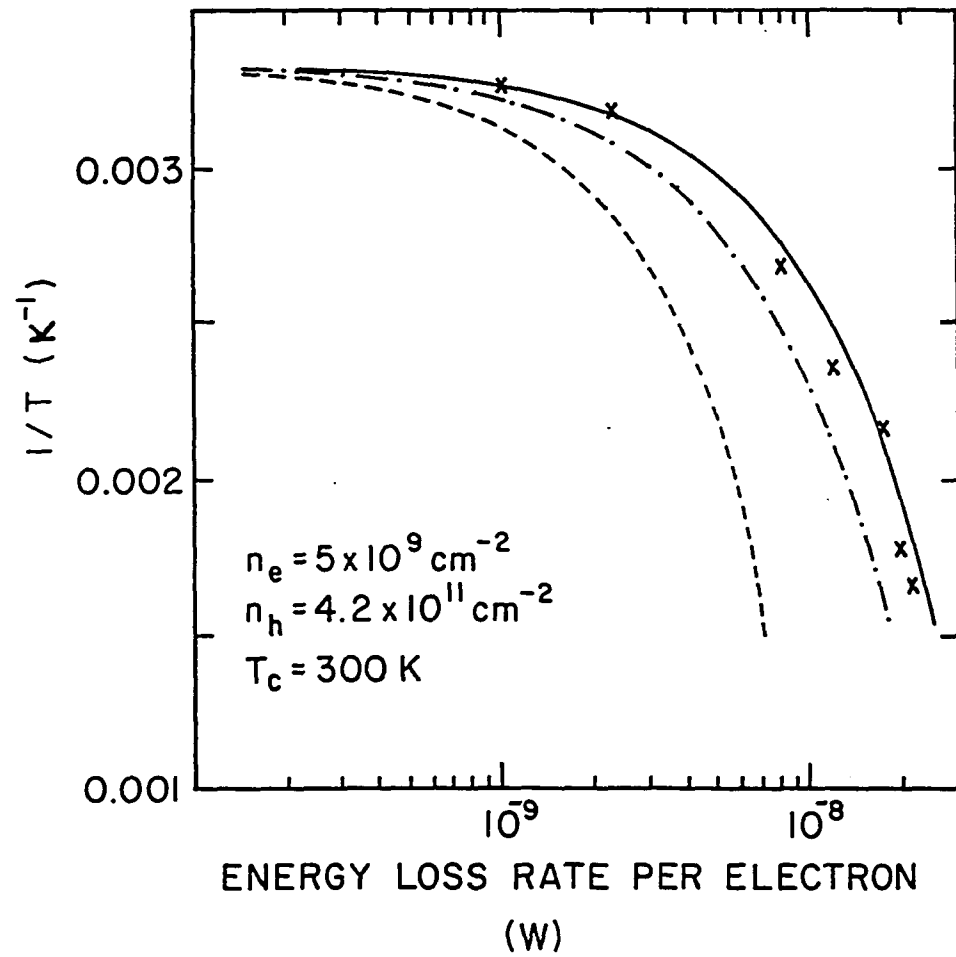


FIG. 5

Part II

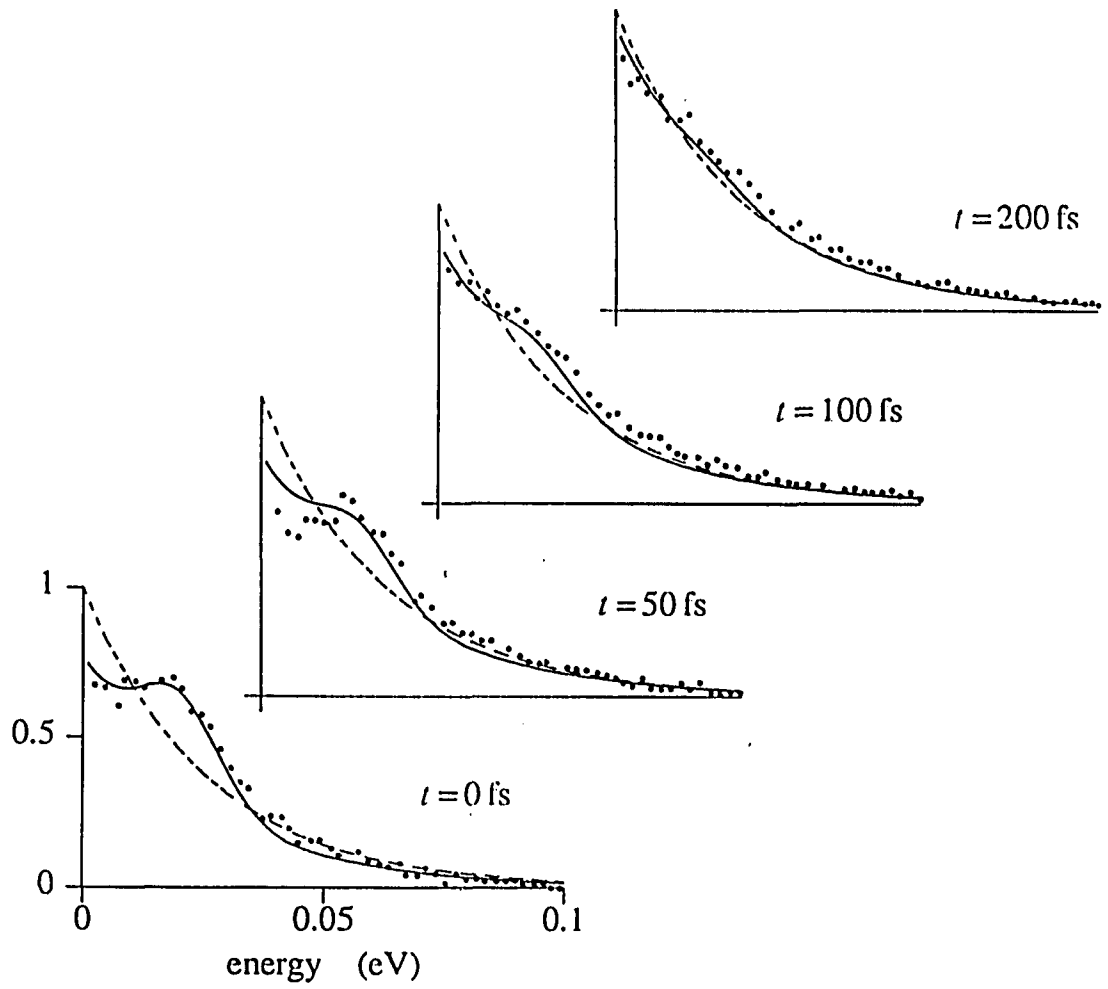


FIG. 1

Part III

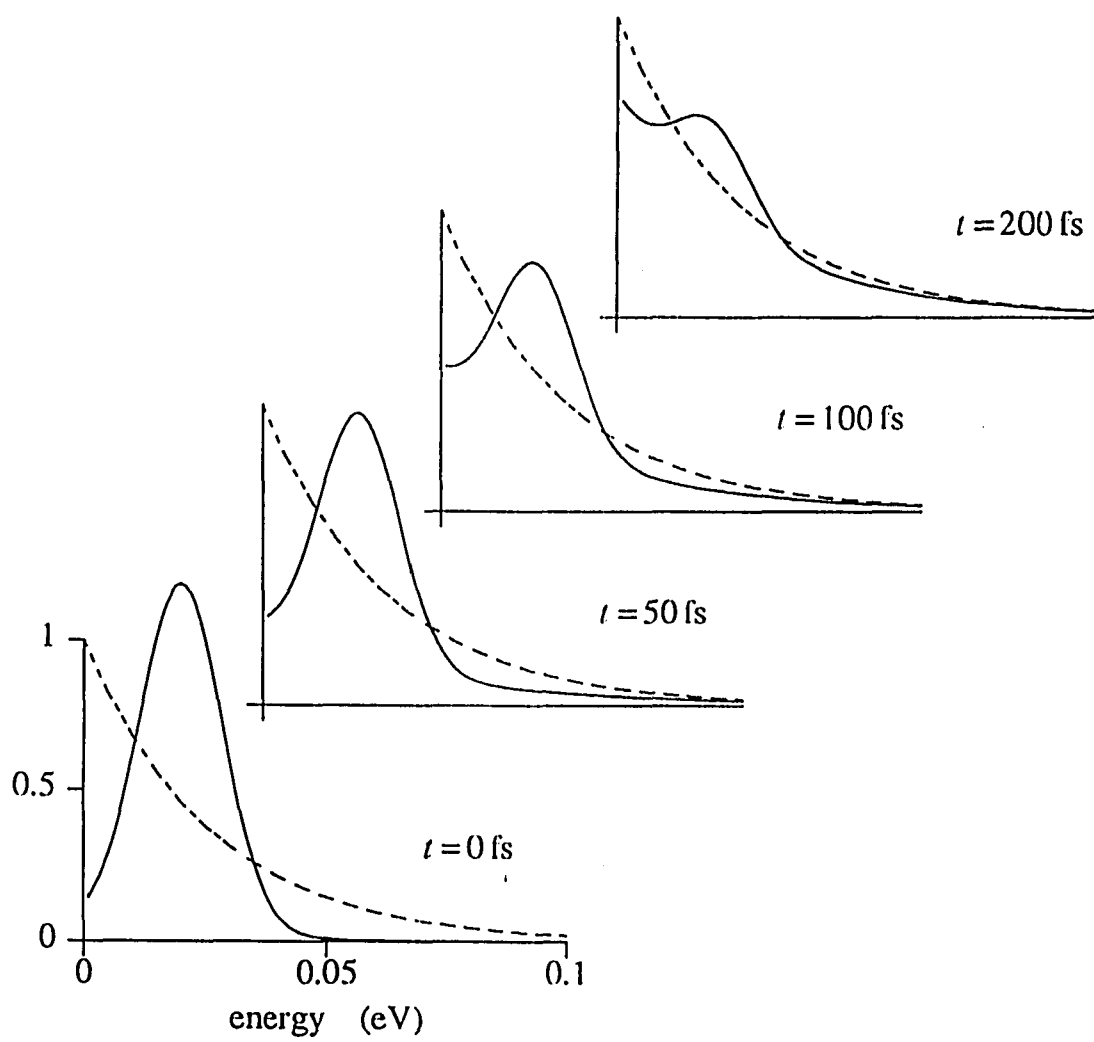


FIG. 2

Part III

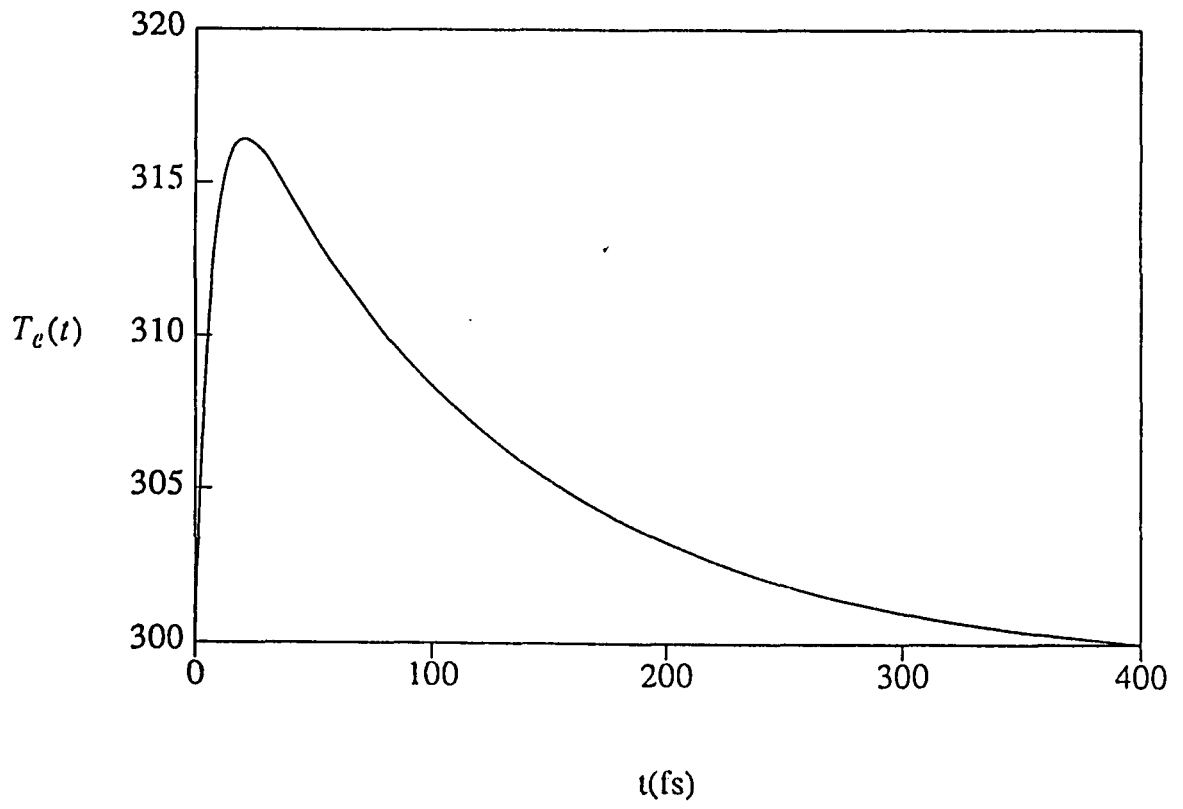


FIG. 3

Part III

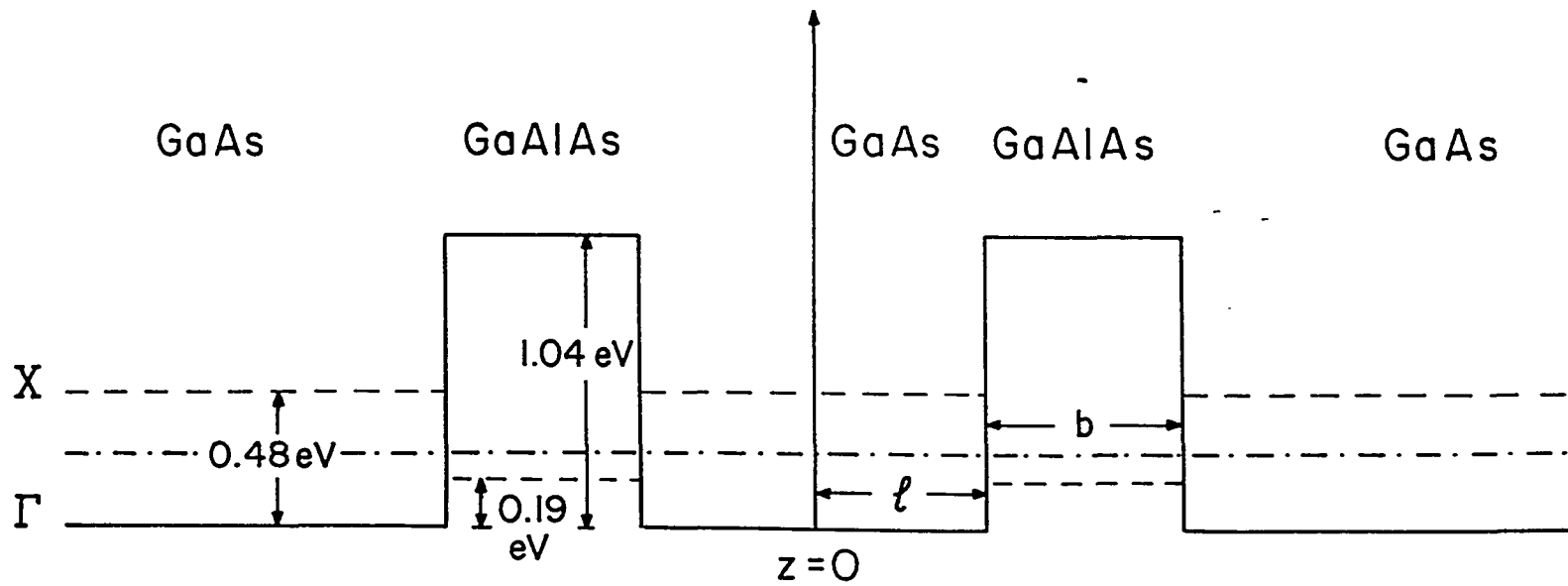


FIG. 1

Part VI

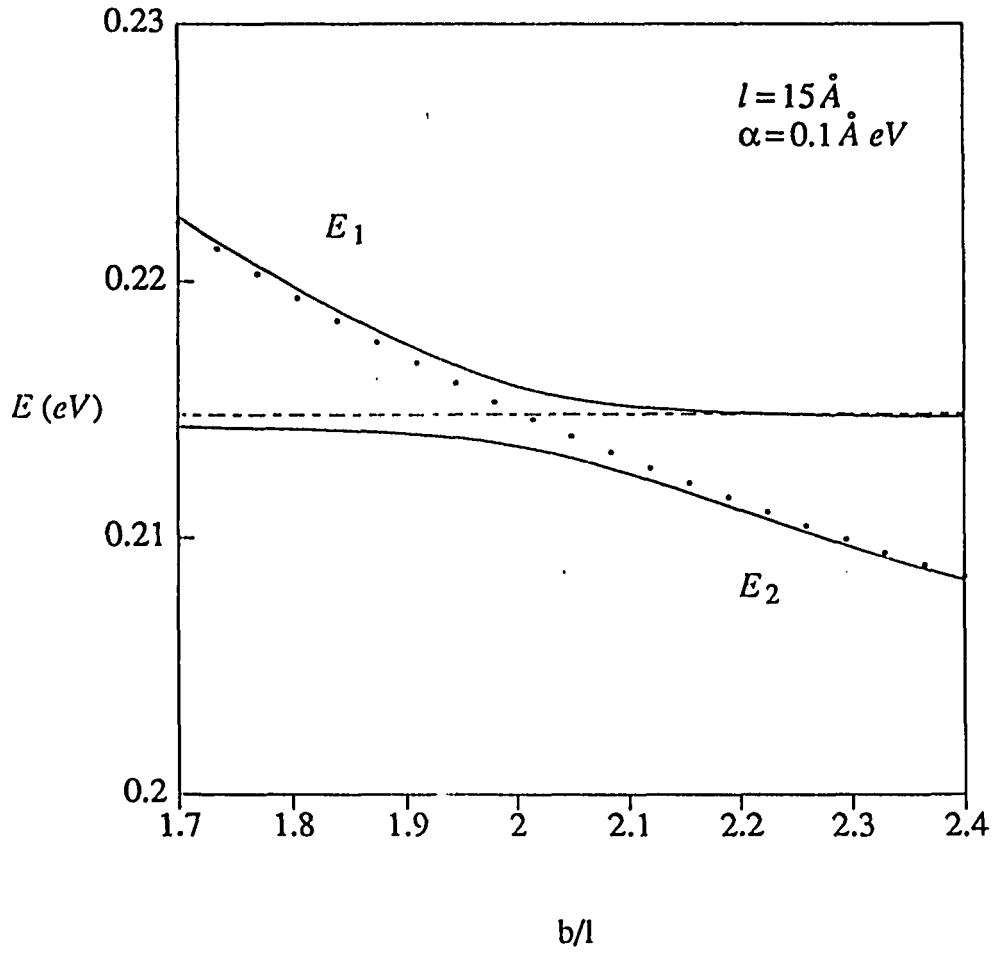


FIG. 2

Part VI

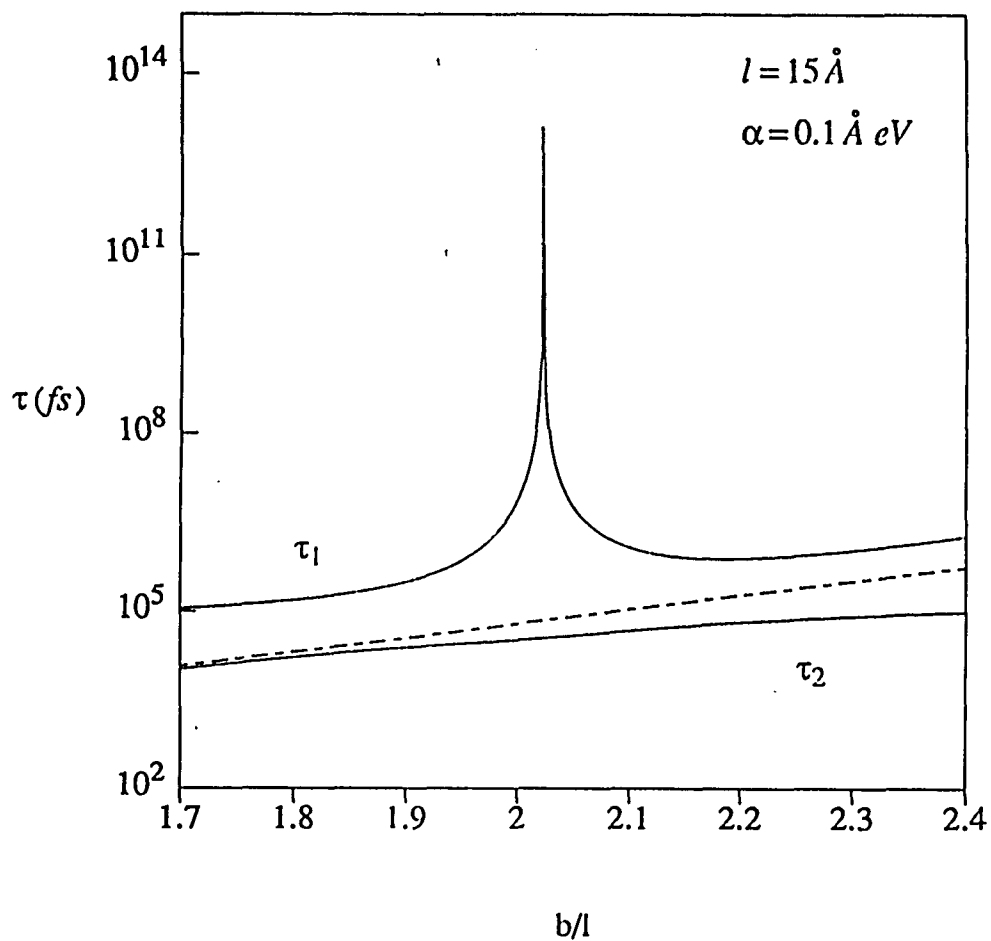


FIG. 3

Part VI

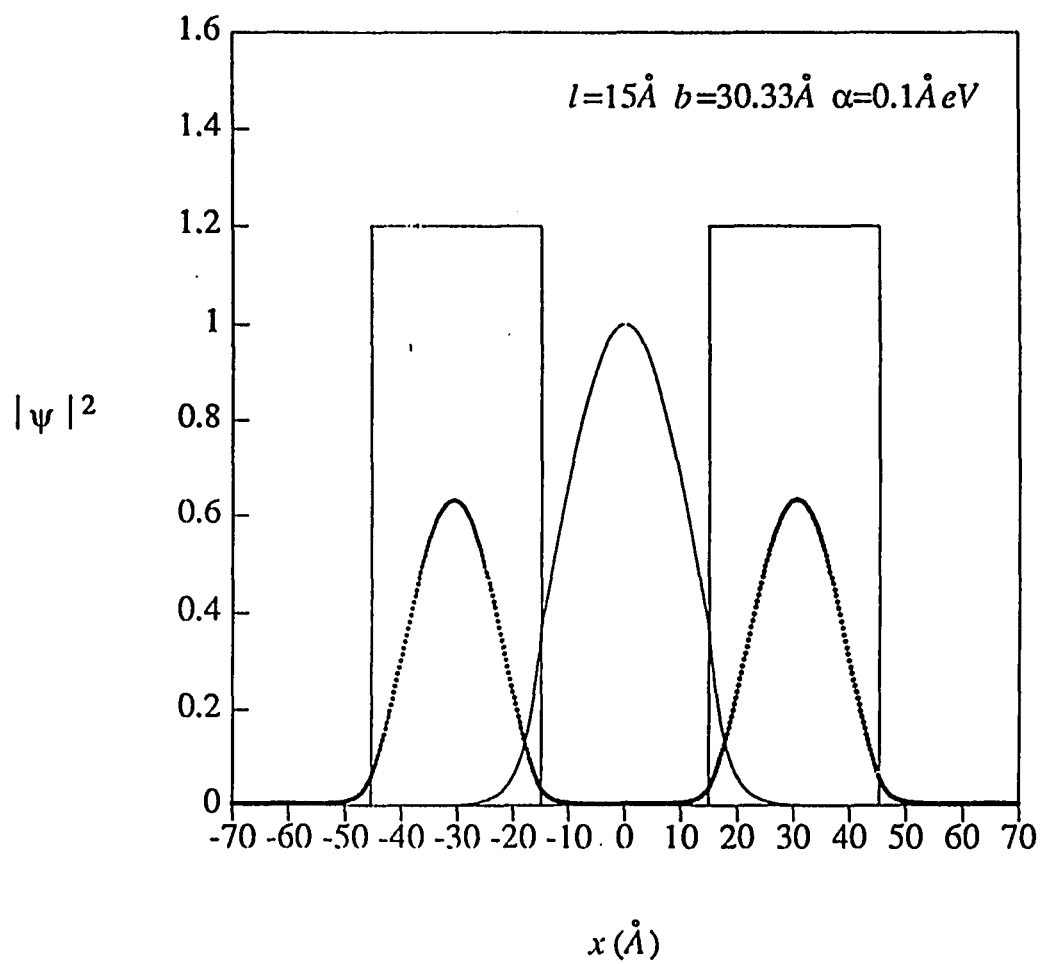


FIG. 4

Part III

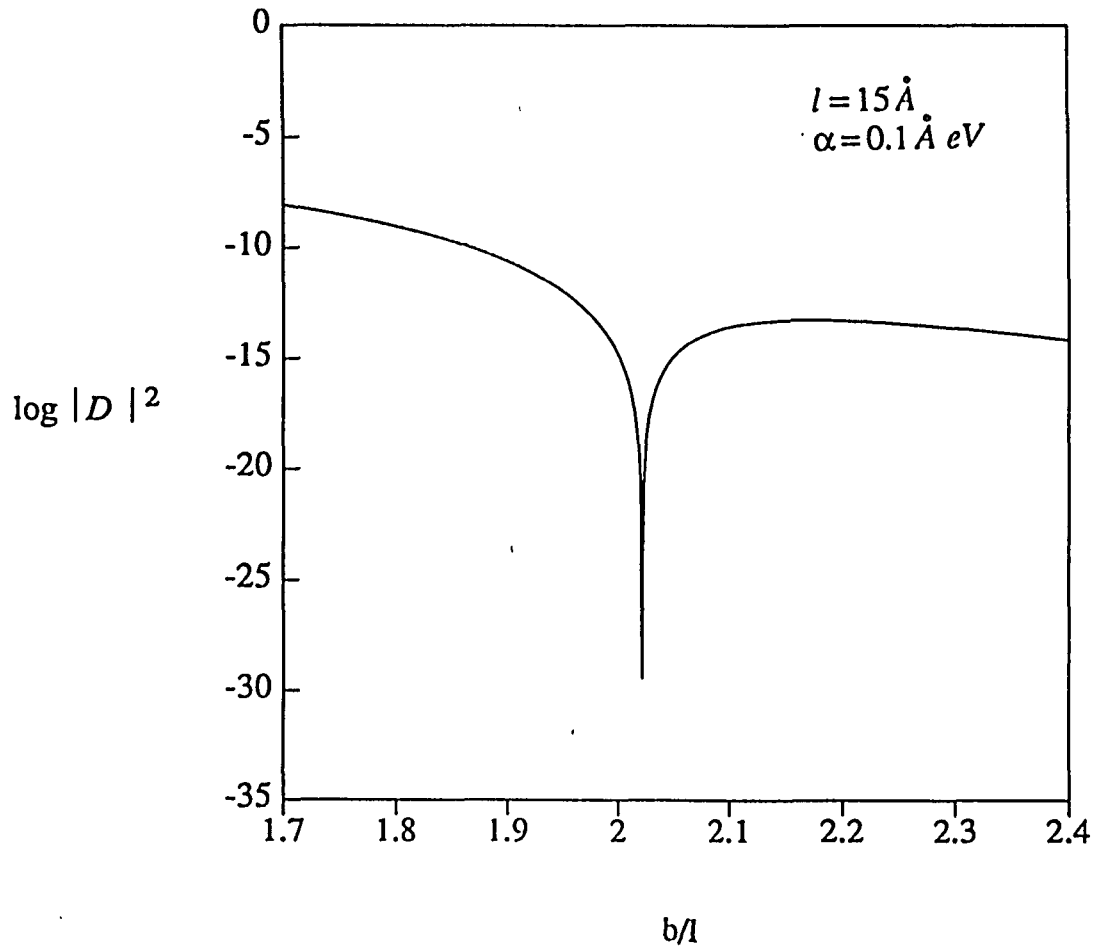


FIG. 5

Part VI

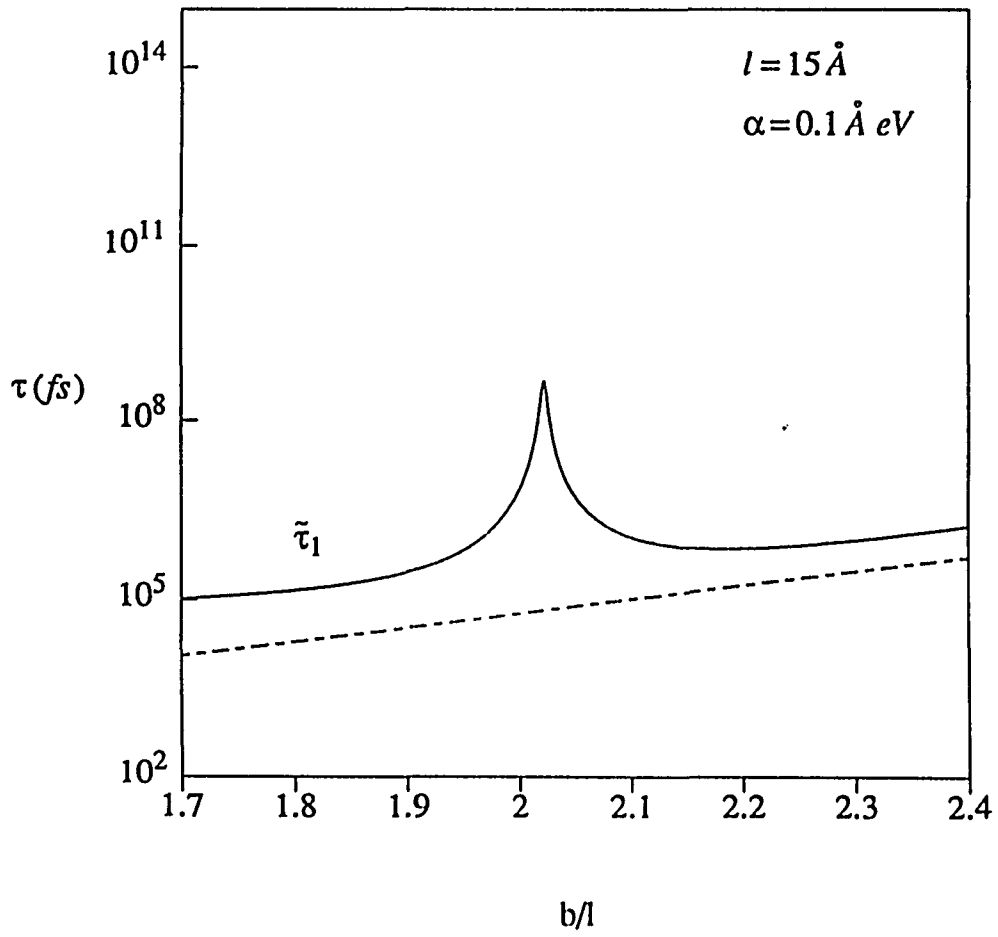


FIG. 6

Part VI

## Bibliography

### Reference of Part I

- <sup>1</sup>L. Esaki and R. Tsu, IBM J. Res. Dev. 14, 61 (1970).
- <sup>2</sup>A. O. Caldeira and A. J. Leggett, Phys. Rev. Lett. 46, 211 (1981); Ann. Phys. (N. Y.) 149, 374 (1983); H. Grabert, U. Weiss, and P. Hanggi, Phys. Rev. Lett. 52, 2193 (1984); 54, 1605 (1985).
- <sup>3</sup>A. J. Leggett, S. Chakravarty, A. T. Dorsey, M. P. A. Fisher, A. Garg, and W. Zwerger, Rev. Mod. Phys. 56, 420 (1986)
- <sup>4</sup>N. S. Wingreen, K. W. Jacobsen, and J. W. Wilkins, Phys. Rev. Lett. 61, 1396 (1988) L. I. Glazman and R. I. Shekhter, Zh. Eksp. Teor. Fiz. 94, 296 (1988); [Sov. Phys. JETP 67, 163 (1988)]
- <sup>5</sup>R. Bruinsma and P. Bak, Phys. Rev. Lett. 56, 420 (1986).
- <sup>6</sup>M. D. Stiles, J. W. Wilkins, and M. Persson, Phys. Rev. B 34, 4490 (1986)
- <sup>7</sup>B. Y. Gelfand, S. Schmitt-Rink, and A. F. J. Levi, Phys. Rev. Lett. 62 1683 (1989).
- <sup>8</sup>M. Büttiker and R. Landauer, Phys. Rev. Lett. 49, 1739 (1982).
- <sup>9</sup>W. Cai, T. F. Zheng, P. Hu, B. Yudanin, and M. Lax, Phys. Rev. Lett. 63, 418 (1989)
- <sup>10</sup>for example, E. Merzbacher, "*Quantum Mechanics*" (Wiley, New York, 1970) Chap. 2
- <sup>11</sup>N. G. Van Kampen, Phys. Rev. 89, 1072 (1952)
- <sup>12</sup>for example, F. W. Byron and R. W. Fuller, "*Mathematics of Classical and Quantum Physics*" (Addison-Wesley, New York, 1969) Chapter 7.
- <sup>13</sup>W. R. Frensley, Phys. Rev. B 36, 1570 (1987).
- <sup>14</sup>for example, L. Landau and E. Lifshitz, "*Quantum Mechanics*" (Pergamon Press, New York, 1962) Chapter 7.
- <sup>15</sup>V. J. Goldman, D. C. Tsui, and J. E. Cunningham, Phys. Rev. B. 36, 7683 (1987)

## Reference of Part II

- <sup>1</sup>D. K. Ferry, M. A. Osman, and R. Joshi, in Proceedings of the Fifth International Conference on Hot Carriers in Semiconductors (unpublished).
- <sup>2</sup>J. Shah, A. Pinczuk, A. C. Gossard, and W. Wiegmann, Phys. Rev. Lett. 54, 2045 (1985).
- <sup>3</sup>R. A. Höpfel, J. Shah, and A. C. Gossard, Phys. Rev. Lett. 56, 765 (1986).
- <sup>4</sup>R. A. Höpfel, J. Shah, P. A. Wolff, A. C. Gossard, Phys. Rev. Lett. 56, 2736 (1986).
- <sup>5</sup>H. J. Polland, W. W. Rühle, J. Kuhl, K. Ploog, K. Fujiwara, and T. Nakayama, Phys. Rev. B 35, 8273 (1987).
- <sup>6</sup>W. Cai, M. C. Marchetti, and M. Lax, Phys. Rev. B 34, 8573 (1986).
- <sup>7</sup>W. Cai, M. C. Marchetti, and M. Lax, Phys. Rev. B 37, 2636 (1988).
- <sup>8</sup>J. D. Wiley, Solid State Commun. 8, 1865 (1970).
- <sup>9</sup>F. Stern and W. E. Howard, Phys. Rev. 163, 816 (1967).
- <sup>10</sup>F. Stern and S. D. Sarma, Phys. Rev. B 30, wrote to me. Finally, let me thank you once again your letter and your help. I greatly appreciate your kindness and your letter does remind me of the days when you were at City College. Looking forward to meeting again here in New York. 840 (1984).
- <sup>11</sup>See, for instance, M. Born and K. Huang, *Dynamical Theory of Crystal Lattices* (Oxford University, Oxford, 1985), pp. 82–100.
- <sup>12</sup>E. M. Conwell, *High Field Transport in Semiconductors* (Academic, New York, 1967).
- <sup>13</sup>J. D. Wiley, *Semiconductors and Semimetals*, edited by R. K. Willardson and A. C. Beer (Academic, New York, 1975), Chap. 2.
- <sup>14</sup>D. C. Tsui, Phys. Rev. Lett. 21, 994 (1968).
- <sup>15</sup>T. Ando, A. B. Fowler, and F. Stern, Rev. Mod. Phys. 54, 437 (1982).
- <sup>16</sup>See, for instance, D. N. Zubarev, *Nonequilibrium Statistical Thermodynamics* (Consultants Bureau, New York, 1974), pp. 411–424 and Appendix III.
- <sup>17</sup>S. Peletminskii and A. Yatsenko, Zh. Eksp. Teor. Fiz. 53, 1327 (1967) [Sov. Phys.–JETP 26, 773 (1968)].
- <sup>18</sup>M. C. Marchetti, W. Cai and M. Lax, in Proceedings of The Fifth International Conference on Hot Carriers in Semiconductors (unpublished).

<sup>19</sup>W. Cai, T. F. Zheng, and M. Lax, Phys. Rev. B. 37, 8205 (1988)

<sup>20</sup>W. Cai, M. C. Marchetti, and M. Lax, Phys. Rev. B 35, 1369 (1987).

<sup>21</sup>S. Das Sarma, J. K. Jain, and R. Jalabert, Phys. Rev. B 37, 4560 (1988).

<sup>22</sup>See, for example, E. U. Condon and G. H. Shortley, *The Theory of Atomic Spectra* (Cambridge University Press, Cambridge, 1967), p. 20.

### Reference of Part III

<sup>1</sup>W. H. Knox, C. Hirlimann, D. A. B. Miller, J. Shah, D. S. Chemla, and C. V. Shank, Phys. Rev. Lett. 56, 1191 (1986)

<sup>2</sup>W. H. Knox, D. S. Chemla, G. Livescu, J. E. Cunningham, and J. E. Henry, Phys. Rev. Lett. 61, 1290 (1988).

<sup>3</sup>J. L. Oudars, D. Hulin, A. Migus, A. Antonetti, and F. Alexandre, Rev. Lett. 55, 2075 (1985).

<sup>4</sup>J. Shah, IEEE J. Quantum Electron. QE-22, 1728 (1986).

<sup>5</sup>C. H. Yang and S. A. Lyon, Physica B+C 134B, 305 (1985).

<sup>6</sup>Z. Y. Xu and C. L. Tang, Appl. Phys. Lett. 47, 692 (1984).

<sup>7</sup>C. V. Shank, R. L. Fork, R. Yen, J. Shah, B. I. Greene, A. C. Gossard, and C. Weisbuch, Solid State Commun. 47, 981 (1983).

<sup>8</sup>P. Lugli and S. M. Goodnick, Phys. Rev. Lett. 59, 716 (1987).

<sup>9</sup>M. A. Osman and D. K. Ferry, Phys. Rev. B 36, 6018 (1987).

<sup>10</sup>D. W. Bailey, M. A. Artaki, C. J. Stanton, and K. Hess, Appl. Phys. Lett. 62, 4638 (1987).

<sup>11</sup>S. M. Goodnick and P. Lugli, Phys. Rev. B 38, 10135 (1988).

<sup>12</sup>W. Cai, T. F. Zheng, and M. Lax, Phys. Rev. B 37, 8205 (1988).

<sup>13</sup>T. F. Zheng, W. Cai, and M. Lax, Phys. Rev. B 38, 1406 (1988).

<sup>14</sup>S. E. Esipov and Y. B. Levinson, Adv. Phys. 36, 383 (1987).

<sup>15</sup>S. E. Esipov and Y. B. Levinson, Pis'ma Zh. Eksp. Teor. Fiz. 42, 193 (1985) [JETP Lett. 42, 239 (1985)].

<sup>16</sup>S. E. Esipov and Y. B. Levinson, Zh. Eksp. Teor. Fiz. 90, 330 (1986) [Sov. Phys.-JETP 63, 191 (1986)].

- <sup>17</sup>S. Mori and T. Ando, Phys. Rev. B 19, 6433 (1979).
- <sup>18</sup>F. Stern and S. Das Sarma, Phys. Rev. B 30, 840 (1984).
- <sup>19</sup>W. Walukiewicz, H. E. Ruda, J. Lagowski, and H. C. Gatos, Phys. Rev. B 30, 4571 (1984).
- <sup>20</sup>See, for instance, Neil W. Ashcroft and N. David Mermin, *Solid State Physics* (Cornell University Press, Ithaca, NY, 1976), pp. 340-344.

#### Reference of Part IV

- <sup>1</sup>E. E. Mendez, W. I. Wang, E. Calleja, and C. E. T. Goncalves da siva, Appl. Phys. Lett. 50, 1263 (1987).
- <sup>2</sup>E. E. Mendez, Bull. Am. Phys. Soc. 32, 615 (1987).
- <sup>3</sup>E. E. Mendez, E. Calleja, C. E. T. Goncalves da Silva, L. L. Chang, and W. I. Wang, Phys. Rev. B 33, 8273 (1986).
- <sup>4</sup>M. H. Meynadier, R. E. Nahory, J. M. Worlock, M. C. Tamargo, J. L. de Miguel, and M. D. Sturge, Phys. Rev. Lett. 60, 1338 (1988).
- <sup>5</sup>G. C. Osbourn and D. L. Smith, Phys. Rev. B 19, 2124 (1979)
- <sup>6</sup>C. Maihiot, D. L. Smith and T. C. McGill, J. Vac. Sci. Technol. UL B1, 637 (1983)
- <sup>7</sup>A. R. Bonnefoi, T. C. McGill and R. D. Burnham, Phys. Rev. B 37 8754 (1988).
- <sup>8</sup>K. V. Rousseau, K. L. Wang and J. N. Schulman, Appl. Phys. Lett. 54 1341 (1989)
- <sup>9</sup>H. C. Liu, Appl. Phys. Lett. 51, 1019 (1987).
- <sup>10</sup>H. Akera, S. Wakahara and T. Ando, Surface Sci. 196 694 (1988)
- <sup>11</sup>J. Batey and S. L. Wright, J. Appl. Phys. 59, 200 (1986).
- <sup>12</sup>S. Adachi, J. Appl. Phys. 58, R1 (1985).
- <sup>13</sup>M. Tsuchiya, T. Matsusue, and H. Sakaki, Phys. Rev. Lett. 59, 2356 (1987).
- <sup>14</sup>Thomas B. Bahder, Clyde A. Morrison, and John D. Bruno, Appl. Phys. Lett. 51, 1089 (1987).
- <sup>15</sup>M. G. W. Alexander, M. Nido, K. Reimann, W. W. Ruhle, and K. Kohler, Appl. Phys. Lett. 55, 2517 (1989)
- <sup>16</sup>G. W. 't Hooft and C. Van Opdorp, Appl. Phys. Lett. 42, 813 (1983)

- <sup>17</sup>Y. Arakaea, H. Sakaki, M. Nishioka, J. Yoshino and T. Kamiya, Appl. Phys. Lett. 46, 519 (1985)
- <sup>18</sup>A. Hariz, P. D. Daphus, H. C. Lee, E. P. Menu, and S. P. Denbaars, Appl. Phys. Lett. 54, 635 (1989)